HYDROGEOLOGY OF FRACTURED-ROCK AQUIFERS AND RELATED ECOSYSTEMS WITHIN THE QOQODALA DOLERITE RING AND SILL COMPLEX, GREAT KEI CATCHMENT, EASTERN CAPE

L Chevallier · LA Gibson · LO Nhleko ·
AC Woodford · W Nomquphu · I Kippie

WRC Report No. 1238/1/04

Water Research Commission

HYDROGEOLOGY OF FRACTURED-ROCK AQUIFERS AND RELATED ECOSYSTEMS WITHIN THE QOQODALA DOLERITE RING AND SILL COMPLEX, GREAT KEI CATCHMENT, EASTERN CAPE

Luc Chevallier, Lesley A. Gibson, Lebogang, O. Nhleko
Council for Geoscience
cnr Oos and Reed Strs.
P.O Box 572
Bellville 7535
luc@geobell.org.za

Alan, C. Woodford
SRK Consulting
Loevenstein Centre
31 Allen Drive
Bellville, 7530
awoody@iafrica.com

W. Nomquphu
DWAF
King William's Town
NomqupW@dwaf.gov.za

Ieptieshaam Kippie / Bekko
Botany Department, UWC
Private Bag X17
Bellville 7535
ibekko@pawc.wcape.gov.za

WRC Report No 1238/1/04
ISN No 1-77005-128-7

FEBRUARY 2004

Disclaimer

This report emanates from a project financed by the Water Research Commission (WRC) and is approved for publication. Approval does not signify that the contents necessarily reflect the views and policies of the WRC or the members of the project steering committee, nor does mention of trade names or commercial products constitute endorsement or recommendation for use.

Printed by Silowa Printers: 012 804 7565

TABLE OF CONTENTS

LIST OF FIGURES

LIST OF TABLES

LIST OF PLATES

ACKNOWLEDGEMENTS

The Steering Committee responsible for the project consisted of the following persons:

Mr. K. Pietersen	Water Research Commission (Chairperson)
Mr. E. Van Wyk	Department of Water Affairs & Forestry
Prof. J.S Marsh	Rhodes University
Mr R. Murray	CSIR
Mr. A.C. Woodford	Research Team – SRK Consulting
Dr. L. Chevallier	Research Team – Council for Geoscience
Mr W. Nomquphu	Department of Water Affairs & Forestry
Ms C. Petersen	Committee Secretary

The financing of the project by the Water Research Commission and the contributions of the Steering Committee are gratefully acknowledged.

The generous support and funding of the project by the Director: Geohydrology of the Department of Water Affairs and Forestry is also acknowledged, in particular for (i) seconding an experienced geohydrologist, Mr. W. Nomquphu, to manage and conduct all the fieldwork at Qoqodala, (ii) the drilling and equipping of 13 exploration boreholes (iii) providing down the hole geophysical logs and video camera operated by B Venter and (iv) organising aquifer-testing i.e pump test and injection test of several holes, (v) The survey of the exploration site.

We also wish to thank our colleagues and their organisation for their scientific and technical support and their assistance:
Mr L. Swart from Department of Agriculture in Queenstown for the spring survey over part of the Great Kei River catchment.
Walter Wheeler and Norsk Hydro (Norway) for the scientific and financial support
Mr. P. Ravenscroft from CSIR for supplying us with bore hole monitoring equipment.
Mr. C. Less for conducting the injection tests.
V. Hallbauer-Zodorozhnaya for the Time Domain Electromagetic survey
Dr B. Low from Coastec for his comments on groundwater dependent ecosystems.
C. and R. McMaster from SAFCOL plantation on the Amatola montane grassland for the checklist of flowering plants.
Carnarvon estate for the list of plants on the Carnarvon mountains.
Dr Ulrike Rivett of the Department of Civil Engineering, University of Cape Town for the supervision Lesley Gibson's Masters thesis.

EXECUTIVE SUMMARY

INTRODUCTION

The present project is a follow-up of a previous Water Research Commission project No 937 on the hydrogeology of Karoo dolerite rings and sills (Chevallier et al., 2001). These saucer-shaped intrusions have induced a complex network of fractures inside the surrounding sediments and are responsible for the formation of numerous shallow and deep seated aquifers. Dolerite ring systems also control to a very large extent the morphology, the recharge and the drainage pattern at surface and influence the emergence of many springs and seepages. It becomes obvious from the hydro-morpho-tectonic model that many of these springs and related ecosystems may be vulnerable to large scale groundwater abstraction from this complex plumbing system of interconnected sills, dykes and fractures.

In the handbook on Hydrogeology of the Karoo Basin (Woodford and Chevallier, 2002b), needs for future research were identified and the study of the relation between groundwater, springs and ecosystems was highly recommended. It was suggested that future project should for that matter adopt a multidisciplinary programme-based approach including hydrostratigraphy, spring census, geomorphology, flow dynamics, biosystems and use of remote sensing.

The study area, i.e. the Qoqodala ring system is situated within the Great Kei river catchment, in the Eastern Cape. It covers four 1: 50 000 sheets and includes Queenstown (**Figure A**). In these Eastern Karoo regions, precipitations are higher than in the Western Karoo, runoff is more important and a large part of the population depends on the numerous springs and seeps coming out from the mountains. Boreholes are very few in the study area (former Transkei) but the numerous springs are associated to dolerite rings.

AIM AND OBJECTIVES

The aim of the project is to investigate ecosystem and spring/seepage dependency on shallow or deep fractured rock aquifers related to dolerite rings and their possible vulnerability to abstraction.

The two objectives as indicated in the memorandum of agreement are:

(i) To assess the occurrence of groundwater associated with the Qoqodala dolerite rings and sills in the Eastern Cape area using:

- Morphological and tectonic 3D analysis
- Hydrocensus of springs and boreholes
- Drainage systems
- Detailed investigation of the dolerite ring systems on a local scale for explorative drilling
- Selection of springs/seeps for detailed studies of their ecosystems
- Spatial analysis and remote sensing

(ii) To define hydro geological domains and the effects on ecosystems, springs recharge:

- By compiling ecosystem maps from available data and remote sensing on a regional scale
- By completing specific fieldwork on a detailed study area
- By selection of a specific spring/seep for detailed study in parallel to the drilling programme

MAJOR RESULTS

Dolerite sill and ring systems of the Great Kei catchment control to a large extent the morphology, the rain fall, the drainage pattern, the occurrence of many springs and therefore the geographic distribution of the local communities and their economic and social life. The Qoqodola sill and ring system comprises several coalescing and overlapping saucer-shape dolerite rings (inner sill, outer sill, inclined sheet), forming an intrusive network which should be conducive to high yielding fractured aquifers at various depths and the emergence of many springs (**Figure A**). The natural vegetation seems to be preserved on the slopes (ring) where it mainly comprises of aloes and shrubs, and few succulent plants . In contrast the middle flat area of the saucer-shape structure, corresponding to the communal land, is severely overgrazed

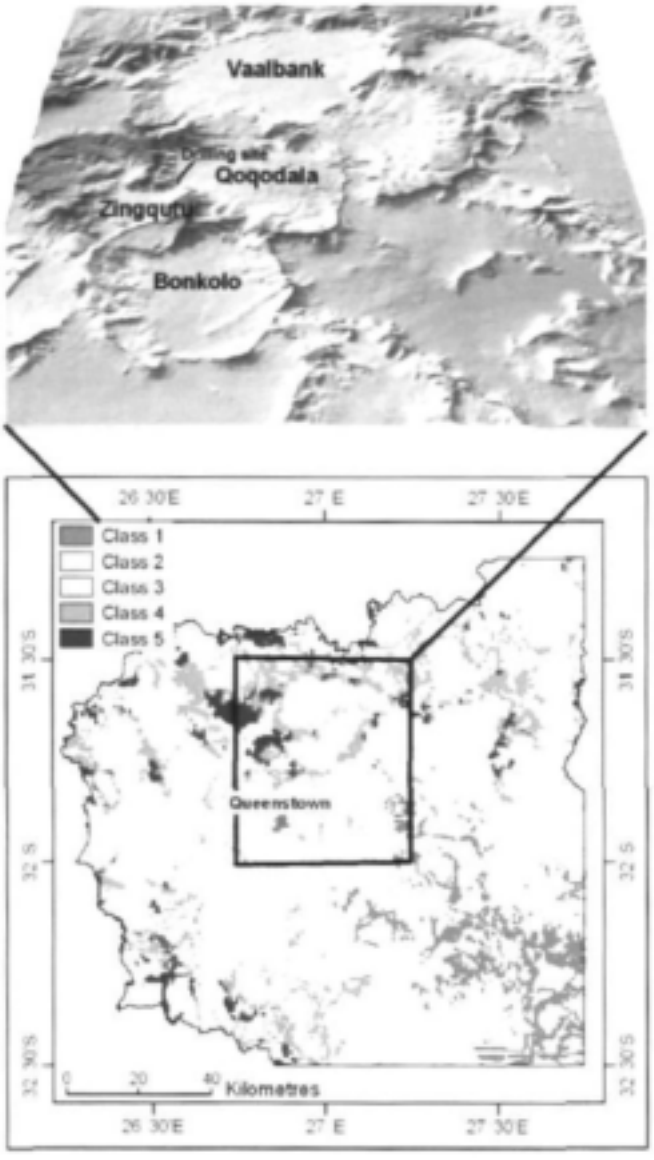

Figure A: Location of the study area inside the Great Kei catchment. The dolerite sills and rings are classified per elevation class (1: 340-942 m, 2: 943-1181m, 3: 1182-1389, 4: 1390-1628, 5: 1629-3000). The Qoqodala system consists of several coalescing rings.

Morpho-tectonic and elevation analysis of the sills completed with drilling results have shown at least six levels of sill intrusion over the study area. Inner sills and outer sills are all interconnected. The outer sill of a specific ring can becomes the inner sill of another ring. For instance one of the outer sill of the Qoqodala ring forms the inner sill of the Bonkolo ring (**Figure B**).

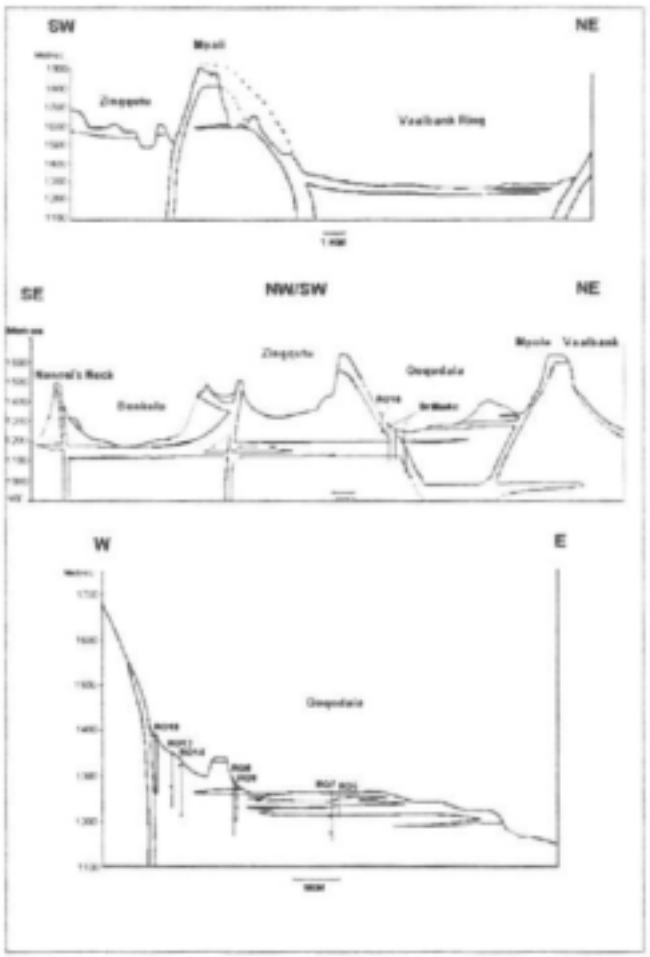

The inclined sheet forms the structural back bone of the ring system and the transition between the inner sills inside the ring and the outer sills outside the ring. Structural analysis over the study area showed that the ring part is densely fractured following major regional trends (dyke intrusion). At the drilling site across the Qoqodala ring, NW fractures are very prominent; the inclined sheet, feeding several sills, is probably fed by a regional dyke.

Figure B. Cross-sections of the Qoqodala dolerite sill/ring system. For location of the cross section see Figure A.

From March 2002 to June 2003, the Department of Water Affairs and Forestry (DWAF) drilled a total of 12 exploration percussion boreholes across the SW rim of the Qoqodala ring, along the road from Qoqodala to Zingqutu. A total drilling depth of 2655m was attained. The inclined sheet and the inner sill of the southwest portion of the Qoqodala ring were the main targets (**Figure C**). This was completed by geological logging, video

camera, geophysical down the hole logging and Time Domain Electromagnetic survey (TDEM), especially for deep structure detection. The profile shows a very thick dolerite inclined sheet feeding two outer sills. The back of the inclined sheet between the two outer sills is structurally very complex with several dolerite offshoots, confirming results obtained at Victoria West. The Qoqodala inner sill and the deeper sill were not intercepted by drilling but detected by TDEM.

Three aquifer-testing schedules, each consisting of a step-drawdown test followed by a 72-hour constant-discharge and waterlevel-recovery test, were conducted on boreholes BH-1, BH-7 and BH-11 over the period 27th June to 22nd July 2003. Qoqodala dolerite ring-system exhibits a typical multi-layered aquifer system, where at least three hydraulically distinct aquifer units are evident (**Figure D**).

A shallow, laterally extensive, unconfined to semi-confined aquifer unit developed in the weathered / uplifted layers above the *Inner Sill*, where the main water-bearing fractures are predominantly sub-horizontal to horizontal. The depth to the waterlevel varies between 9 and 11 m.bgl. When flowing, the river is effluent into the groundwater system. The deeper, sub-horizontal fracture zone associated with the relatively thin dolerite 'offshoot' may only be weakly connected to the overlying fracture network and, if this is the case, could be considered as separate aquifer layer.

A shallow, semi-confined to confined aquifer developed within the intensely fractured sediments behind *Inclined Sheet* and *Outer Sill* of the ring system. The confined nature of the undisturbed aquifer resulted in boreholes BH-4 and BH-5 becoming artesian soon after drilling as well as the spring near BH-5 becoming dry. At this point, it is also likely that the aquifer was effluent to the river.

A deeper-seated, confined aquifer associated with discrete, open, fractures in the dolerite and meta-sediments at the base of the *Outer Sill* and *Inclined Sheet*, as well as presumably the *Inner Sill*. High yields were struck in a fracture system at the base of the *Outer Sill*. The temperature of the groundwater in borehole BH-7 is slightly elevated at

24° C, indicating upward movement of groundwater from a greater depth. The water is generally of good quality and varies around 44 mS/s. No chemical data was available yet from DWAF when the present report was compiled.

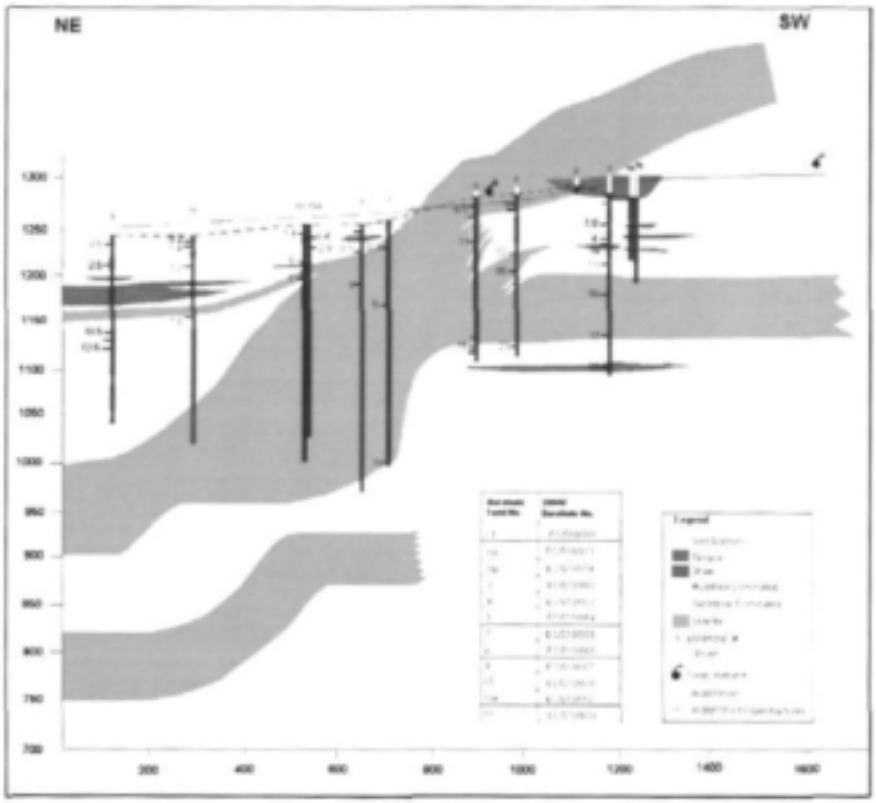

Figure C : Geohydrological profile at Qoqodala exploration drilling site.

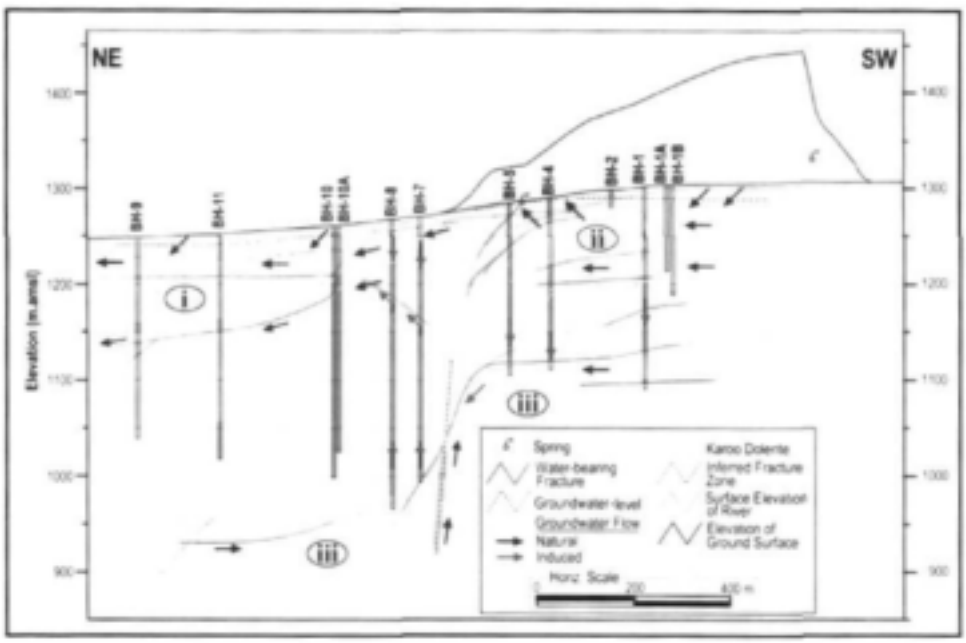

Figure D: Natural and 'Induced' Groundwater Flow Regime at the Qoqodala Test Site

The ecosystem mapping part of the project aimed to produce a high resolution vegetation map by using remote sensing technique. Secondly, any wetlands present in the study area were mapped using moisture and greenness indices derived from multi-temporal satellite imagery. Finally, the spectral properties of a known seep were used to map this groundwater dependant ecosystem.

The results of the vegetation mapping revealed that it is possible to use medium resolution satellite image for broad vegetation mapping however it is not suitable for mapping at community level. The nature of the landscape lends itself more to land use mapping than vegetation mapping (**Figure E**).

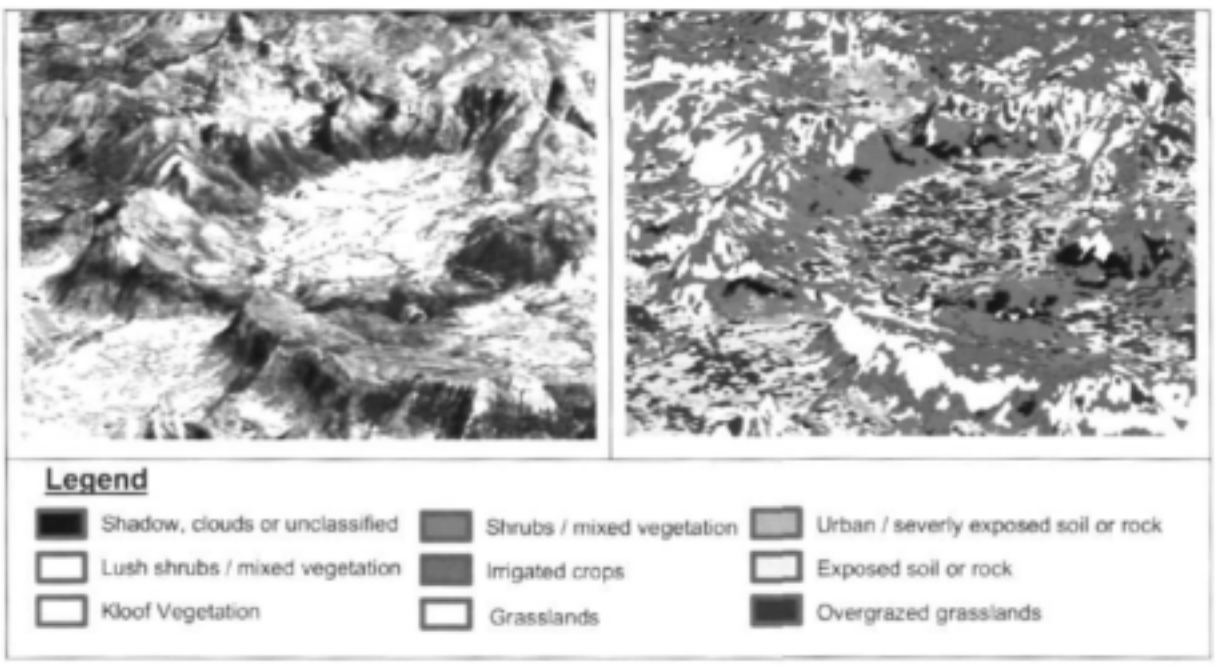

Figure E: 3 dimensional view of the Qoqodala Ring showing the vegetation classification results (right) with an Aster image (lef). Looking from South to North.

The wetland mapping proved that large wetlands are not present on the upland dolerite regions where rain fall and moisture are important, but instead vast grassland areas are present (**Figure F**). Small seeps on the slope of the dolerite rings are such that they were not successfully mapped using either Aster or Landsat imagery.

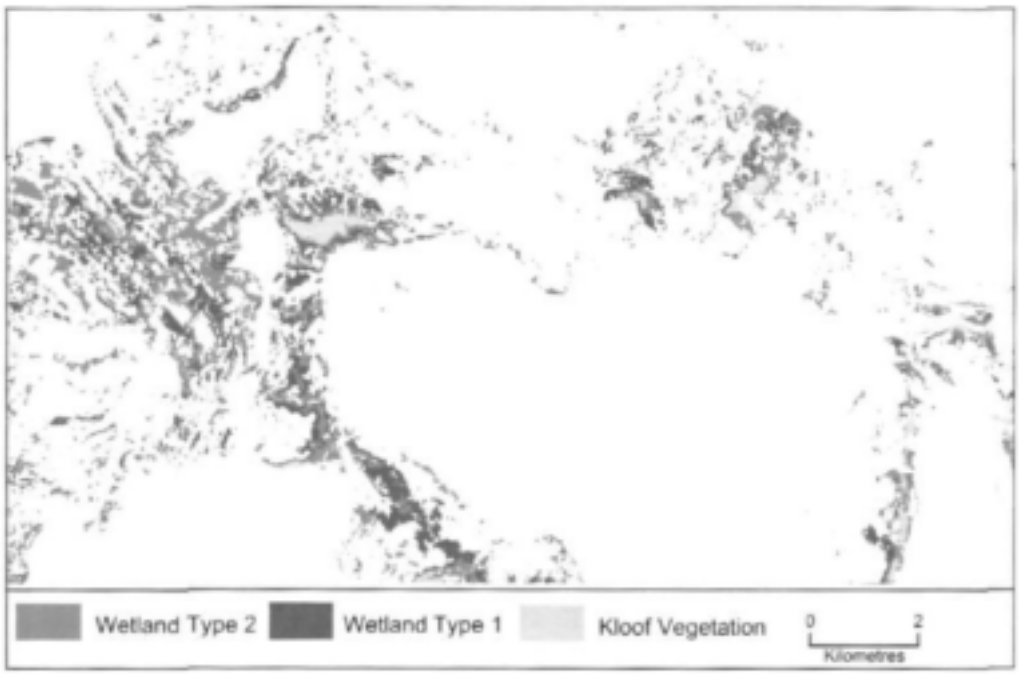

Figure F: Results of the Aster Classification Approach for wetland mapping

Finally, using the spectral properties of a known seep to map other seeps in the area revealed interesting trends (**Figure G**). When the results of the seep mapping are compared with the slope analysis and dolerite elevation classes, it was seen that in general, the density of seeps decreases with elevation and with slope steepness. The optimal slope on which the 'seeps' occur at these altitudes is on slopes of less than eight degrees closely followed by slopes of between eight and 14 degrees.

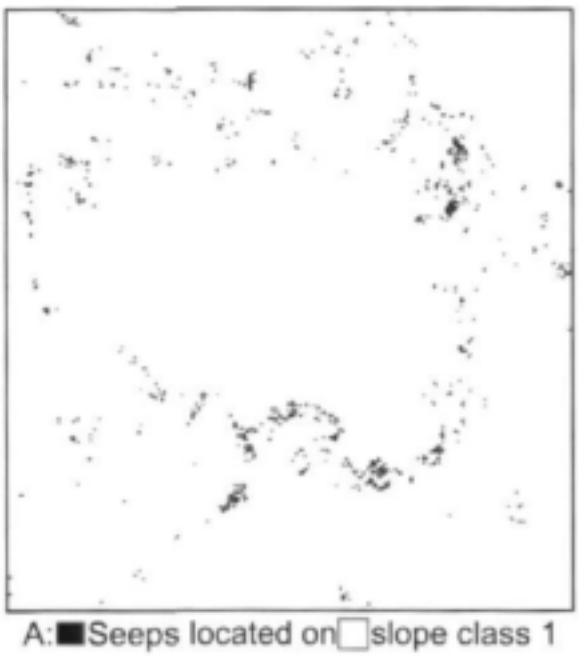

Figure G: Distribution of potential seeps on slopes between 8° and 14°. No field verifications

Ecosystem studies have shown that grassland is very common on high lying outer dolerite sills in recharge areas but do not however host large wetlands that could act as water reservoir (**Figure H**). Aloe dominated shrubs and succulent thicket occurs on North facing and East facing slopes of the dolerite rings being adapted to more arid conditions that the grassy highlands (**Plate A**). None of these plants however are likely to be groundwater dependant. Lush tall shrubs with a tree component dominate in the kloofs and at the foot of dolerite cliffs and seem to prefer South and West facing steep exposures. These luxuriant thickets may be terrestrial to phreatophytic i.e. a combination of moist conditions in valley or shadowy places and periodic use of non-perennial seeps at the base of dolerite cliffs. Groundwater dependent plants occur around perennial seeps where the vegetation consists mainly of grass and sedges growing on peaty black soil forming small wet areas from few meters to several tens of meters wide. Shrubs adapted to harsher conditions are unable to grow. They typically occur in depressions along fractures or created by morphological breaks along lithological contact zone i.e mudstone-sandstone or dolerite sediment. They also tend to occur at low elevation and on slopes no more than 14°. These seeps and small wetlands might not significantly contribute to the overall water recharge but they are very vulnerable to change in groundwater regime via drilling or abstraction as proven at Qoqodala drilling site. In the middle of the ring extreme land degradation occurs; bare soil and overgrazed grassland dominate. This does not mean that wetland vegetation did not exist in the past.

The most vulnerable eco-hydrogeological system corresponds to the upper unconfined aquifer above the low outer sill and to the seeps occurring at low elevation. The bulk of the groundwater recharged during rainfall events is stored in this aquifer layer. Because of the high density of fracturing of the ring and the high connectivity of these shallow fractures, badly planned drilling can induced water flow regime and deplete the aquifer and therefore affect these ecosystems. The location of wetlands or seeps at low elevation, the direction and density of fracturing, the slope of the inclined sheet, and the presence of an outer sill at depth are factors that should be taken into account when developing dolerite ring related groundwater.

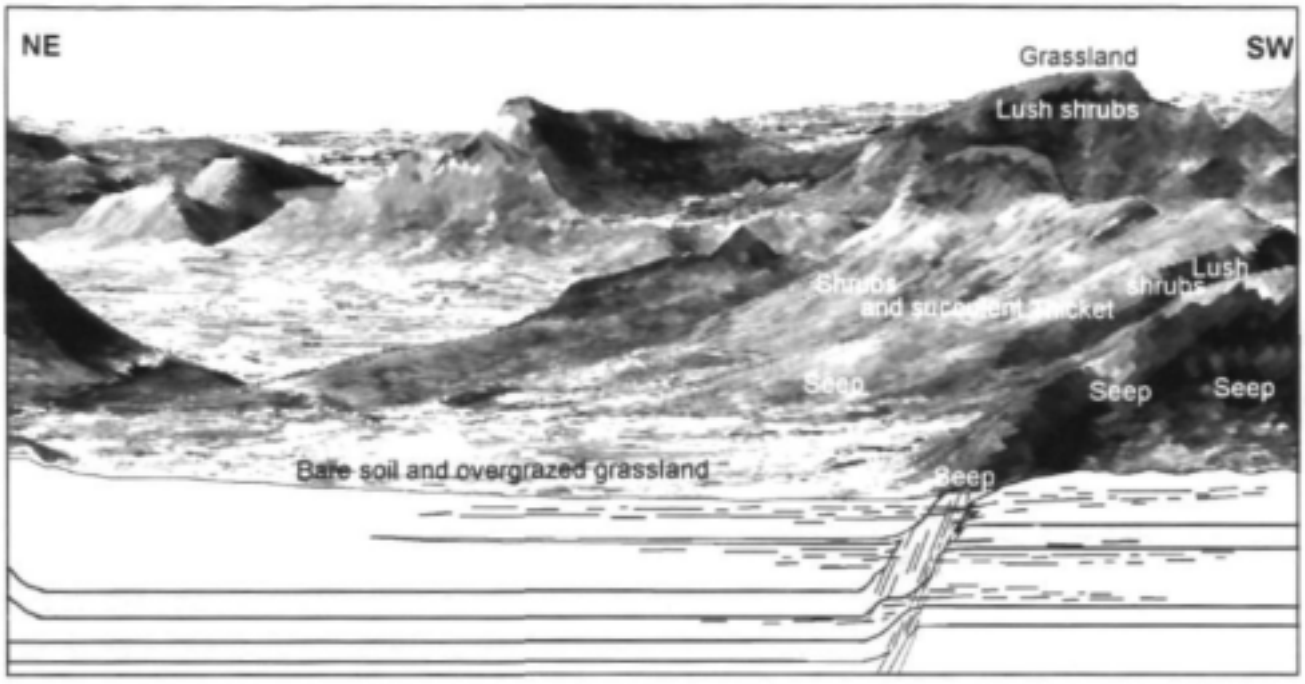

Figure H: The Eco-geohydrological model of the Qoqodala dolerite ring system.

Plate A : Ecosystem and dolerite ring at Qoqodala drilling site. The foreground is occupied by the shrubs and succulents typical of dolerite slopes.

1. INTRODUCTION

1.1 PROJECT BACKGROUND AND LOCATION OF STUDY AREA

This project is a follow-up of a previous Water Research Commission project No 937 on the hydrogeology of Karoo dolerite rings and sills (Chevallier et al., 2001). These saucer-shaped intrusions typically consist of a flat inner sill, an inclined sheet on the circumference (the ring) and an outer sill forming the rim of the saucer but often eroded away (**Figure 1**).They have induced a complex network of fractures inside the surrounding sediments and are responsible for the formation of numerous shallow and deep seated aquifers. Dolerite ring systems also control to a very large extent the morphology, the recharge and the drainage pattern at surface and influence the emergence of many springs and seepages.

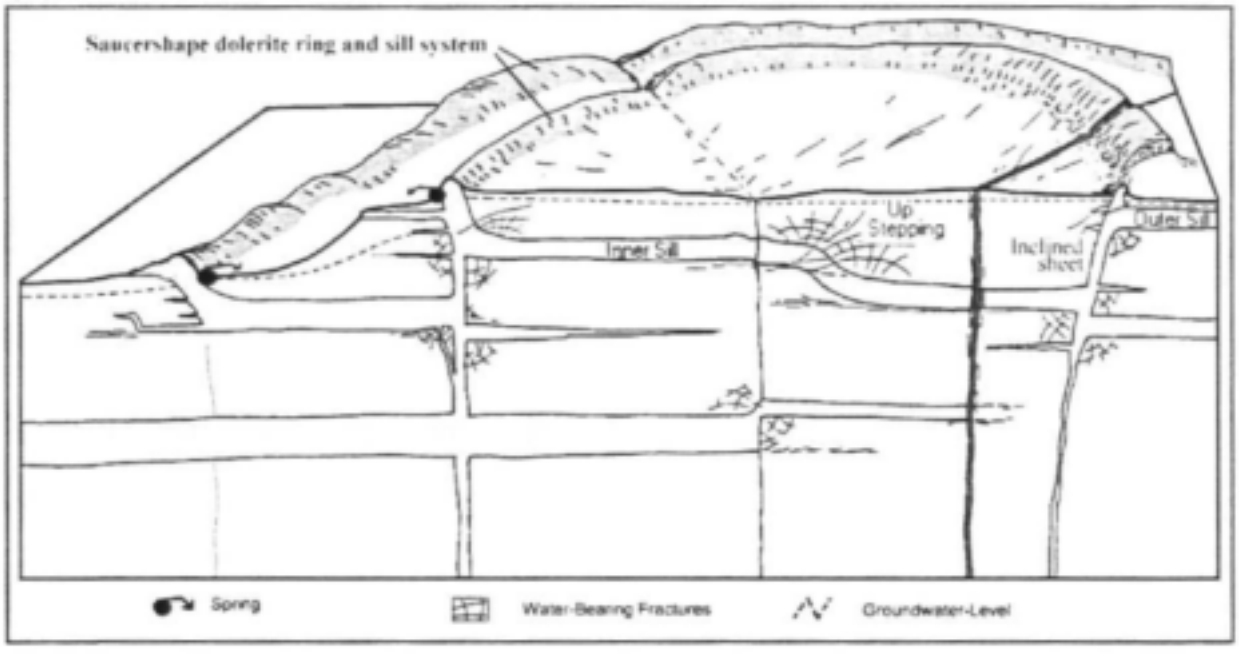

Figure 1: Hydro-morpho-tectonic model of Karoo dolerite sill and ring complex (after Chevallier et al., 2001), This typical saucer-shape structures controls the morphology, the springs, the drainage and the ecosystem at surface.

It becomes obvious from the hydro-morpho-tectonic model of figure 1 that many of these springs and related ecosystems may be vulnerable to large scale groundwater abstraction from this complex plumbing system of interconnected sills, dykes and fractures.

As an example, during exploration drilling for WRC project 937, on the farm Vrede, next to Victoria West, a high yield artesian borehole was sunk in a shallow inclined dolerite sheet, 400 m from a spring. During pump testing in January 2002, the spring and the vegetation dried out and water levels in other boreholes dropped by 26m. After the heavy rains of February 2002 (250 mm) the spring was flowing again. Any assessment of the hydro-ecosystems in the Karoo will therefore have to take into account the hydrogeology of dolerite sills and rings.

In the handbook on the hydrogeology of the Karoo Basin (Woodford and Chevallier, 2002a), needs for future research were identified and the study of the relation between groundwater, springs and ecosystems was highly recommended. It was suggested that all future projects should for that matter adopt a multidisciplinary programme-based approach including hydrostratigraphy, spring census, geomorphology, conceptual flow dynamics, biosystems and the use of remote sensing.

Previous WRC projects on Karoo dolerite (Burger et al., 1981; Chevallier et al. 2001, Woodford and Chevallier, 2002b) were situated in the Western Karoo i.e. in semi-arid to arid areas where recharge is low and springs and seepages are few. In these regions the springs do not represent large and reliable water supply and are solely used by individual commercial farmers for local application (garden, bottling).

Conversely, in the Eastern Karoo regions, precipitation is higher, runoff is more important and a large part of the population depends on the numerous springs and seeps coming out of the mountains. This region is therefore more suited to a study on the relationship between dolerite rings fractured rock aquifers, springs and ecosystems (the results of the study could be applied latter to drier parts of the Western Karoo Basin). The study area is situated within the Great Kei River catchment, covers four 1: 50 000 sheets and includes Queenstown (**Figure 2**).

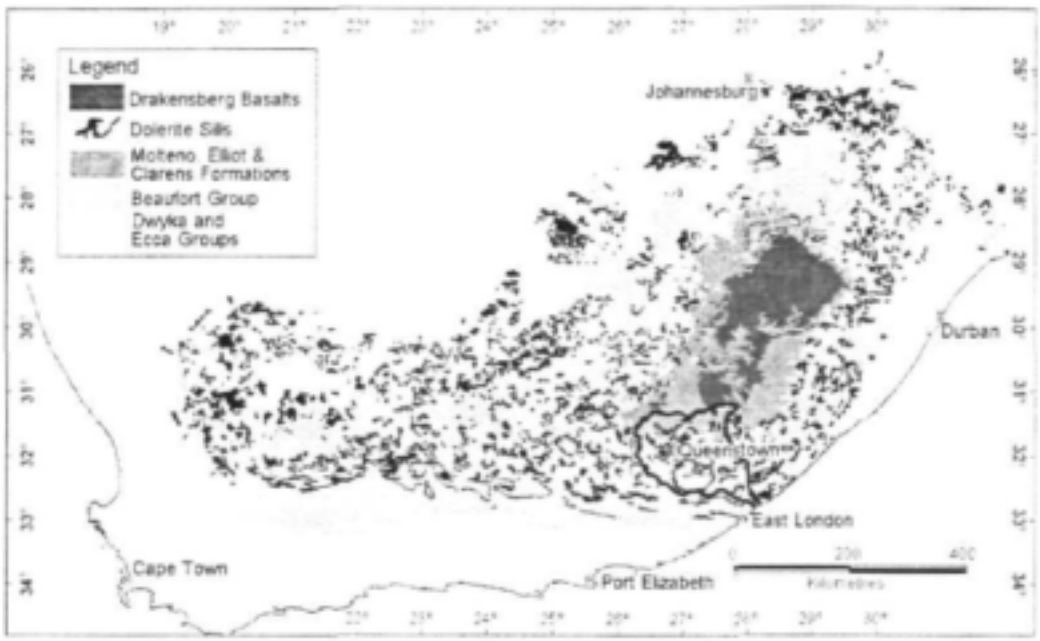

Figure 2: The Qoqodala study area is situated in the Great Kei River Catchment around Queenstown.

1.2 AIM AND OBJECTIVES OF THE PROJECT

The aim of the project is to investigate ecosystem and spring dependency on shallow or deep fractured rock aquifers related to dolerite rings and their possible vulnerability to abstraction.

The two objectives as indicated in the memorandum of agreement are:

(i) To assess the occurrence of groundwater associated with the Qoqodala dolerite rings and sills in the Eastern Cape area using:

- Morphological and tectonic 3D analysis
- Hydrocensus of springs and boreholes
- Drainage systems
- Detailed investigation of the dolerite ring structures on a local scale for explorative

drilling

- Selection of springs for detailed studies of their ecosystems
- Spatial analysis and remote sensing

(ii) To define hydro-geological domains and the effects on ecosystems, springs recharge:

- By compiling ecosystem maps from available data and remote sensing on a regional scale
- By completing specific fieldwork on a detailed study area
- By selection of a specific spring for detailed study parallel to the drilling programme.

1.3 LITERATURE REVIEW

A very large part of the literature related to the structure of the Karoo dolerite fractured-rock aquifers and their hydrogeology has been covered by previous projects. This extensive literature can be found in Woodford and Chevallier (2002a). New ideas on dolerite geometry and associated fluid transfers have been developed during a collaborative project with a Norwegian research team led by Volcanic Basin Petroleum Research in Oslo. The rifted margin of offshore Norway shares the same geological environment: sedimentary basin intruded by dolerite sill and ring complexes which are the potential pathways for fluid migration and traps (oil). Of special interest is the study of the connections between dolerite intrusions and volcanic vents which can be seen on seismic profiles. Similar volcanic vents are found just north of our study area above the sills intruded into the Elliot Formation (Jamtveit et al., in press; Svensen et al., 2001).

Literature on springs in the Eastern Cape, especially in the study area, is scarce. The paper on Karoo springs by Kok (1992) remains the only published document to date.

It is apparent from the literature review that remote sensing can be used to aid groundwater detection. The infrared wavelengths are particular useful for water, moisture and vegetation detection. Of concern is the fact that, the majority of studies consulted mentioned that

inaccuracies occurred when trying to detect small area of wetlands, surface water or areas of moisture. It has been suggested by Conrad et al (2000) that the use of other spatial data such as digital elevation models and drainage may complement and verify the results obtained from satellite image processing. Many remote sensing papers were consulted but the most relevant to the study in the South African context was the study by Thompson et al (2002). This study details, in the form of a pilot project, the image processing steps followed in order to map wetlands using Landsat imagery. In another South African example, Hartnady & Hay (2000) investigated whether vegetation anomaly mapping could be used as a tool in spring mapping unfortunately, groundtruthing was not carried out due to budgetary constraints.
Introductory texts on remote sensing were consulted extensively and included Mather (1999); Sabins (1997); and Lillesand & Kieffer (2000).

Few publications in South Africa refer to groundwater dependency and vulnerability of selected ecosystems and spring (Cleaver et al., 2003, Smart, 2003). Extensive literature is available for Australia where groundwater dependent ecosystems form a very important part of water management and sustainable development (literature review from the Water and Rivers Commission, 2001). Although Australian ecosystems are different from South African ecosystems the methodology for identifying probable relationship between ecosystems and groundwater occurrence and the level of dependency remains the same.

There is presently no floral species list for the study area or for the Great Kei catchment in general, and no literature of previous floristic work, other than Acocks (1988) and Rutherford (1997), was found for the study area. The National Botanical Institute was visited and the archives of Acocks' work were consulted. Although some sample sites occurred within the study area, locations were not recorded accurately so this was of little use. In addition, the Acocks' photographic archive was browsed for photographs of the study area with some success. These photographs can be seen in Appendix A. Our literature review was less sites specific and related to interactions between groundwater and vegetation (Le Maitre *et al*, 1999), soil identification, Karoo shrubland (Milton S.J., 1990). However a checklist for flowering plants could be obtained locally such as the Eastern Amatola Montane Grassland (McMaster, C. and McMaster, R. 2001).

1.4 DATA ACQUISITION

The list of data obtained for this project is quite extensive and can be found in **Table 1**. The data sources were varied but the Department of Water Affairs and Forestry, the Council for Geoscience, Surveys and Mapping and the Department of Agriculture in Queenstown were the main data suppliers. The extent of the data coverage of the main datasets used in the research is shown in ***Figure 3***. The data used in this research project and listed in Table 1, as well as the data resulting from this project, will be stored on the server at the Council for Geoscience in Bellville. In addition, the data will be written to CD ROM and will be stored in the safe in the same building. Metadata has been captured and is stored with the data.

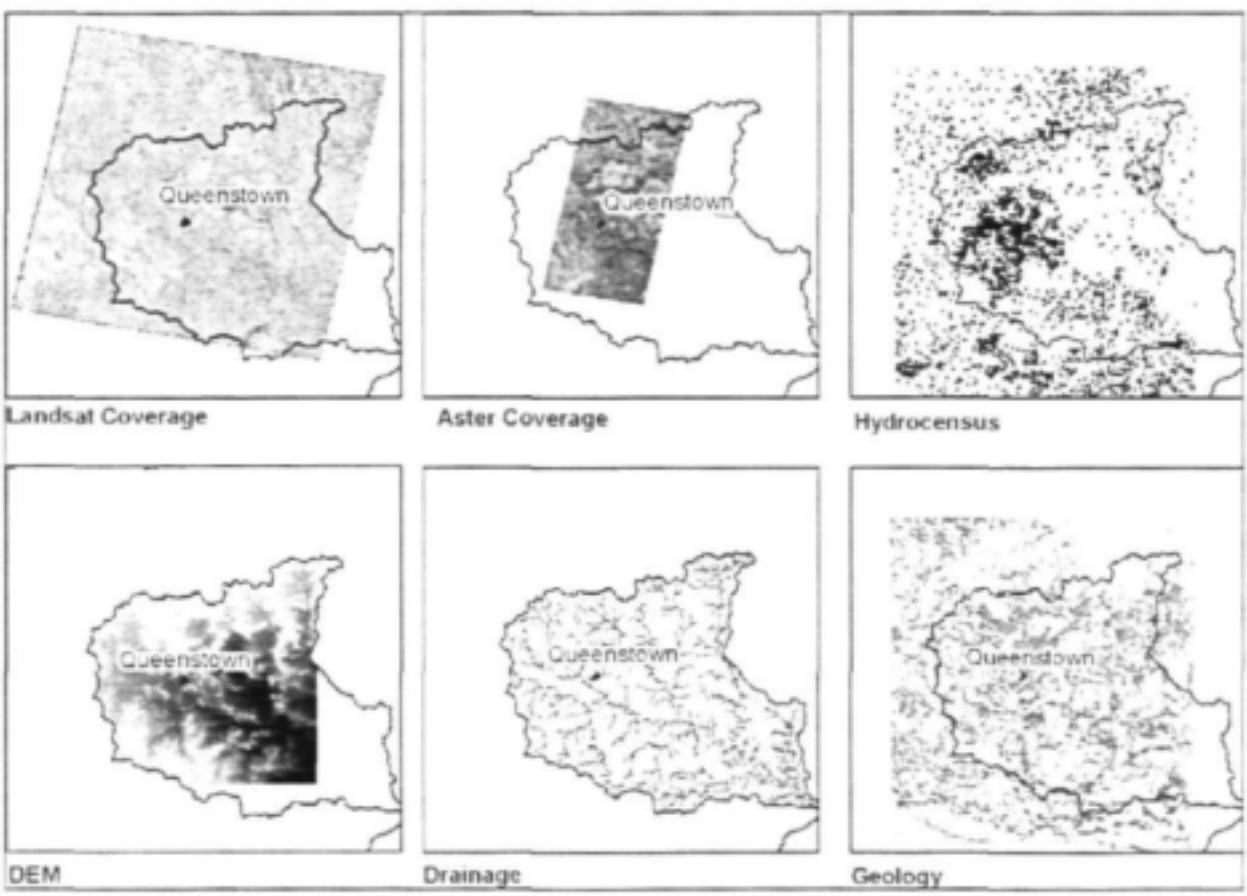

Figure 3: The extent of data coverage for the main datasets used in this research.

Table 1: Data obtained for the research project

DATASET	EXTENT	SOURCE	FORMAT	SCALE
Geological Data				
Dolerite Sills	Study Area	(CGS)	ArcView® shape file	1 : 50 000
Geology	Map sheets 3126 & 3226	CGS	ArcView® shape file	1 : 250 000
Lineaments	Study Area	CGS	ArcView® shape file	1 : 50 000
Dolerite Dykes	Study Area	CGS	ArcView® shape file	1 : 50 000
Borehole logs	Drill site	DWAF and CGS	Report	
Geophysical Data				
TDEM	Drill site	Terra Sounding	Report	
Magnetic fabric	Map sheets 3126 & 3226	CGS	GeoTiff	1 : 250 000
Climate Data				
All climate data	South Africa	CCWR	ArcInfo® grid	Pixel resolution = 0.016667 Decimal Degrees
Hydrogeological data				
Bore holes	Map sheets 3126 & 3226	DWAF	Spread sheet	
Springs	Map sheets 3126 & 3226	DWAF Agriculture RSS	Maps Spread sheets	1 : 50 000
Hydrological Data				
Rivers (stream-ordered)	Catchment S	DWAF	ArcView® shape file	1 : 50 000
Catchment delineation	Catchment S	DWAF	ArcView® shape file	1 : 50 000
Topographical Data				
Contours and Spot heights	Most of Catchment S	Chief Directorate: Surveys and Mapping	ArcView® shape file	1 : 50 000
Digital elevation model	Most of Catchment S	CGS from Contour and Spot height data	ArcInfo® grid	Pixel resolution = 50 metres
Satellite Imagery				
Landsat 7 ETM+	See Figure 3	Satellite Application Centre (SAC)	GeoTiff	Pixel resolution = 15m, 30m & 60m
Landsat 5 TM	See Figure 3	SAC	GeoTiff	Pixel resolution = 30m & 60m
Aster	See Figure 3	Internet		Pixel resolution = 15m, 30m & 90m
Botanical Data				
Acock's Veld Types	South Africa		ArcView® shape file	1 : 1 000 000
Mucina & Rutherford's preliminary vegetation map	South Africa	National Botanical Institute	ArcView® shape file	

2. GENERAL DESCRIPTION OF GREAT KEI CATCHMENT

2.1 PHYSIOGRAPHY AND CLIMATE

The Great Kei River catchment is made up of the Great Kei River and its tributaries. Within the catchment the terrain varies, with elevation increasing from sea level at the coast to almost 2500m in the far north. In the northern parts of the catchment, the topography is greatly influenced by the dolerite rings which result in circular shaped upland regions giving rise to the local highs in elevation. The catchment includes areas of the former Transkei and Ciskei as well as the towns of Queenstown, Stutterheim, Cathcart and Lady Frere. The catchment is bounded by The Winterberg, The Bamboesberg, The Stormberg and The Amatole Mountains. The Mount Arthur Range is situated within the catchment to the north east of Queenstown (**Figure 4**).

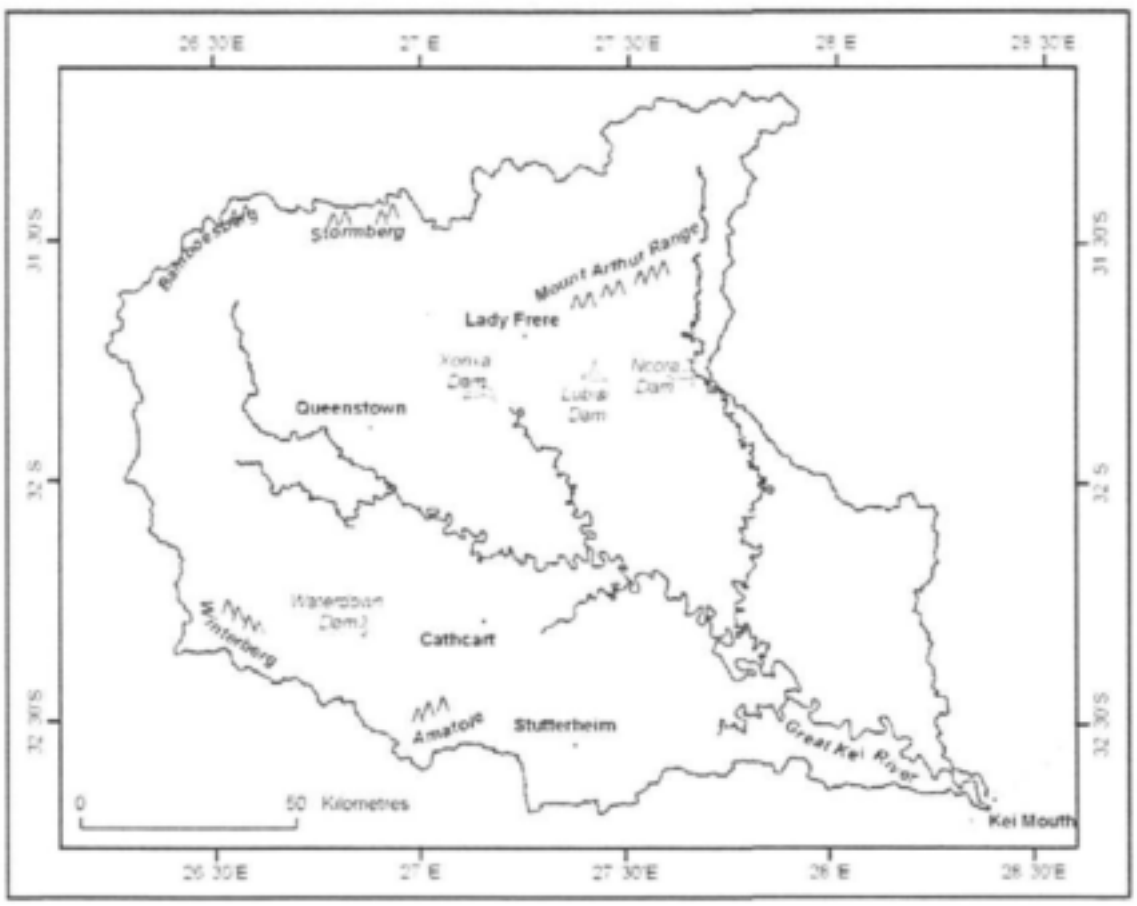

Figure 4: The major physiographic features and towns of the Great Kei River Catchment

At a catchment scale the drainage pattern can be described as dendritic however variations may occur at a local scale. The tributaries feed the Great Kei River which drains into the Indian Ocean at Kei Mouth. Three large dams are found in the catchment to the east of Queenstown; the Xonxa, the Lubisi and the Ncora Dams and to the south of Queenstown, near Whittlesea, is the Waterdown Dam.

The mean annual precipitation is in the region of 1000mm at the coast and in areas of great elevation. Elsewhere, mean annual precipitation is between 400 and 800mm (Schultz et al., 1997). The coastal regions receive rainfall throughout the year whereas the inland regions have a seasonal summer rainfall (Smart, 1998). The mean annual runoff interpreted from Midgely et al (1994) also differs from coast to inland; 50 - 200mm and 10 – 50mm respectively. Mean annual temperature, decreases with elevation ranging from 18° at the coast to 12° in the high-lying areas.

The soils of the catchment are varied in depth, texture and relief. Two thirds of the catchment consists of moderate to deep sandy loam soils on flat relief. Moderate to deep clayey loam soils are found on the undulating coastal terrain in the extreme south and on the steep slopes in the North East. Around the Great Kei River itself, moderate to deep sandy loam soils occur on the steep relief. (Smart, 1998)

2.2 GEOLOGY

The Great Kei catchment covers part of the Karoo Basin underlain by the continental sediments of the Permo-triassic Beaufort Group, and the Triasso- Jurassic Molteno and Elliot Formations (**Figure 5**). The Cape Fold Belt tectonics in that part of the basin was very mild, characterised by gentle folding with a centripetal dip towards Lesotho, resulting for the study area in a shallow, less than 5°, northwards dipping of the strata. These deposits were subsequently intruded by the Karoo dolerites during a period of extensive magmatic activity that took place over the Southern African continent during the Mid-Jurassic Gondwanaland break-up.

2.2.1 The Karoo Supergroup

The sediments correspond to the progressive infilling, shrinking and concomitant shallowing of the Basin, with subaerial depositional environments (fluvio-lacustrine) characterised by mudstone, siltstone and sandstone (Cole, 1992; Smith et. al, 1993; Johnson et al., 1997; Catuneanu et al., 1998).

The Permian (~260 Ma) Adelaide Subgroup occupies the lower part of the catchment. It consists of bluish-grey mudrock with alternating grey, fine to medium-grained sandstone that generally constitutes 20–30% of the total thickness, sometimes as little as 10%. Individual sandstone units average 6m in thicknesses but can reach several tens of meters locally. The mudstone represents deposition in a flood plain and lacustrine environment whereas the sandstone units formed by the lateral migration of meandering rivers.

The early Triassic (~240 Ma) Tarkastad Subgroup occupies the middle and larger part of the catchment. It is characterized by a greater abundance of red mudstone and sandstone. In the Great Kei catchment the Subgroup comprises a lower, sandstone-rich Katberg Formation and an upper, mudstone-rich Burgersdorp Formation. In the Katberg Formation the sandstone – mudstone ratio decreases steadily from 90% in the South to 30 % in the North when it becomes indistinguishable from the overlying Burgersdorp Formation.

Our study area (the Qoqodala ring system) lies within the Burgersdorp Formation which is approximately 700 m thick in the Queenstown area (Groenewald, 1996; Hancox, 1998). The Middle part of the Burgersdorp Formation is well exposed in Nonesi's Nek road section, North East of Queenstown, just outside the Bonkolo Ring (**Figure 6**). The section is dominated by red to purple mudstone with localised thin sandstone channels. Halfway up the section a prominent laterally extensive sandstone horizon occurs. It is some 10 -15 m thick and composed of stacked bar elements.

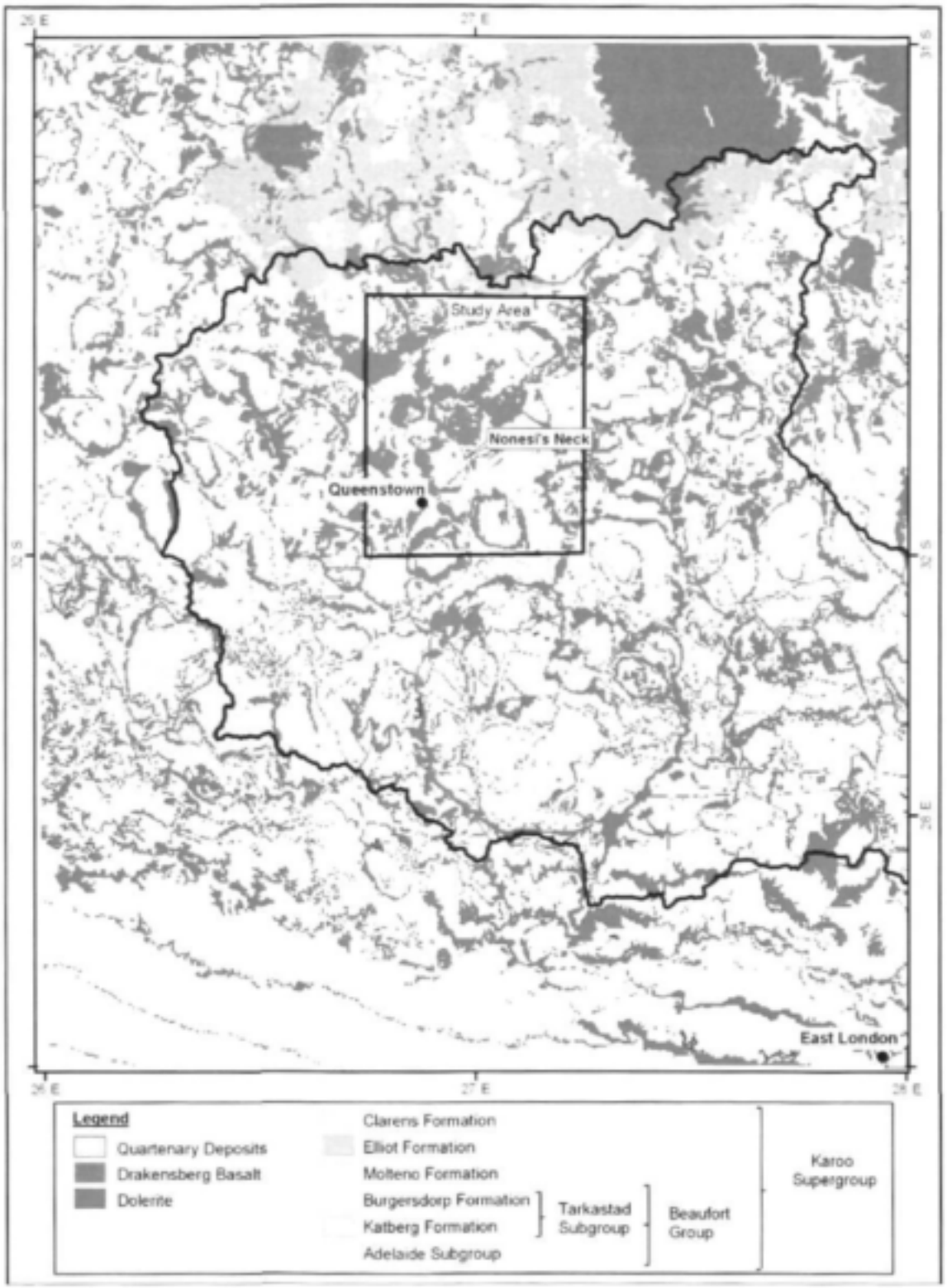

Figure 5: General geology of the Great Kei catchment. Extensive flat dolerite sills are intruded in the Adelaïde Subgroup whereas dolerite ring and sill complexes are developed in the Tarkastad Subgroup.

The late Triassic Molteno Formation (~220 Ma) and Early Jurassic Elliot Formations (~195 Ma) underlie the northern part of the catchment area where they attain a total thickness of about 800 m. The Molteno formation comprises alternating pale, medium- to coarse-grained sandstone (30 to 75 %), and pale olive mudstone. The Elliot Formation is composed predominately of greyish-red mudstone, with subordinate fine to medium-grained sandstone (30 %), generally occurring as fining-upward cycles.

2.2.2 The Karoo dolerites

The Karoo dolerite represents the roots and the feeders of the extrusive Drakensberg basalts dated around 180 Ma (Duncan et al., 1997). They consist of an interconnected network of dykes and sills that probably acted as a shallow stock work-like reservoir (Chevallier & Woodford, 1999).

Dyke intrusions show four major trends in the catchment area: NW, E-W, NNE and NE. These four directions are also commonly found in the Western Karoo (Woodford & Chevallier, 2002a,b). The E-W direction is prominent in the southern part of the catchment where it forms a swarm of long and thick dykes (up to 300m). Their trend varies along their trajectory, becoming curvi-linear and feeding into the NW trending intrusions. It has been suggested that these long regional dykes might have propagated laterally along strike (and not vertically) from a magma source located further East (Woodford & Chevallier, 2002a).

The dolerite sills and rings are by far the most common tectonic style controlling the geomorphology of the landscape and the shape of the Great Kei catchment to a large extent. Du Toit (1905, 1920) was the first researcher to describe these structures in the vicinity of Queenstown. He also pointed out the existence of preferential horizons of intrusion inside the Karoo basin, such as lithological boundaries within the Beaufort Group. It seems to be true for the Great Kei catchment area where:

- Extensive flat lying sills are intruded inside the Adelaide Subgroup (sills between King William's Town and Stutterheim)

- Large size dolerite sill/ring complexes are intruded in the Katberg Formation (Cathcart ring)
- Smaller size dolerite rings are intruded in the Burgersdorp and Molteno Formations (The Qoqodala ring system)
- Very few dolerite rings are cutting through the Elliot Formation.

Dolerite sill and ring complexes display the typical sub-circular saucer-shape structure described by Chevallier et al. (2001) with a flat lying inner sill, an inclined sheet (the ring) and a flat lying outer sill (see **Figure 1**). They form coalescing or cross-cutting structural units. Each unit can in itself be composed of several sub-units of smaller size resulting in the so-called "*ring-within-ring*" patterns. Many feeder dykes can be seen branching onto the rings or cutting through them. Their mode of emplacement and the relations between dykes and rings are discussed in Chevallier et al. (2001).

A cross-section at the latitude just North of Queenstown shows the complex interference between the different rings (**Figure 6**).

The cross section shows that dolerite sill and ring complexes are characterized by a "box-type" intrusive pattern. Several sills are intruded at the small elevation, i.e. an inner sill of a specific ring system becomes the outer sill of another system, or outer sills of two ring systems can merge into one. Ring systems therefore do not represent a series of basins and domes, nor do they result from the propagation of undulating sills as suggested by Du Toit (1905) in the early days (model still referred to by some authors). In fact they are flat lying sills connected together with inclined sheets similar to the second model proposed by Du Toit (1920).

The figure does not show the dolerite intrusions below the layer of sills and ring complexes, but according to the regional stratigraphy very large size sill/ring complexes and extensive flat lying sills should be present.

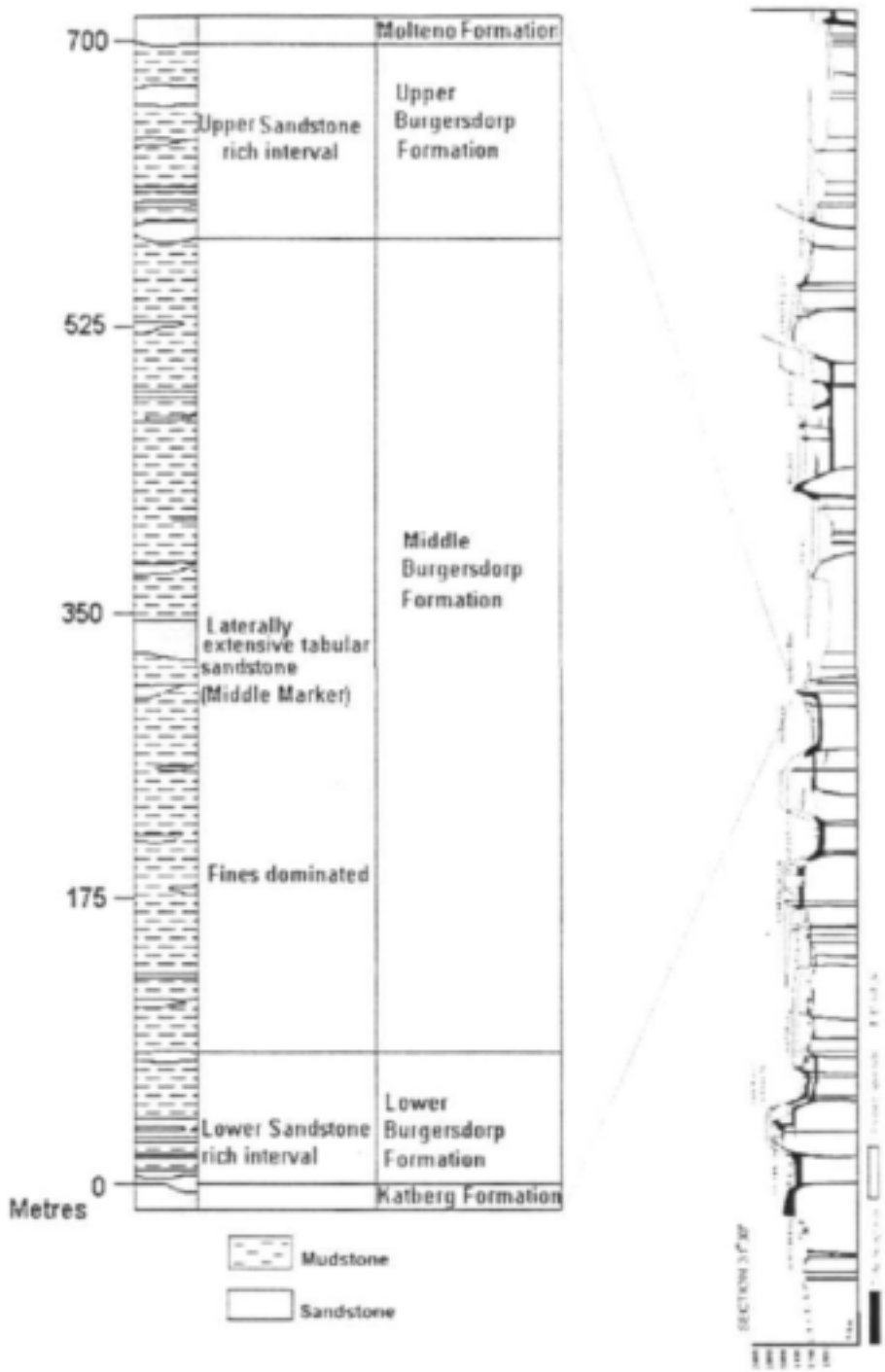

Figure 6: The composite lithostratigraphic section of the Burgersdorp Formation based on Nonesi's Neck exposures (From Hancox, 1998). It is illustrated within the regional context by an E-W cross section at the latitude of Queenstown showing the complex relations between the dolerite sills and rings intruded inside the Burgerdorp Formation. The elevation of many of the inner sills has been estimated. The geology below the layer of sill and ring complexes is not shown.

2.3 REGIONAL HYDROGEOLOGY

2.3.1 Borehole hydrocensus

The Great Kei River forms the boundary between former South Africa and former Transkei homeland. The distribution of boreholes (DWAF's NGDB) clearly shows the difference between the developed commercial farmlands to the south west of the Great Kei River and the communal grazing grounds to the north-east (**Figure 7**). Water supply in the former homeland is done via spring development and few shallow and low yielding boreholes.

Due to its virtual absence of primary porosity and permeability, the sediment of the Beaufort Group is very seldom targeted for groundwater (Woodford & Chevallier, 2002.b). However, shallow boreholes sunk in the weathered zone (20 to 30m deep) can sometime be sufficient for windpump supply between 0.5 and 1.0 l/s (Vandoolaeghe, 1979, 1980,b).

The water yielding capacity of the Karoo sediments can be largely improved by fracturing, especially close to dolerite dykes. On the Queenstown map sheet Vandoolaeghe (1980a) and Smart (1998) show that boreholes targeting dolerite dykes are more successful than boreholes not - targeting dykes, especially in the medium-range yields between 4 and 7 l/s. An exhaustive hydrogeological investigation of the Karoo dolerite dykes was carried out by Woodford & Chevallier (2002.a,b). With the exception of the big valleys, they have always been, and still are, the preferred drilling targets for groundwater in the Karoo. Dyke contact aquifers are confined and yields around 2 to 3 l/s.

Very few boreholes target the water-yielding portions of the dolerite rings (Chevallier et al., 2001). Those boreholes sited within the vicinity of these intrusives are not drilled deep enough to adequately test their water-bearing potential. Vandoolaeghe (1980a) investigated the Lehman's Drift inclined sheet west of Queenstown. He concluded that "exploration of these aquifers is not straightforward, even in the best cases" and that they do not stand out for their prolificacy, a blow yield of 10 l/s is considered to be good but 4 l/s is closer to average.

Figure 7: Map of the dolerite dykes, rings and sills of the catchment area also showing the distribution of borehole and spring occurrences.

Primary intergranular aquifers in modern alluvial deposits are far inferior to the fractured-dolerite aquifers and do not form an important part of the groundwater town supply. Alluvial deposits with a substantial shallow aquifer are developed in the Zwart Kei River subcatchment west of Queenstown (Vandoolaeghe, 1980a, b). The only alluvial deposit of geohydrological significance occurs in the Lehmansdrift area along the Klaas Smits River, where it is used for irrigation purpose. The mean saturated thickness of the fine grain alluvial aquifer is 8 m. Good yields are exceptional, but can locally reach 5.5 l/s. Its dimensions are limited and it makes better storage reservoir ($1.5\ 10^6\ m^3$) than a production field. The piezometric depression at Hopefield is caused by heavy abstraction from wells tapping the unconfined alluvial aquifer. The water quality of the alluvial aquifer is reported as below average. (Vandoolaeghe, 1980a).

2.3.2 Springs

A spring database was built for the Great Kei catchment using:

- The NGDB
- Hydrocensus carried out by DWAF during the compilation of the Queenstown hydrogeological map (Smart, person. Com.)
- Hydrocensus carried out by DWAF in parts of the study area in 2001
- Hydrocensus carried out by Department of Agriculture in parts of the Chris Hani District in 2002, specifically for the project
- Hydrocensus carried out by Rural Support Services (1994) in Qoqodala

The database is still patchy and incomplete and a proper statistical analysis could not be performed. However it appears that the large majority of springs are linked to dolerite rings (**Figure 7**). All the spring water of the catchment is derived from meteoric water circulating at depths along secondary aquifers such as fractures and faults in the same manner as most of the springs in the Karoo basin (Kent, 1972). Kok (1992) supported this meteoric origin by finding a linear relationship ($r = 0.977$) between average annual rainfall and recharge of a number of Karoo springs. He estimated that in areas with more than 100mm rainfall (such as our study area), recharge to the springs could be, on average, about 8% of the rainfall for that area.

Springs can emerge at different places along the dolerite ring (**Figure 8**).

- Perennial springs can be found at high altitude at the top of the ring or the outer sill. This is the case for the Amatola range that forms the southern boundary of the Cathcart dolerite ring where several spring eyes have been mapped. According to SAFCOL plantation and the local farmers the spring is perennial and feeds the Toise River. This type of spring implies a perched water table, wetlands and marshy areas in very fractured dolerite that acts as a sponge. These springs need to be constantly recharged by rain, dew or mist.

- The majority of springs occur on the lower slope and on the inner side of the ring. They result from water following shallow dipping cracks and more specifically fractures parallel to the walls of the intrusion. In our study area, local communities depend largely or entirely on these springs for their water supply. A stream an also be fed by several of these springs.

- The third type of spring occurs below the outer sill, in the sediment. They result from water seeping through the vertical cooling cracks of the sill, through the sediment and emerging at a more impermeable sedimentary layer.

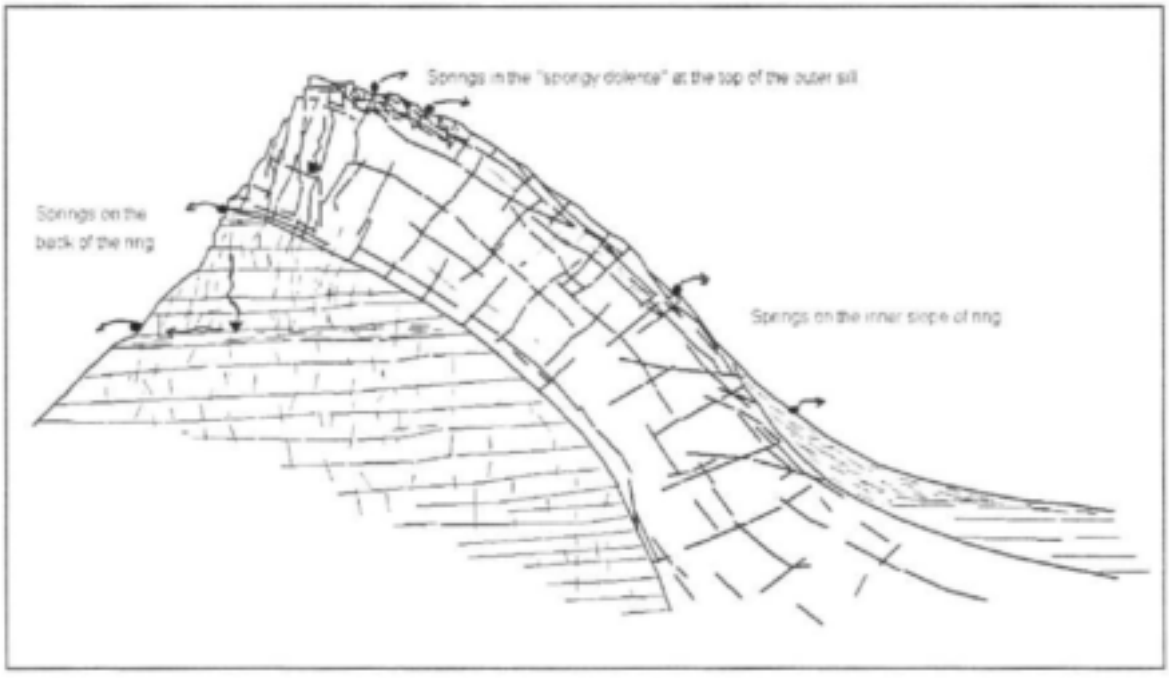

Figure 8: The different types of spring occurrences associated with dolerite sill and ring complexes in the Great Kei Catchment.

2.3.3 Water quality

DWAF's national groundwater hydrochemical database does not contain any information for the study area, although a number of records are available for the Queenstown district to the south. DWAF's 1:500,000 scale hydrogeological 3126 mapsheet (Smart, 1998) confirms the above, and indicates that the electrical conductivity (EC) of the groundwater is typically less than 70 mS/m, although it may be as high as 300 mS/m locally.

The exploration boreholes drilled on the dolerite ring system at Qoqodala would confirm the mapping carried out by Smart, where the electrical conductivity measured during the pump-testing of boreholes BH-1, BH-7 and BH-1 varies between 39 and 55 mS/m.

2.4 VEGETATION

The Great Kei Catchment is situated within a zone of transition and it is a meeting place of many different vegetation types. The floristic components of this area include components of forest families; Cape flora and karoo and karroid types of vegetation. Vegetation types such as high forest, macchia, thorn savannah, grassland, karroid scrub and succulent karoo are often found adjacent to one another (Batten and Bokelmann, 1966). Acocks (1988) described this area as a mixture of grassveld, sourveld, bushveld, false thornveld and scrub. Acocks' veld map (**Figure 9**) illustrates the various veld types present within the Great Kei River catchment.

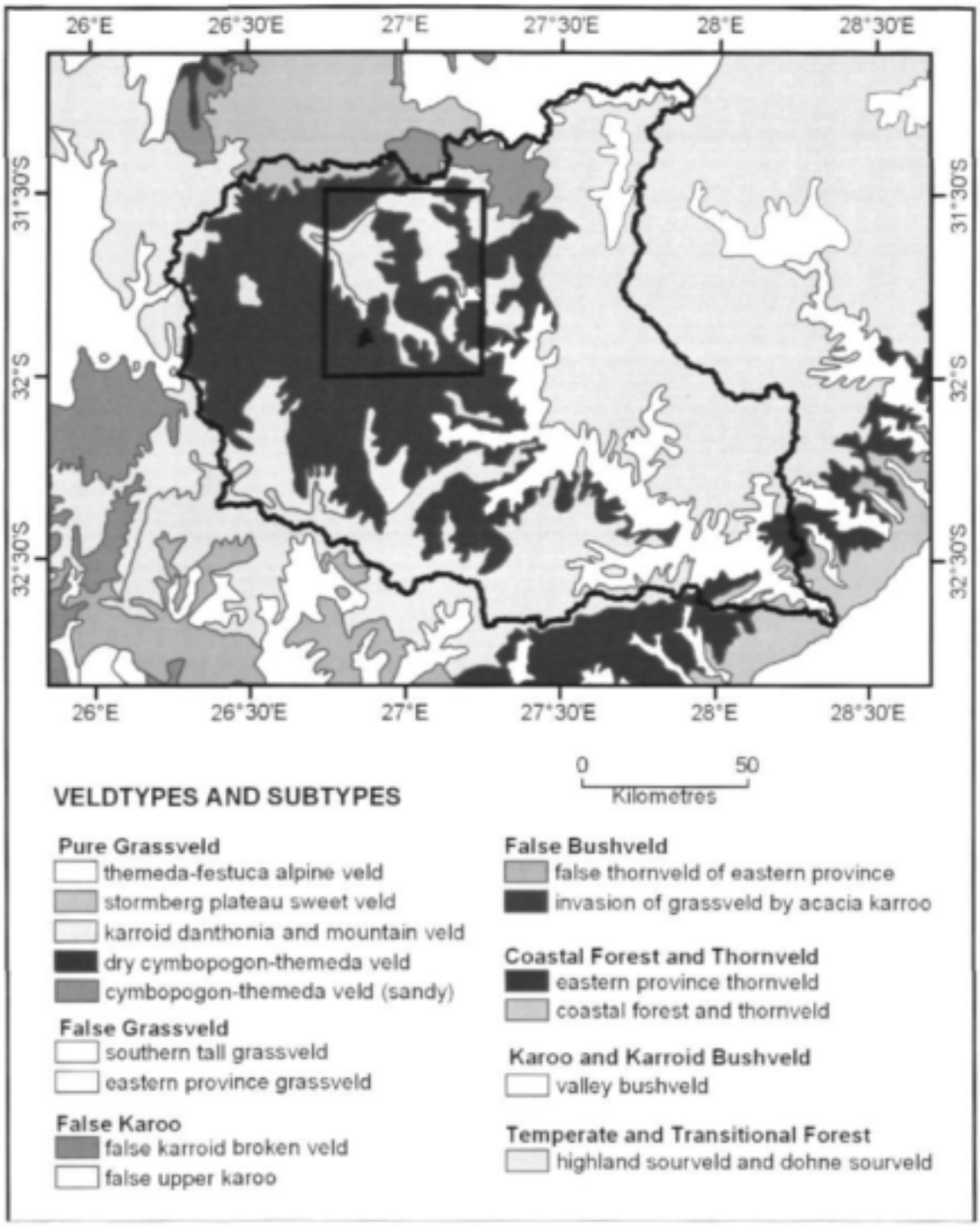

Figure 9: The veldtypes and veld subtypes present within the Great Kei River Catchment as mapped by Acocks.

2.5 DEFINITION OF THE STUDY AREA

The study area straddles the former boundary between South Africa and Transkei and covers four 1: 50 000 scale topocadastral maps (**Figure 10**): 3126DD Queenstown, 3126DB Vaalbank, 3127CC Bolotwa and 3127CA Lady Frere

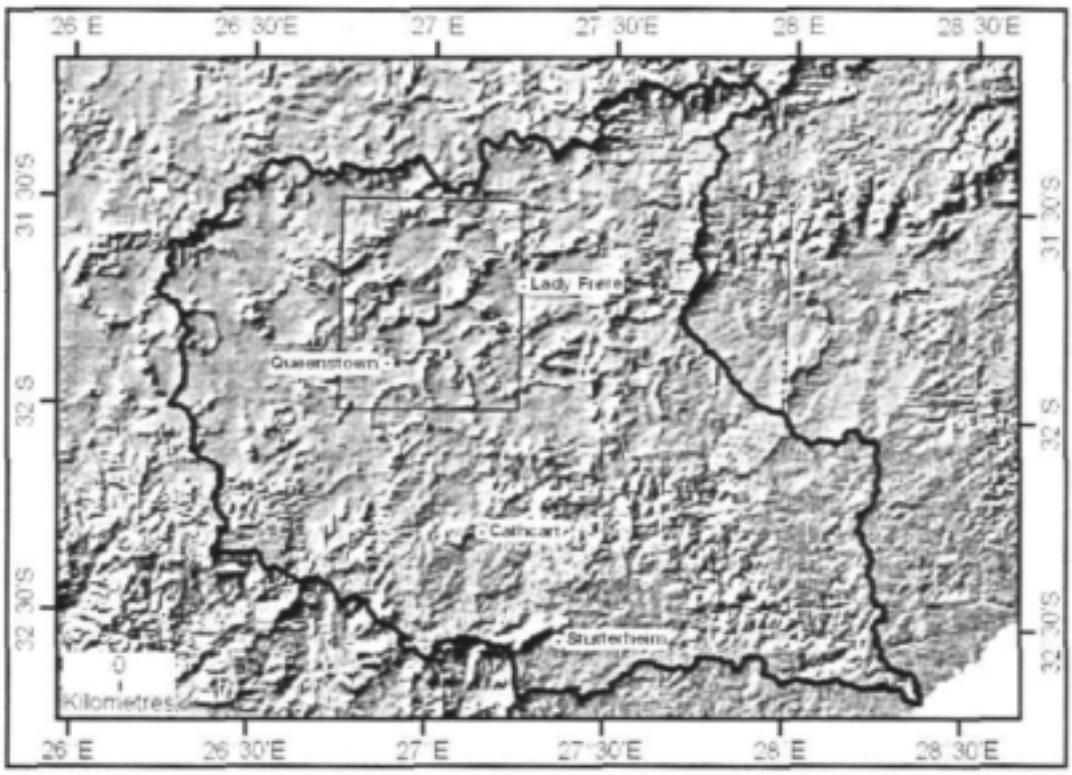

Figure 10: Regional DEM showing position of study area within the Great Kei Catchment

The study area was chosen for the following reasons:

- it includes a well developed system of rings: the Qoqodala Ring System
- the rugged topography covers a wide range in elevation
- the area is relatively dry compared to the southern part of the catchment
- it includes commercial farmlands and the communal lands of the former Transkei
- portions of the study area have been neglected in the past in terms of water supply
- springs and seepages are known to occur in the region
- different veld types occur in the study area making it of interest botanically.

3. ECO-GEOHYDROLOGY OF THE QOQODALA RING COMPLEX

3.1 INTRODUCTION

The study area (**Figure 11**) encompasses both the former Transkei and the former South Africa, and the human needs and land use patterns in these areas are very different.

In the former Transkei, subsistence farming and live stock grazing occurs on the tribal lands. Overgrazing has placed immense pressure on the land which has resulted in severe land degradation on the flat inner sill. Heavily eroded gullies are common place, and hardy shrubs, typical of the Karoo are found on the mountain slopes. Grasslands characterize mountaintops where grazing sometimes takes place.

The settlement pattern in the old South Africa constitutes urban settlement in a formal town (Queenstown), and rural settlement on evenly distributed commercial farms. In the former Transkei the settlement pattern is quite different, an urban setting in the form of Illinge Township, situated approximately five kilometres east of Queenstown. Settlement in the rural context is in the form of villages comprised of scattered dwellings located at the base of the mountain slopes.

The topography of the study area is greatly influenced by the dolerite rings which are circular shaped upland regions, giving rise to the local highs. The elevation in the area is from approximately 900m above sea-level in the Southeast, and increases steadily to approximately 2000m above sea-level in the North and the Northwest (at Mount Steep in Black Eagle Reserve).

Rainfall in the study area is influenced by orography, as a result the mountaintops are wetter than the flat inner sills. Irrigation of the commercial farmlands takes place in the 'old' South Africa and water used in urban areas is taken from surrounding dams as well as redistribution from other areas. The former Transkei relies on unpredictable rainfall, springs and ad hoc water supply schemes. Several boreholes have been drilled in this region however the boreholes have proven to be unsustainable.

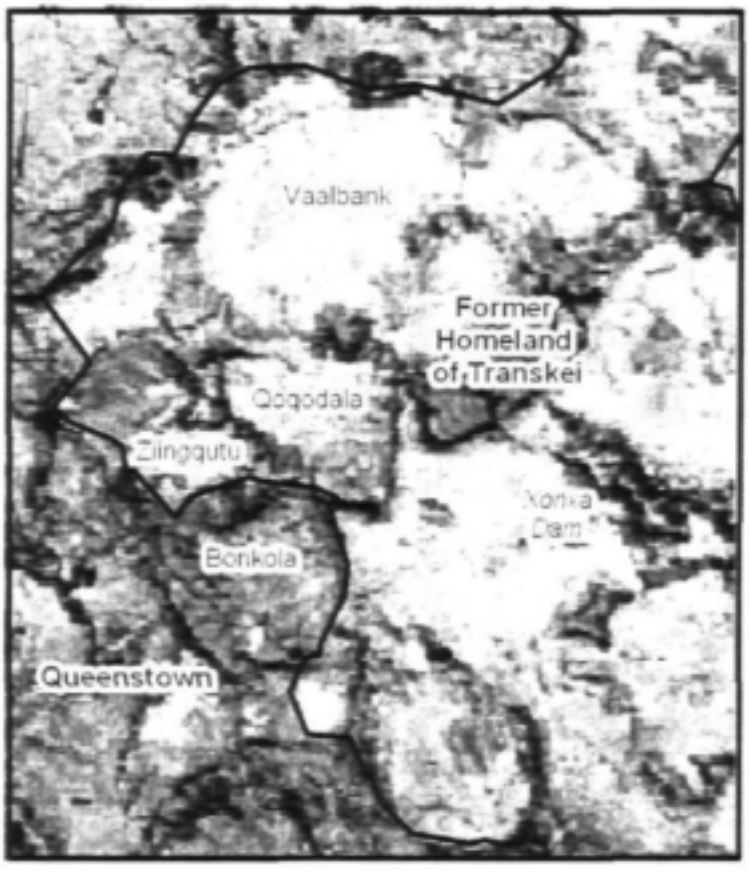

Figure 11: Satellite image of the study area showing the border between the former Transkei and South Africa

The mean annual precipitation for Queenstown is given as approximately 600mm (Schultz et al. 1997). The mean annual temperature is approximately 15° (Schultz et al. 1997), with temperatures ranging from below zero at night in the winter months to up to 40° during the day in the summer months. These extreme temperatures are also experienced in the former Transkei. Most winter mornings are characterized by frost, at worst there is an occasional snowfall.

Figure 12 shows the demographic statistics and levels of services provided across the study area (Statistics South Africa, 2001). A young population characterizes the study area as a whole. There are areas with an illiteracy rate of up to 25% and unemployment levels reach 80% in places. As implied by these figures, poverty is a severe problem in many parts of the study area.

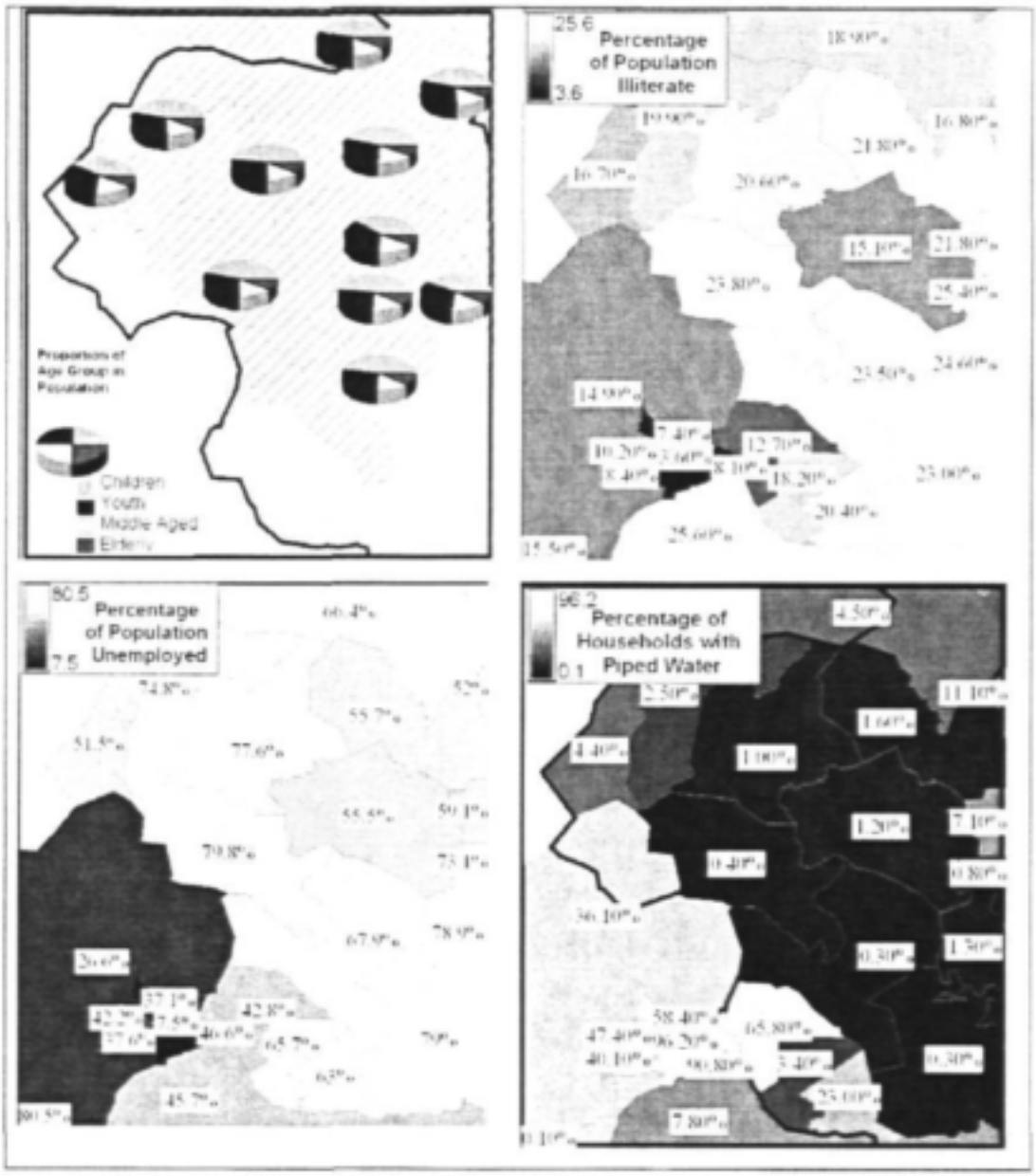

Figure 12: Demographic and level of services in the study area. (Children: All persons between 0 and 15 years old; Youth: All persons between 16 and 35 years old; Middle Age: All persons between 35 and 64 years old; & Elderly: All persons over 65 years)

Levels of service were politically biased in the past which is apparent by looking at the percentage of houses with piped water. In Queenstown, 96% of household are equipped with piped water whilst, barely 15kms north, only 0.4% of dwellings have piped water.

Similar trends are picked up on examining the statistics for sanitation and electricity: and hydrocensus data of the area also highlights these past inequalities. There is obviously a great need for services in the parts of the study area which included the former Transkei. With an adequate supply of water, it may be possible for more extensive cultivation to occur thus creating an opportunity for the local population to turn to farming as a source of employment and income.

3.2 MORPHOTECTONICS OF THE QOQODALA SILL/RING COMPLEX

The geology (dolerite sills, rings and dykes) of the study area was compiled from the existing CGS 1: 50 000 scale field maps and completed by air-photo and Landsat interpretation in conjunction with field work.

The Qoqodola sill and ring complex comprises several coalescing and overlapping saucer-shape dolerite rings, forming an interesting intrusive network which, according to our hydro-morpho-tectonic model of Figure 1 should be conducive to different fractured aquifers at various depths and the emergence of many springs (**Figure 13**).

The dykes have intruded along three major regional directions, i.e NW, NNE and NE, found all over the Great Kei catchment (see Figure 5). These dykes control the emplacement and the shape of the rings. The NW trend seems to be predominant, controlling for instance the alignment of the three Cokoyi, Bonkolo, Zingutu rings. The NE direction is materialized by an intrusive feature that runs across the study area from the south where it forms the straight and linear trace of the south west part of the Bonkolo ring to the north where the dyke outcrops inside the Vaalbank ring. At Nonesi's neck the dyke forms an inclined sheet dipping 78° to the West. The NE direction has controlled the emplacement of the northern part of the Vaalbank ring.

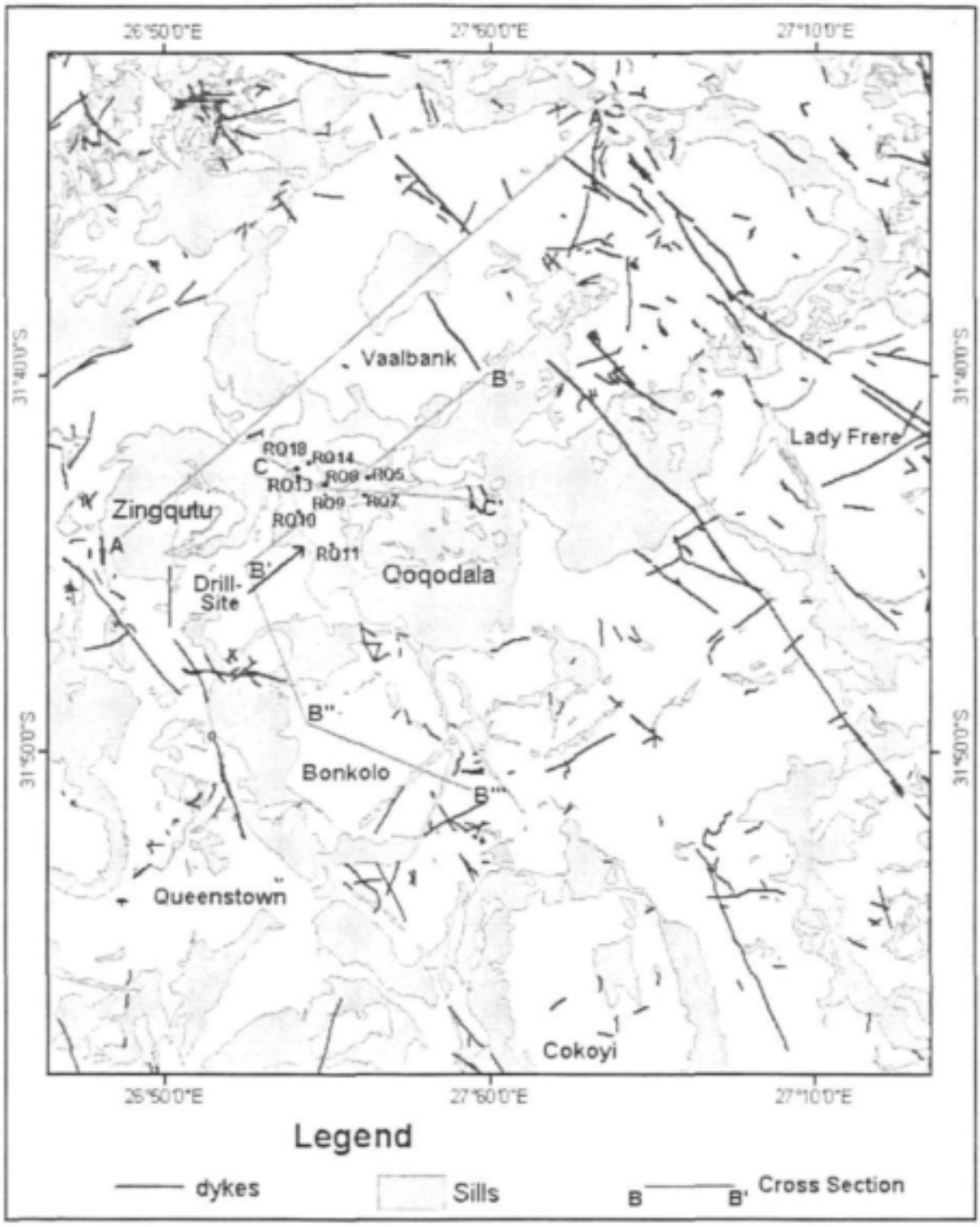

Figure 13: Geological map of the Qoqodala dolerite sill/ring complex. Note the tectonic control by the NW and NE trending dykes. RQ boreholes are from Rural Support Services (1994).

Three cross-sections were compiled from the existing 1: 50 000 scale field maps (**Figure 14**). These sections were further constrained by logs from boreholes drilled in the Qoqodala ring by Rural Support Services (1994) and logs from our exploration drilling site on the south-west rim of the Qoqodala ring. These sections show 5 levels of sill intrusions:

Between 900 and 1000 m (on section B-B‴). It forms the deep inner sill of the Qoqodala ring. Too deep to be intercepted by exploration drilling it was found using Time Domain Electro Magnetic method (see chapter on exploration drilling).

Between 1100 and 1150 m (on sections B-B‴). It forms the inner sill of Bonkolo ring and the lowest outer sill of Qoqodala, and was intercepted during exploration drilling. This outer sill probably forms the base of the Zingqutu inter-ring valley.

Between 1200 and 1300 m (all sections). It corresponds to a series of thin offshoots especially well developed in Qoqodala on section C-C" .

Between 1600 and 1650m (sections A-A' and B-B‴). It forms the inner sill of the Zingqutu ring and the high outer sills of Qoqodala.

Between 1800 and 1900 m (section A-A"). It forms the outer sill of Zingqutu ring, at Mpali Mountain.

A 50m Digital Elevation Model was built for part of the catchment area, from data supplied by Surveys and Mapping (see Chapter 1.4). In **Figure 15**, the 3D model shows that the different rings intersect each other or coalesce together and that the sills have been emplaced at different elevation. An analysis of the elevation of the outcropping dolerite was done at two scales: first at catchment scale and secondly at the scale of the study area.

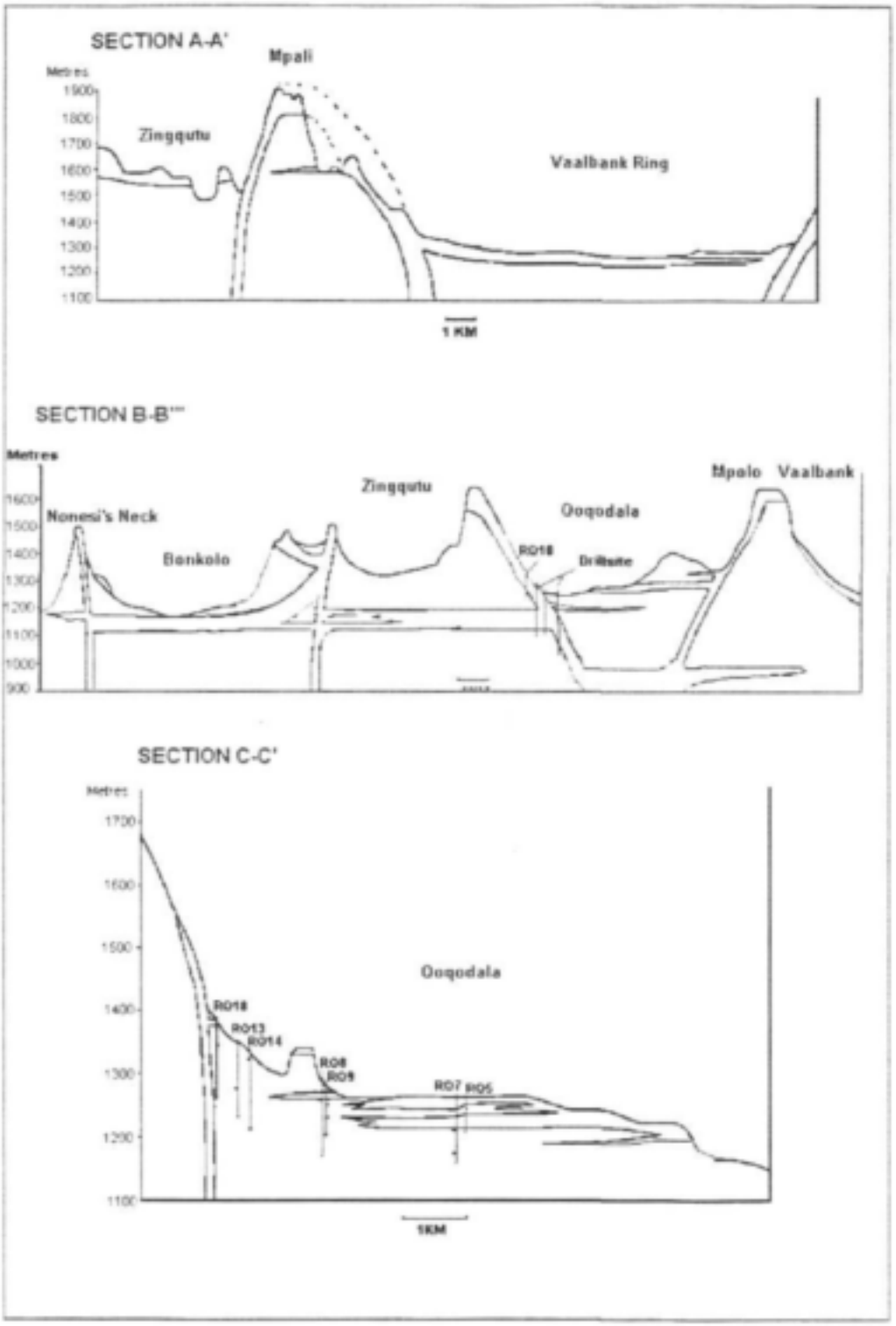

Figure 14: Cross-sections of the Qoqodala dolerite sill/ring complex. For location of the cross section and the boreholes, see Figure 13.

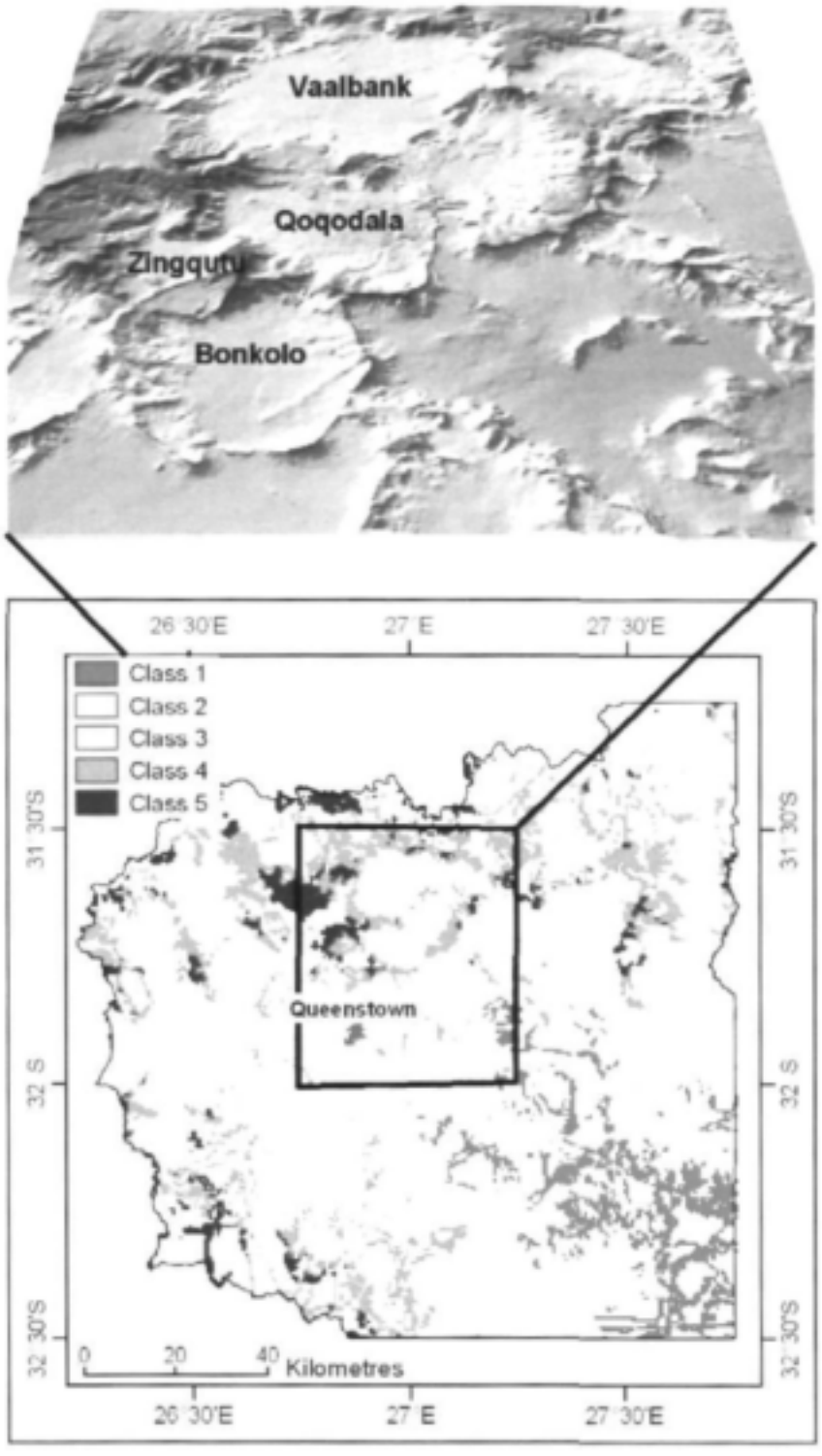

Figure 15: Classification of dolerite elevation for the catchment and hill shade DEM with perspective view of the study area.

The manner in dolerite elevation classes were created at catchment scale was to extract the dolerite from the 1: 250 000 geology shapefile. The dolerite was then converted to a raster dataset with a resolution of 50m which matched the resolution of the digital elevation model (DEM). The dolerite had a pixel value of 1 and non dolerite pixels had a null value. The DEM was then multiplied by the raster dolerite dataset to create a dataset whereby every outcrop of dolerite had a height value attached to it. The height values were then classified into five classes based on the natural breaks classification method. The height intervals of the five dolerite elevation classes are given in **Table 2**.

Table 2: The elevation range of each dolerite elevation class

Dolerite Elevation Class	Elevation (metres)
Class 1	340 - 942
Class 2	943 - 1181
Class 3	1182 - 1389
Class 4	1390 - 1628
Class 5	1629 - 3000

A few correlations between sill levels of the geological cross sections and dolerite elevation class can be made:

- The lower inner sill at 900m at Qoqodala corresponds to the lower intrusions of Class 1 at the south-east corner of the catchment.
- The series of outer sills and offshoot between 1100 and 13000 m correspond to Class 2 and 3. That is mainly the elevation range within which the inclined sheets are intruded. They occur in the middle part of the catchment.
- The series of outer sills between 1600 and 1900 m correspond to Class 4 and 5. As expected they occur on the side of the catchment in the water shed areas (Amatole range in the south west and highlands in the north).

The study of the elevation of the dolerite was then taken to the study area by combining the DEM in the manner mentioned above, with the dolerite digitized at a scale of 1:50 000. The class intervals noted above were then applied to the study area to create a map of the different classes of dolerite elevation. A slope analysis was carried out on the DEM and the proportion of each dolerite class occupying different slopes classes was studied and definite trends were highlighted. Slopes were divided into 5 categories based on the natural breaks in statistics (**Table 3**).

Table 3: Definitions of Slope Categories

Slope Category	Slope Angle
Category 1	slopes $\leq 8°$
Category 2	$8° <$ slopes $\leq 14°$
Category 3	$14° <$ slopes $\leq 20°$
Category 4	$20° <$ slopes $\leq 28°$
Category 5	slopes $> 28°$

The results of the slope analysis reflect the morphology of the dolerite ring (**Figure 16**):

Contact Zone: Steep slopes at the foot of cliffs

Class 1: Flat slopes transition to flat sill

Class 2 – 4: The inclined sheet

Class 5: Outer sill

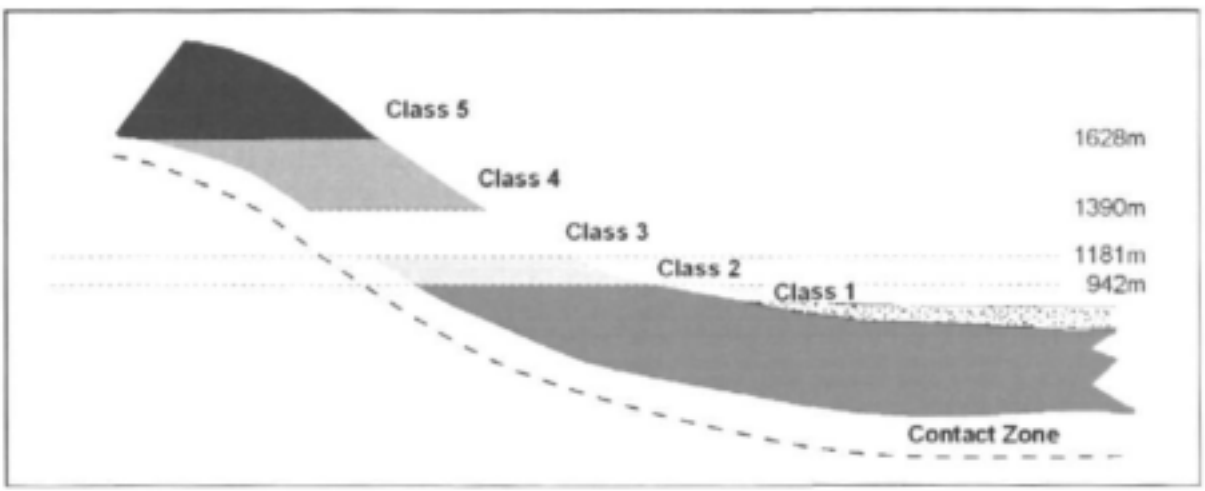

Figure 16: Elevation class morphology of the ring structure as highlighted by elevation and slope analysis.

The results of each category of slope found in each of the dolerite classes are shown in the graphs in **Figure 17**

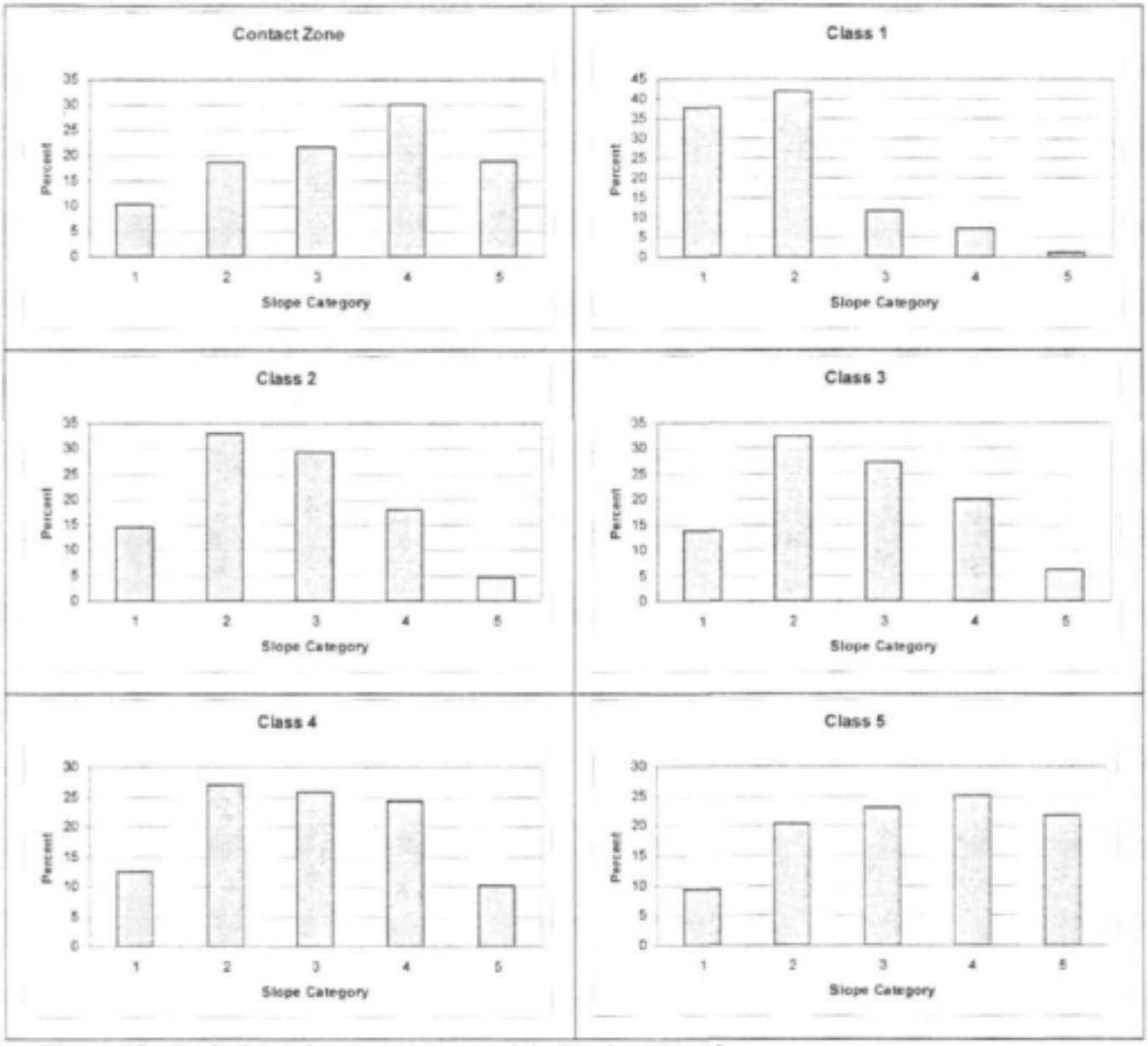

Figure 17: Analysis of slope category per dolerite elevation class

3.3 LINEAMENT MAPPING

Lineaments were digitized onscreen from Landsat ETM+ multispectral band combination and panchromatic band. The lineaments were mapped at two scales, firstly at a scale of 1: 40 000 and secondly, at a scale of 1: 100 000. The two scales were used in order to pick up both large and micro lineaments. The resultant satellite lineaments coverage is shown in **Figure 18**.

The dolerite rings are heavily fractured, whereas inner sills and outer sills are less fractured. NW and NE directions dominate the structural fabric, forming a very dense network of fractures at right angles. These trends also correspond to the main direction of dyke intrusion. The SW side of the Qoqodala ring, where the exploration site is located, appears to be the most fractured. This could have implications in term of secondary porosity and recharge potential. This part of the ring also lies on a NW trending structural feature that is running along the NE side of the Cokoyi, Bonkolo and Zingqutu rings. Such a feature could be linked to a prominent NW trending feeder dyke at depth as suggested in our hydro-morpho-tectonic model shown in Figure 1. Woodford & Chevallier (2002) have shown that NW trending major lineaments and fracture density play a very important role in the occurrence and yield of dolerite related fractured aquifers.

Figure 18: Lineament map of the Qoqodala sill/ring complex. The exploration site is located over a prominent NW fracture zone possibly corresponding to a regional feeder dyke at depth.

3.4 BOREHOLE INFORMATION

The study area falls within the 1.5 – 2.0 l/s borehole yield range on DWAF's regional hydrogeological map (3126), and greater than 15% or boreholes drilled are likely to fall within the 3.0 – 10.0 l/s range (Smart, 1998).

DWAF's National Groundwater Database (NGDB) contains information for 84 waterpoints in the study area (**Table 4**), although quite a large number occur in the Queenstown area further to the south. Very little information is attached to each record and most of the waterpoints (55) are located in groundwater management unit S31F-b (the Bonkolo Basin). Groundwater management units S31F-a, S31F-c, S10D-b and S10D-c contain 2, 6, 16 and 4 waterpoints, respectively. The average depth of 70 boreholes is 62 m (standard deviation of 26, maximum depth of 120m) and the median depth is 55m. Information for 35 'wet' boreholes indicates an average yield of 7.4 l/s (standard deviation of 6) and a median yield of 7.0 l/s. This is well above the yield range anticipated by Smart (1988) and is generally high for such Karoo fractured-rock aquifers. The 'wet' borehole yield variations per lithological unit are summarized in **Table 4.** The highest borehole yields appear to be obtained in boreholes drilled where Quaternary alluvium outcrops, although borehole drill depths indicate that these wells penetrated the bedrock below. Thick coarse-grained alluvial aquifers are not common in the area and it is more probable that it is the structural-geomorphological setting (lowest point in catchment, shallow watertable, structurally controlled drainage system etc.) of these deposits that exerts a control on the yields records.

Table 4: DWAF NGDB Yield Statistics per Lithological Unit

Lithological Unit	Number Records	Yield (L/s)				
		Min	Max	Average	Standard Deviation	Median
Quaternary Alluvium	8	7.6	15.1	11.0	2.3	10.1
Karoo Dolerite	10	0.2	10.1	5.0	3.5	4.2
Burgersdorp Formation	17	0.5	29.0	7.0	7.6	4.4
Note: No information for the Molteno Formation						

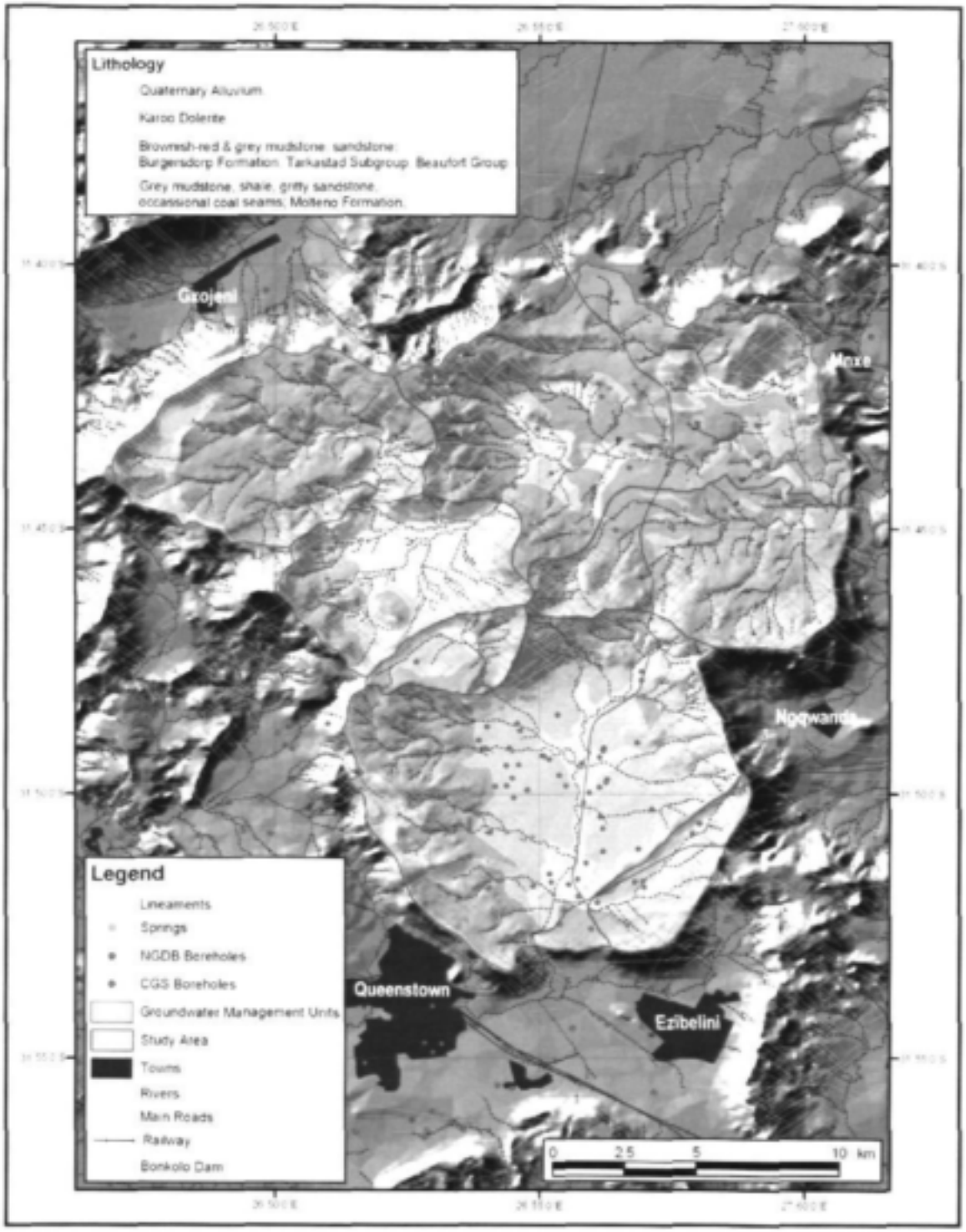

Figure 19: Location of boreholes and springs in the study area, overlain with lithology and remote sensing lineaments

3.5 EXPLORATION DRILLING

Project WRC 37 has shown that the inclined sheet and the bottom of the inner sill are the most rewarding target for groundwater exploration in term of strikes and yields (see hydro-morphotectonic model of Figure 1). With our model in mind the best site for drilling the inclined sheet was the southwest portion of the Qoqodala ring (along the road from Qoqodala to Zingqutu (**Figure 20**). The Department of Water Affairs and Forestry (DWAF) drilled a total of 12 exploration percussion rotary boreholes from March 2002 to June 2003 and a total drilling depth of 2655m was attained. The elevation and position of the boreholes, river and two springs were surveyed by DWAF (PE).

3.5.1 Drilling results

Borehole 1 was sited behind the inclined sheet. Two monitoring boreholes 1A and 1B were drilling 46m and 57m away respectively.

Boreholes 2 and 3 were drilled in a palaeo-terrace where terrain was unstable, and drilling was stopped at shallow depth. Of the two, borehole 2 is the deepest and was used for logging and monitoring.

Boreholes 4 and 5 were drilled on each side of the road and a wetland characterised by a seep covered by grass, with peaty collapsing soil, situated 4 m above the river. The wetland is on a fault.

Borehole 6 was not drilled for access reason.

Boreholes 7 and 8 were also on each end of a similar grass patch with peat soil but no sign of seep.

Boreholes 9 and 11 were drilled north of the road in the flat area. They were supposed to intercept the inner sill, unfortunately the latter appears at greater depth than expected.

Borehole 10 and 10A were drilled, south of the road, next to each other (10 m) in order to intercept the change from inner sill to inclined sheet.

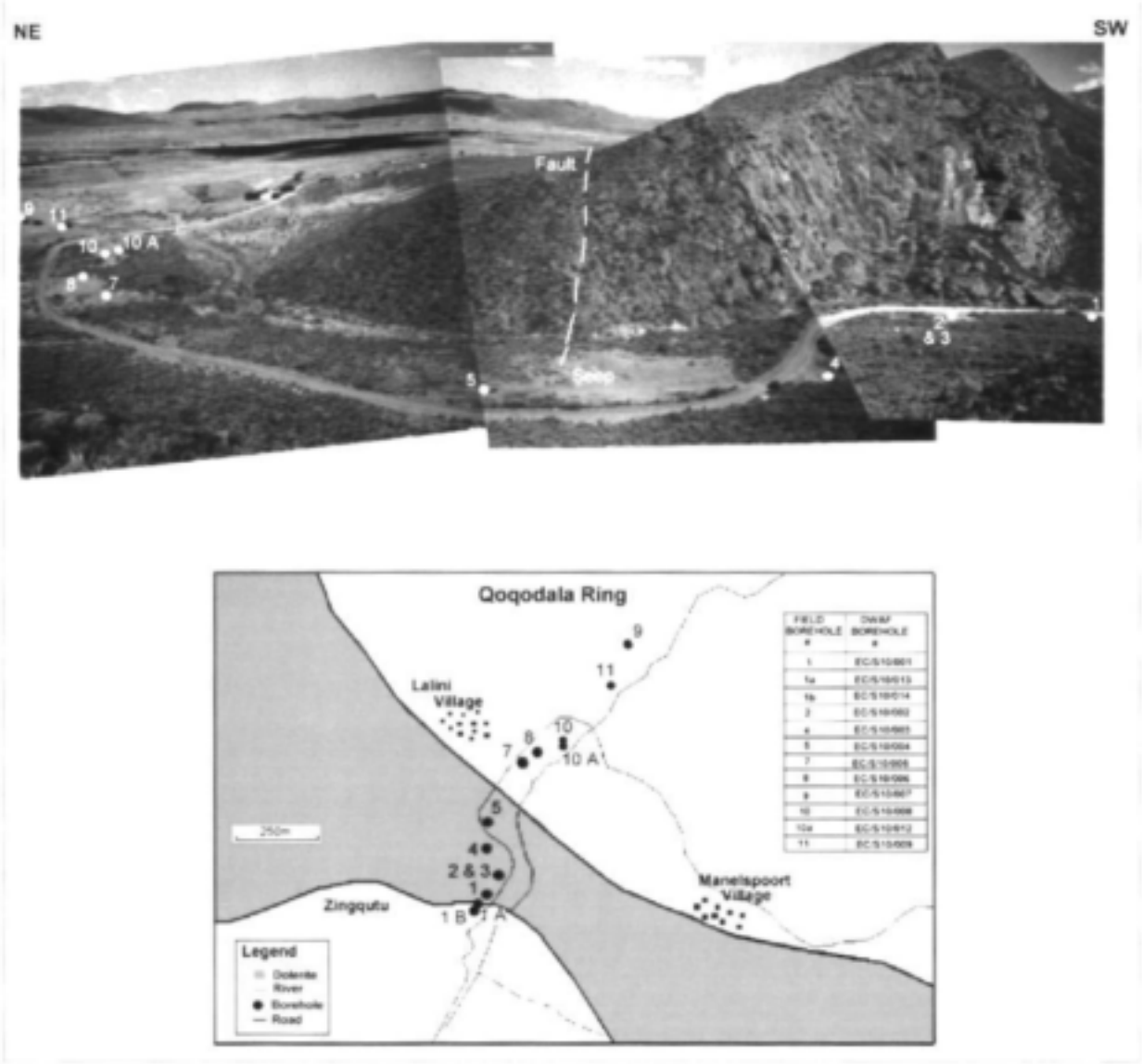

Figure 20: The Qoqodala exploration drilling site: map and panoramic view (see Figures 18 and 19 for general location). The 1.5 km long profile straddle across the dolerite inclined sheet. Note the fault in the dolerite sheet and the presence of a wetland land between boreholes 4 and 5.

Logging of the borehole chips was done by the research team. Downhole video camera and geophysical wireline survey were also done by DWAF on borehole 1, 4 (incomplete), 5, 7, 8, 9, 10A and 11.

Geohydrological and technical results are summarised in **Table 5.**

Table 5: Summary of the Exploration Borehole Information

DWAF No.	Borehole Field No.	Depth (m.bgl)	Waterlevel (m.bgl)	Date Measured	Final Blow Yield (l/s)	Total EC (mS/m)	pH
EC/S10/001	1	212	14.8	12/12/2002	38	44	7.51
EC/S10/013	1a	90	23.2	25/06/2003	-		
EC/S10/014	1b	115	23.8	25/06/2003	-		
EC/S10/002	2	31	7.1	25/06/2003	seep		
EC/S10/003	4	181	3	12/12/2002	23	41	7.5
EC/S10/004	5	181	4.2	12/12/2002	16	47	7.57
EC/S10/005	7	277	12	12/12/2002	10		7.83
EC/S10/006	8	300	14	12/12/2002	1		7.02
EC/S10/007	9	211	9.7	12/12/2002	12		
EC/S10/008	10	263	13.9	08/03/2003	8.5		
EC/S10/009	10a	247	11.2	25/06/2003	-		
EC/S10/010	11	248	15	25/06/2003	7.5	44	7.91

The cross section shown in **Figure 21** was compiled from geological logging, video camera, geophysical logging and completed by a Time Domain Electromagnetic survey (TDEM), especially for deep structure detection. The profile shows a very thick dolerite inclined sheet feeding two outer sills. It is interesting to note that the added thickness of the two outer sills equal the thickness of the inclined sheet. The back of the inclined sheet between the two outer sills is structurally very complex with several dolerite offshoots, confirming results obtained at Victoria West (Chevallier et al., 2001). The Qoqodala inner sill and the deeper sill were not intercepted by drilling but were detected by TDEM.

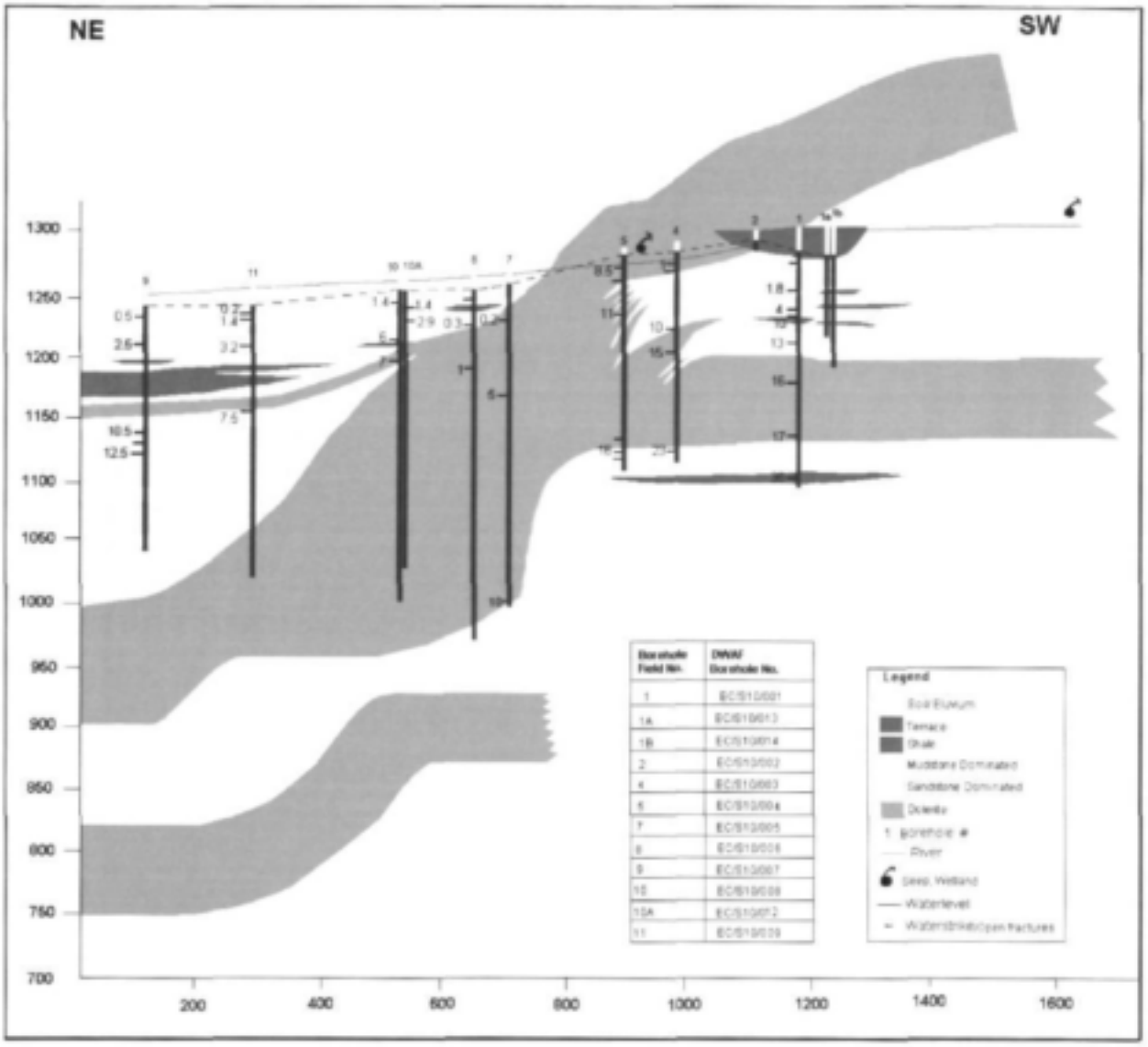

Figure 21: Geohydrological profile at Qoqodala exploration drilling site (see Figure 20 for location). The sandstone bar has been uplifted by the dolerite inclines sheets. The deep structures (inner sills) have been detected by Time Domain Electro Magnetics. Water strikes and fractures are present at lithological contacts.

A major sandstone bar has been displaced by the intrusion of the inclined sheet. This 100m thick bar could be the equivalent of the middle bar of the Burgersdorp Formation as seen at Nonesi's Neck (see Figure 6).

3.5.2 Time Domain Electromagnetic (TDEM) results

The inner sill could not be reached by drilling, therefore in March 2003, a Time-Domain-Electro-Magnetic (TDEM) survey was conducted (Hallbauer-Zadorozhnaya et al., 2003; Terra Sounding and Analytical Ltd, 2003). The TDEM survey, using "Tsickl-5" equipment aimed to detect deep-seated dolerite bodies and water-bearing sediments in excess of 350m depth. Two readings were taken at each of the 12 stations (**Figure 22**) using two receiver loops of effective areas of $625m^2$ and $6400m^2$. With the $625m^2$ receiver loop, information from 25m depth to 300-400m is obtained. The $6400m^2$ receiver loop gave results from 50m to 600m, and deeper. For the 12 stations a transmitter loop of size 100m x 100m was used. A larger transmitter loop (200m x 200m) was also used at the three northern stations above the deep inner sill. For purposes of this project, the depth 'limit' was set at 500m.

Interpretation of the recorded signals involved the use of visualisation of TDEM signals, compilation of the S-plane version, mathematical modeling and geological interpretation. On the flat area, TDEM signals were slightly distorted by polarisation effect (IP) or structural influences. The slight distortion shows that the lithology is mainly horizontal. On the mountainous area, the signals were distorted even more. These recordings cannot be interpreted using a multi- layered, non-polarisable model, since the distortions are not typical for the curves.

TDEM data was then interpreted using the Sτ-version, where depth is plotted against apparent longitudinal conductivity (ALC). An increase in ALC would show a layer of low resistivity. The Sτ-version indicates the placement of conductive layers into a cross-section and this information can then be used for the process of mathematical modelling. The first low resistance layer observed, i.e. the first increase of ALC, indicated a water-bearing layer. Larger increases also meant water saturated sediments, while the lowest increases meant sediments underlying the dolerite sill.

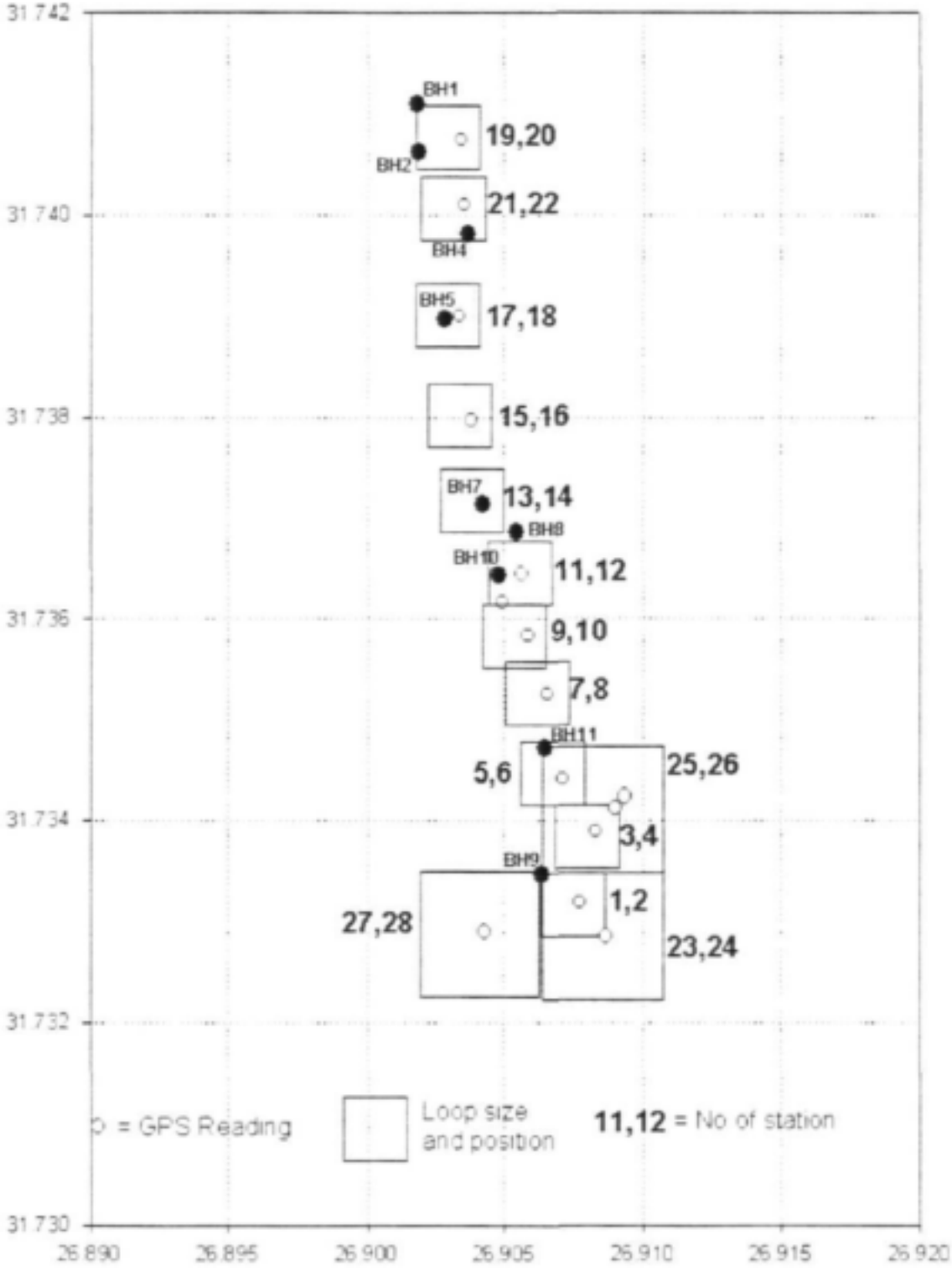

Figure 22: Time Domain Electromagnetic survey at Qoqodala Exploration drilling site, map showing reading station and size of loops.

This method enabled the detection of the Qoqodala inner sill lying between 900 and 1000 m depth (high resistivity). Another dolerite sill and an inclined sheet were detected at greater depth. Water saturated sediments were also detected (**Figure 23**).

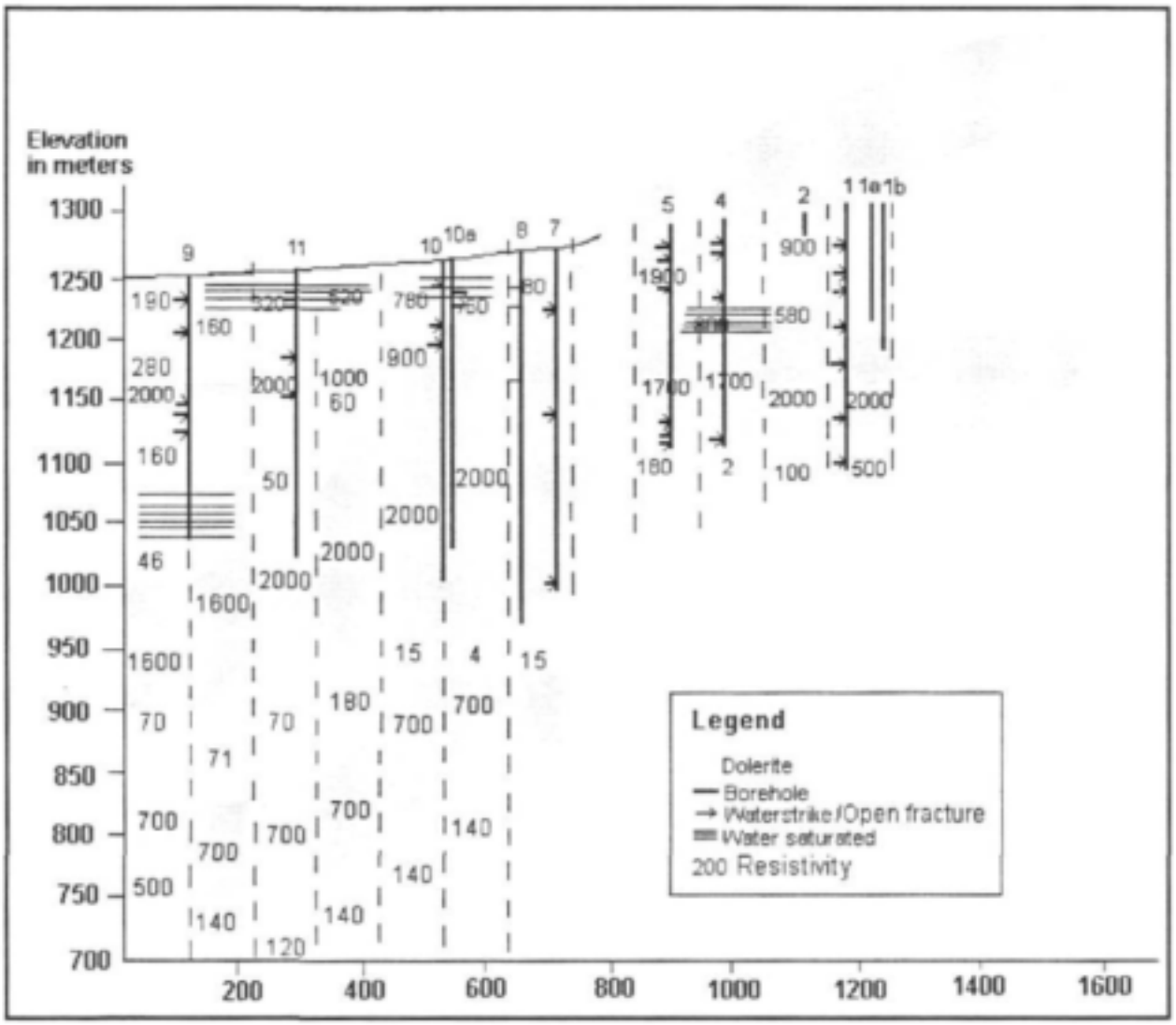

Figure 23: Time Domain Electromagnetic survey at Qoqodala Exploration drilling site, cross section.

3.5.3 Groundwater occurrences and water movement

Water strikes and fractures mainly occur at lithological contacts (dolerite contacts or sandstone contacts). The sandstone seems to be the most water saturated lithological unit, and the video camera recording showed it to be the most fractured. The profile shows fractured-rock aquifers at different depths.

The top fractured-rock aquifer is between 20 and 80 m, situated above the Zingqutu outer sill and the Qoqodala thin off shoot. Water movement within this aquifer has been seen from video camera in borehole1, where the water disappears into a horizontal fracture at depth of 54m.When borehole 5 was drilled in July 2002 it was artesian. Borehole 4 was then drilled and after 97m, the nearby wetland dried out. The waterlevel dropped by four meters (the seep located between boreholes 4 and 5 dried out and emerged four meters below, in the river bed) and borehole 5 stopped being artesian. Shallow boreholes 2 and 3 were subsequently drilled in the terrace affecting artesian borehole 4. Borehole 1 was then drilled and when it reached the depth of 30 – 40m, borehole 4 stopped being artesian. The waterlevels in borehole 1, 2, 4 and 5 have been dropping since. It appears that since the drilling took place, the system has been leaking water from the top.

A series of water bearing fractures occur at the base of the Zingqutu outer sill and the Qoqodala thin offshoot. In borehole 5, water is moving into a series of joints and fractures at a depth of 155m at the base of the outer sill. At the same elevation in borehole 9, a series of permeable subvertical joints and cracks below the sandstone bar is letting the water in.

A deep aquifer (250m depth) occurs at the bottom of the deeper Qoqodala inner sill and the inclined sheet. It has been intercepted by borehole 7. At the bottom of the hole the water is turbid and could be coming out of a fracture. The water is warm (24°) and moving up the borehole.

Monitoring of the boreholes only started end of 2002 - beginning of 2003 (see table 5). Water levels were taken on a monthly basis through out 2003. In September 2003 two divers, supplied by the CSIR were installed in boreholes 5 and 7. The borehole data was entered into Aquimon, software designed by one of the authors (A. Woodford) for well field monitoring.

3.6 PUMP-TEST ANALYSIS

Three aquifer-testing schedules, each consisting of a step-drawdown test followed by a 72-hour constant-discharge and waterlevel-recovery test, were conducted on boreholes BH-1, BH-7 and BH-11 (**Figure 21**) situated on the Qoqodala dolerite ring-complex, over the period 27th June to 22nd July 2003 by Hippo Contractors from Bloemfontein. In all cases a mono-type, positive displacement pump was utilized. Unfortunately, the waterlevel response was not monitored in borehole BH-5 during pump-testing of boreholes BH-7 and BH-1.

3.6.1 Borehole BH-11

A multi-rate test was conducted on borehole BH11 and the relevant information is summarized in **Table 6** and graphically presented in **Figure 24**. The pumping rate was increased from 1 to 15 l/s over 9 steps of 60 minutes each. Localised dewatering of the fractures at 22 and 27 m.bgl are evident in the waterlevel drawdown curves during step 5 and 6, respectively. The optimum short-term pumping rate for BH-11 is estimated at 6 l/s.

Table 6: Summary of Results of Step-Drawdown Test on Borehole BH11

Borehole Depth (m)			230.0	Water Interception (Yield l/s)	22 (0.2), 27 (1.2), 42 (1.8), 72 (4.3).
Pump Intake (m.bgl)			120.0		
Rest Waterlevel (m.bgl)			14.91		
Step	Yield (l/s)	Duration (min)	Maximum Drawdown (m)	Specific Drawdown	Transmissivity (m^2/day)
1	1.0	60	1.57	0.0181	68
2	2.0	60	2.68	0.0153	80
3	3.0	60	3.87	0.0146	84
4	4.0	60	5.42	0.0152	80
5	6.0	60	8.54	0.0160	76
6	8.0	60	12.40	0.0174	70
7	10.0	60	16.43	0.0184	66
8	12.0	60	24.39	0.0227	54
9	15.0	60	57.42	0.0437	23
Volume Pumped (m^3):			220	-	Est: 75
Well Losses (B):				1.62×10^{-3}	n = 7.42
Aquifer Losses (C):				2.86×10^{-5}	

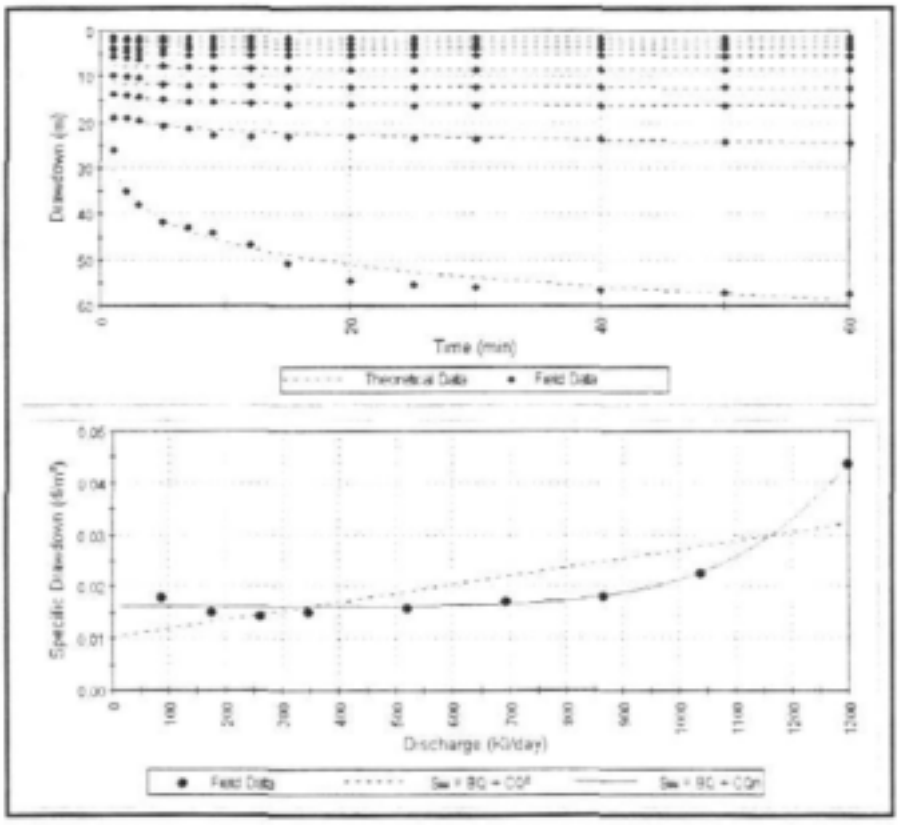

Figure 24: Step-Drawdown Test on Borehole BH-11 - Waterlevel- and Specific-Drawdown Plots

A 72-hour constant discharge test was conducted on borehole BH-11 at a rate of 10 l/s (860 m^3/day), in order to induce as large as possible a decline in the waterlevel in the borehole without reaching pump-suction at 120 m.bgl. The results of the test are summarized in **Table 7** and graphically presented in **Figure 25**. The waterlevel in BH-11 declined by 22.5m during the test, due to the abstraction of 2592 m^3 of groundwater. The waterlevels in boreholes BH-8, BH-9, BH-10 and BH-10A were monitored during the test, but only BH-9 showed a response to pumping. In the production borehole an inflection point occurs at 1700 minutes (30-Jun-03 in **Figure 25A**) at a drawdown of 18.2 (i.e. 34 m.bgl), which is probably related to the dewatering of a water-bearing fracture at this depth. Similarly, a second inflection point is evident at 3800 minutes (01-Jul-03) that may also indicate a water-bearing fracture at 36 m.bgl. Three days after pump-shutdown, a waterlevel deficit of just over a metre remained. The long-term sustainable yield of this borehole is estimated at 7 600 m^3/month or 90 000 m^3/annum. Note that this estimate does not include the abstraction from any other nearby production boreholes tapping the same aquifer unit.

Table 7: Summary of Results of Constant Discharge Test on Borehole BH11

Borehole Number	Radial Distance (m)	Rest-Waterlevel (m)	Maximum Drawdown (m)	Waterlevel Deficite	Transmissivity (m^2/day)	Storativity
BH-11	0	15.67	22.46 [4320]	-1.16 (4320)	91	-
BH-09	139	11.74	3.71 [4320]	-1.20 (4320)	235	5.5×10^{-5}
Volume Pumped (m^3):			2592			

Notes: [Duration of Pump Test in minutes] (Time in minutes since pump-shutdown)
EC varied between 48 and 50 mS/m.

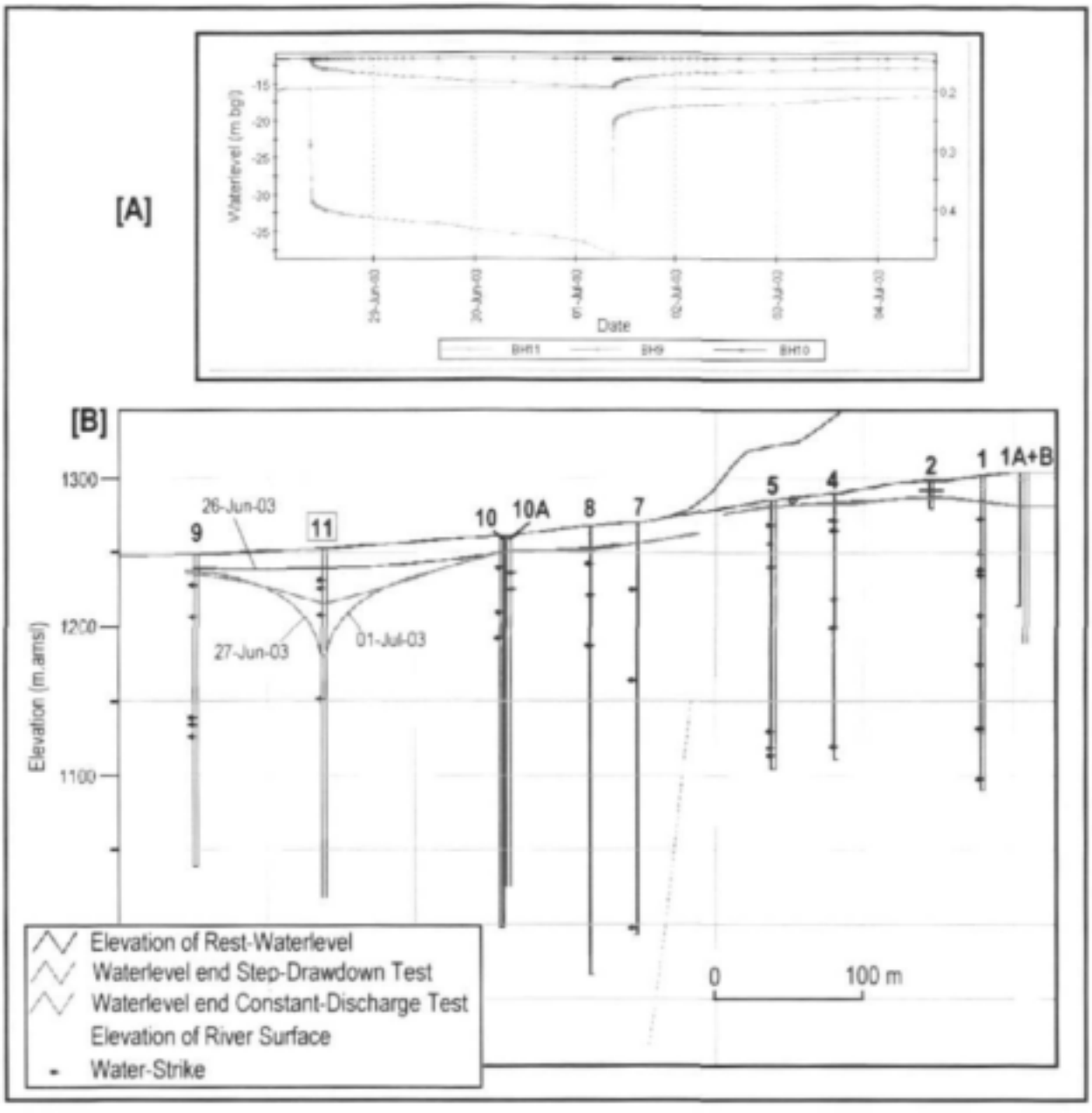

Figure 25: Constant Discharge Test of Borehole BH-11 and Waterlevel Response in Observation Boreholes BH-9 and BH-10

3.6.2 Borehole BH-7

A multi-rate test was conducted on borehole BH-7 and the relevant information is summarized in **Table 8** and graphically presented in **Figure 26**. The pumping rate was increased from 1 to 15 l/s over 9 steps of 60 minutes each. The first four points (steps) on the specific-drawdown graph are 'anomalous' and this may be due to the development (removal of drill material from the fractures) of the borehole during this portion of the test. The optimum short-term pumping rate for BH-7 is estimated at 4 l/s.

Table 8: Summary of Results of Step-Drawdown Test on Borehole BH-7

Borehole Depth (m)			277.0	**Water Interception (Yield l/s)**	44.5 (0.2), 106 (4.8), 273 (5.0)
Pump Intake (m.bgl)			120.0		
Rest Waterlevel (m.bgl)			15.64		
Step	**Yield (l/s)**	**Duration (min)**	**Maximum Drawdown (m)**	**Specific Drawdown**	**Transmissivity (m^2/day)**
1	1.0	60	2.96	0.0336	36
2	2.0	60	3.85	0.0217	56
3	3.0	60	4.92	0.0188	65
4	4.0	60	5.98	0.0169	72
5	6.0	60	8.58	0.0163	75
6	8.0	60	12.73	0.0164	75
7	10.0	60	18.22	0.0201	61
8	12.0	60	40.16	0.0376	32
9	15.0	60	65.56	0.0482	25
Volume Pumped (m^3):			220	-	**Est: 74**
Well Losses (B):				1.26×10^{-2}	**n = 3.66**
Aquifer Losses (C):				1.91×10^{-10}	

A 72-hour constant-discharge test was conducted on BH-7 at a rate of 12 l/s (1 037 m^3/day). During the test, the waterlevel in borehole BH-7 declined by almost 85m after the abstraction of 3 110 m^3 of groundwater. The pertinent results of the test are summarized in **Table 9** and graphically presented in **Figure 27**. A narrow deep cone of waterlevel depression developed around the production borehole, which extended beyond observation boreholes BH-8 and BH-

10 situated in the same aquifer unit. The waterlevel in borehole BH-4 that is situated in the adjoining aquifer unit also declined by 1.4m due to the pump-test.

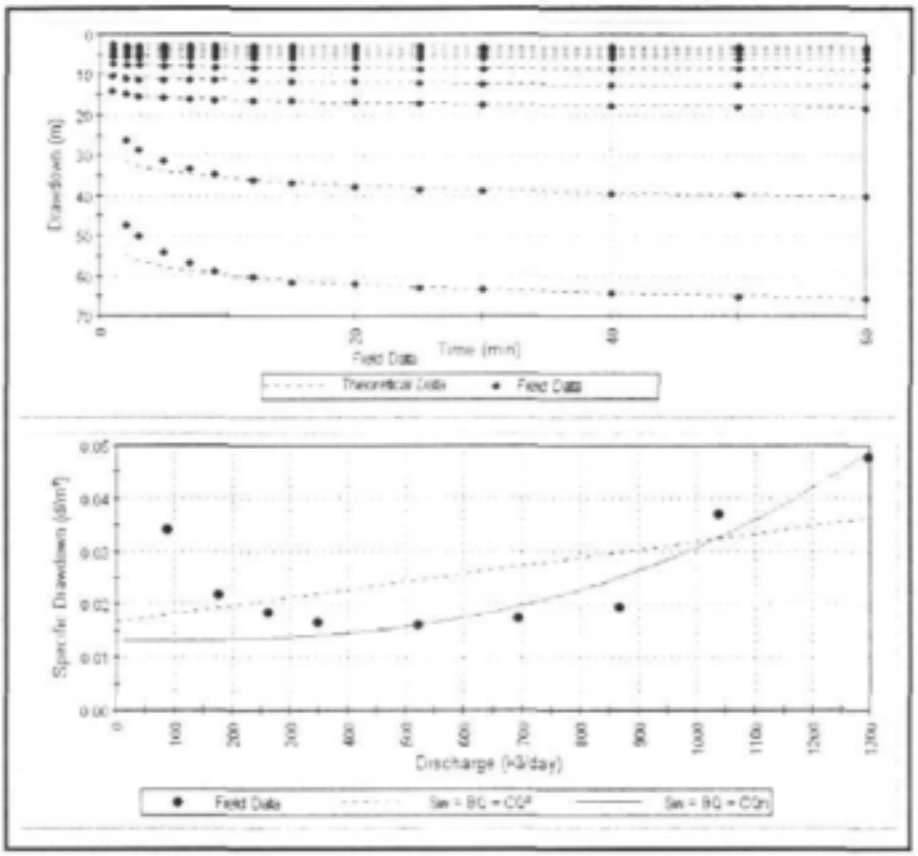

Figure 26: Step-Drawdown Test on Borehole BH-7 - Waterlevel- and Specific-Drawdown Plots.

This response is attributed to the 'artificial' hydraulic connection created by the drilling activities between the two aquifer units (discussed in **Chapter 3.7**). A relatively large waterlevel deficit of over 2m remained some 72-hours after pump-shutdown, indicating a relatively slow rate of lateral inflow of groundwater into the production borehole from the surrounding aquifer. The unrealistically low transmissivity value obtained for BH-7 (**Table 9**) is ascribed to unusually high 'borehole' losses within the vicinity of the well. The long-term sustainable yield of this borehole is estimated at 5 200 m^3/month or 62 000 m^3/annum. Note that this estimate does not include the abstraction from any other nearby production boreholes tapping the same aquifer unit.

Table 9: Summary of Results of Constant Discharge Test on Borehole BH-7

Borehole Number	Radial Distance (m)	Rest-Waterlevel (m)	Maximum Drawdown (m)	Waterlevel Deficite	Transmissivity (m^2/day)	Storativity
BH-07	0	17.37	84.84 [4320]	-2.49 (4320)	19^{7}	-
BH-08	64	18.36	8.24 [4320]	-2.47 (4320)	110	2.9×10^{-4}
BH-10	161	12.56	6.34 [4320]	-2.42 (4320)	145	5.8×10^{-5}
BH-04	411	8.57	1.38 [4320]	-1.14 (4320)	200	1.2×10^{-3}
Volume Pumped (m^3):			2592	**Average**	**152**	**5.2×10^{-4}**

Notes: [Duration of Pump Test in minutes] (Time in minutes since pump-shutdown)
EC varied between 48 and 51 mS/m.

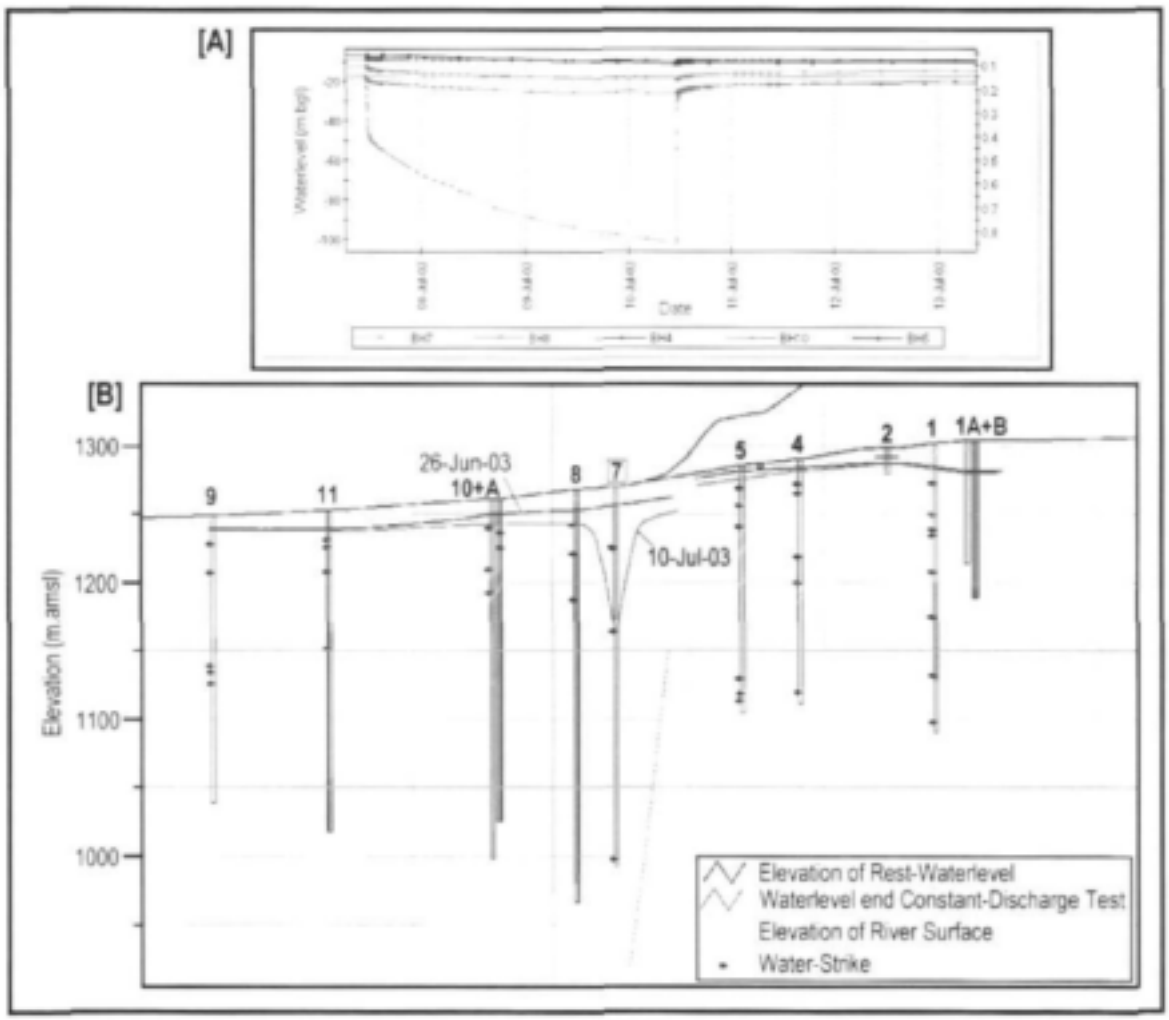

Figure 27: Constant Discharge Test of Borehole BH-7 and Waterlevel Response in Observation Boreholes BH-4, -5, -8 and BH-10.

3.6.3 Borehole BH-1

A multi-rate test was conducted on borehole BH-1 and the relevant information is summarized in **Table 10** and graphically presented in **Figure 28**. During the test the pumping rate was increased over 9 steps of 60 minutes each from 1 to 15 l/s, which resulted in a maximum waterlevel drawdown of only 14.3m at the end of step number 9. In terms of the aims of the step-test and the depth of the main water-bearing fractures the test is regarded as inconclusive. The maximum yield of BH-1 could not be determines due to the relatively narrow diameter (165mm) of the borehole and limited yield capability of the contractors pump. The optimum short –term pumping rate of BH-1 is estimated at 8 l/s.

Table 10: Summary of Results of Step-Drawdown Test on Borehole BH-1

Borehole Depth (m)			204.0	**Water Interception (Yield l/s)**	64 (4.0), 68 (6.0), 95 (3.0), 128 (3.0), 171 (1.0), 205 (17)
Pump Intake (m.bgl)			120.0		
Rest Waterlevel (m.bgl)			21.23		
Step	**Yield (l/s)**	**Duration (min)**	**Maximum Drawdown (m)**	**Specific Drawdown**	**Transmissivity (m^2/day)**
1	1.0	60	0.66	0.00765	160
2	2.0	60	1.09	0.00578	211
3	3.0	60	1.74	0.00329	194
4	4.0	60	2.60	0.00676	181
5	6.0	60	4.33	0.00770	159
6	8.0	60	6.48	0.00885	138
7	10.0	60	8.06	0.00882	138
8	12.0	60	11.33	0.01030	119
9	15.0	60	14.34	0.01040	117
Volume Pumped (m^3):			220	-	**Est: 206**
Well Losses (B):				2.08×10^{-3}	**n = 1.41**
Aquifer Losses (C):				4.45×10^{-4}	

A 72-hour constant discharge test was conducted on BH-1 at a rate of 15 l/s (1 296 m^3/day), in order to induce as larger as possible a drawdown in the borehole with the limited capacity of the pump-equipment. The waterlevel response was monitored in observation boreholes BH-1A, -1B and BH-4 in the same aquifer unit, all of which showed a response. The results are summarized in **Table 11** and graphically presented in **Figure 29**.

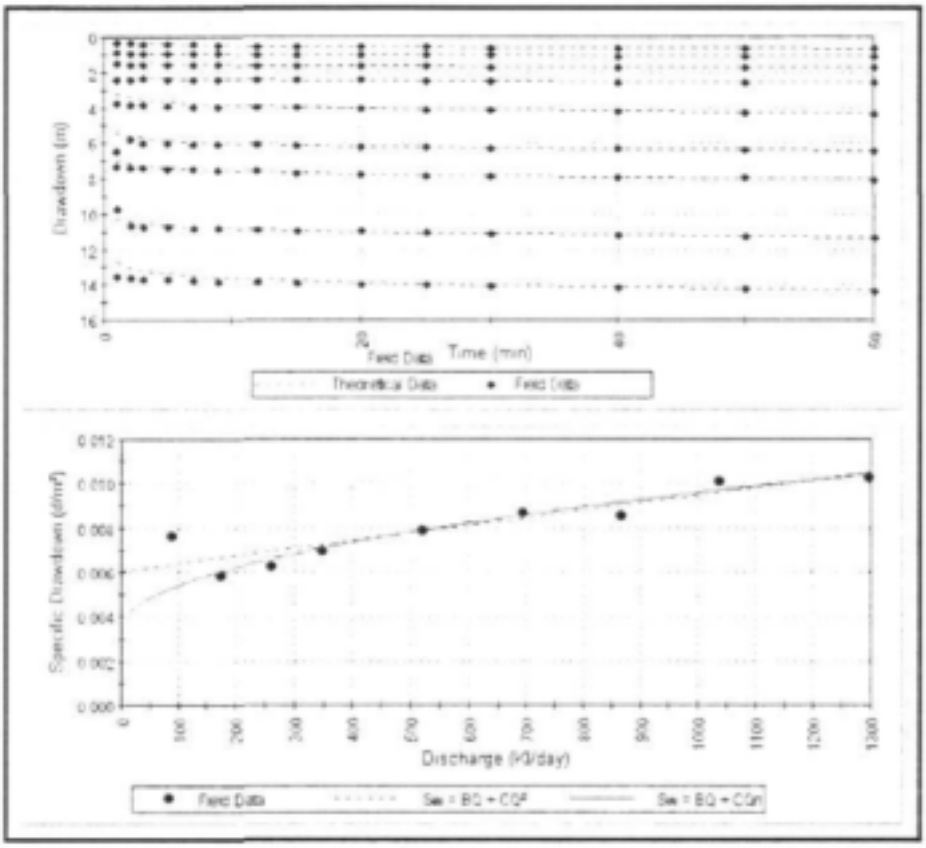

Figure 28: Step-Drawdown Test on Borehole BH-1 - Waterlevel- and Specific-Drawdown Plots.

The waterlevel in BH-1 declined by almost 23m due to the abstraction of 3 888 m^3 over the period of the test. A relatively large waterlevel deficit of ±4 m remained three days after pump-shutdown. The drawdown curve shows and inflection point at 250 minutes and a drawdown of 13.8 m (i.e. 36 m.bgl), where after the rate waterlevel decline increases steadily. This would indicate a poor hydraulic connection between the aquifer unit and the adjacent river at this locality, where it was anticipated that pumping would have induce recharge of aquifer from the river system. The transmissivity and storativity values (**Table 11**) determined from the pump-test data are considered to most accurately characterize the hydraulic properties of the aquifer system at Qoqodala. The long-term sustainable yield of borehole BH-1 is estimated at 5 700 m^3/month or 68 400 m^3 per year.

Table 11: Summary of Results of Constant Discharge Test on Borehole BH-1

Borehole Number	Radial Distance (m)	Rest-Waterlevel (m)	Maximum Drawdown (m)	Waterlevel Deficite	Transmissivity (m^2/day)	Storativity
BH-01	0	21.72	20.88 [4320]	-3.92 (4320)	105	-
BH-1A	46	25.80	11.55 [4320]	-4.92 (4320)	110	2.5×10^{-4}
BH-1B	57	26.36	11.50 [4320]	-4.21 (4320)	80	2.8×10^{-4}
BH-04	212	10.13	10.27 [4320]	-4.22 (4320)	80	2.2×10^{-5}
Volume Pumped (m^3):			3888	**Average**	**94**	**1.8×10^{-4}**

Notes: [Duration of Pump Test in minutes] (Time in minutes since pump-shutdown)
EC varied between 39 and 47 mS/m.

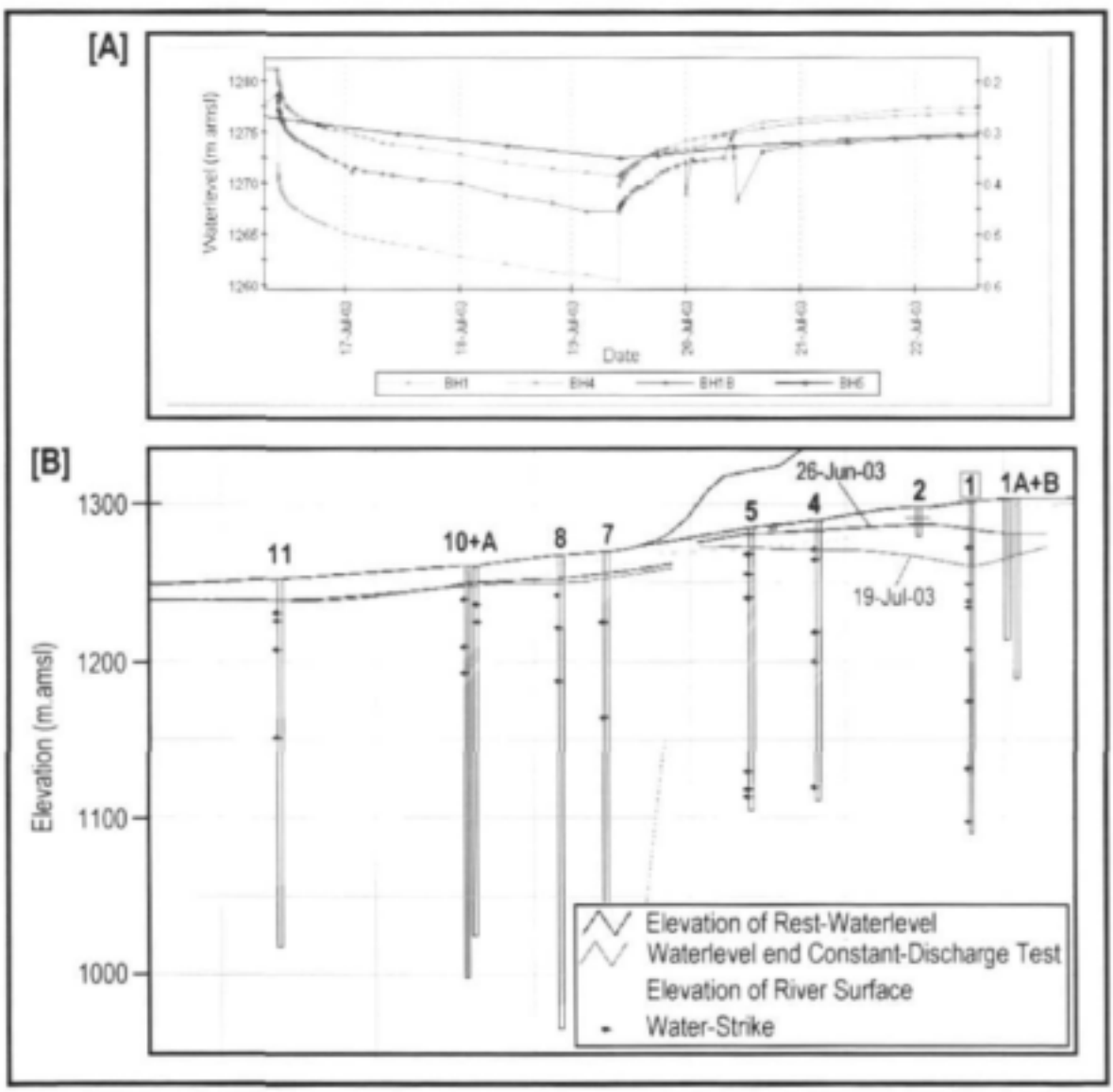

Figure 29: Constant-Discharge Test of Borehole BH-1 and Waterlevel Response in Observation Boreholes BH-1B, -4, and BH-5

In all three constant-discharge tests the waterlevel drawdown curves show a steepening of the curve, i.e. an increase in the rate of waterlevel decline, during the later half of the test - a response that is commonly observed in shallow, semi-confined, Karoo fracture-rock aquifers. This is indicative of the various flow regimes that evolve over time in such 'dual porous' aquifer systems, where water abstracted is initially derived from the macro-fractures (fracture-type flow) during the early portion of the pump-test, whilst towards the end of the test the majority of the water is derived from the dense network of connected micro-fractures and joints (pseudo-Darcian flow).

3.7 AQUIFER DESCRIPTION AND FLOW CONCEPTUALIZATION

The Karoo fractured-rock aquifer systems are generally multi-layered, in basic terms consisting of:

(i) a shallow (less than 30m below waterlevel), relatively thin but laterally extensive, unconfined to semi-confined aquifer comprised of well jointed and weathered rock developed mainly during processes of local structural deformation, weathering, erosional unloading etc; and

(ii) a deeper-seated (in excess of 90m below waterlevel), semi-confined to confined aquifer comprised of discrete fractures developed associated with regional structural features formed within the current and/or a previous regional tectonic regimes.

Of course, a particular aquifer system may comprise a vertical stacking of any number of these layers. The permeability and degree of interconnectivity between the aquifer layers can be greatly enhanced when associated with a favourable tectonic structure (i.e. dyke, fault etc.).

On the macro-scale, the upper aquifer layer can be viewed as an intergranular or porous medium due to the dense, interconnected network of variably orientated, joints and fractures where quasi-radial flow occurs. The bulk of the groundwater recharged during rainfall events is stored in this aquifer layer. The deeper aquifer layer often consists of one or more discretely orientated, open fracture zones, which is generally of relatively limit lateral extent. This aquifer layer stores

significantly less groundwater than the upper aquifer layer and isotropic, fracture-type flow is dominant. The various aquifer layers are commonly in hydraulic connection, resulting in some degree of 'leakage' between layers. Boreholes drilled into the upper aquifer unit generally strike a relatively large number of low-yielding water interception (see zone above 75 m.bgl in **Figure 30**), whilst infrequent, discrete, higher yielding water interceptions are typical of the deeper aquifer units.

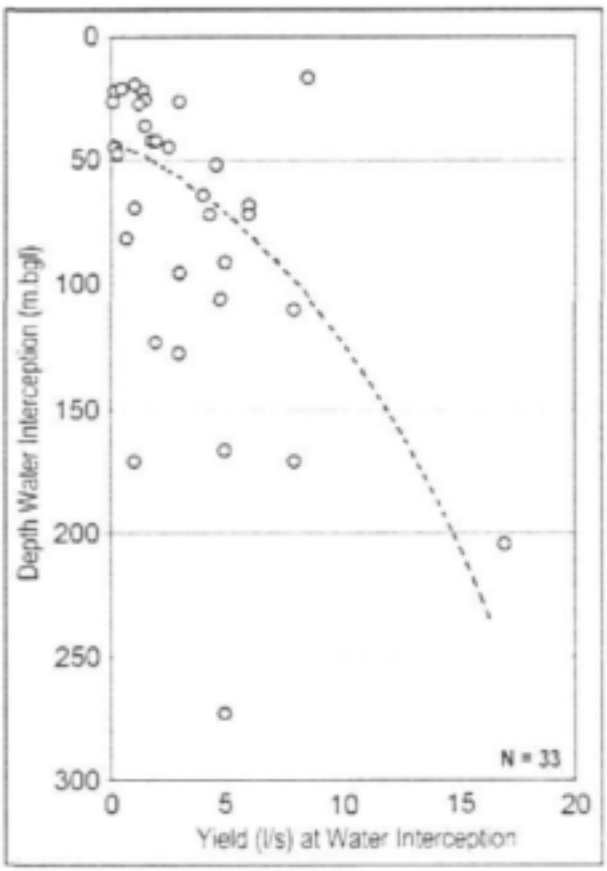

Figure 30: Water interception yield variations with depth below ground surface in Qoqodala exploration boreholes BH 1 to 11

The Qoqodala test site developed on the edge of the Qoqodala dolerite ring-structure exhibits such a typical multi-layered aquifer system, where at least three hydraulically distinct aquifer units are evident, namely (**Figure 31**):

(i) A shallow, laterally extensive, unconfined to semi-confined aquifer developed in the weathered / uplift zone sandstone and mudstone layers above the *Inner Sill*, where the main water-bearing fractures are predominantly sub-horizontal to horizontal. The depth to the waterlevel varies between 9 and 11 m.bgl. When flowing, the river is effluent into the groundwater system. The deeper, sub-horizontal fracture associated with the relatively thin dolerite 'offshoot' may only be weakly connected to the more elevated fracture network and, if this is the case, could be considered as separate aquifer layer.

(ii) A shallow, semi-confined to confined aquifer developed within the intensely fractured sediments and dolerite 'sandwiched' between the *Inclined Sheet* and *Outer Sill* of the ring-complex. A spring is developed, near BH-5, adjacent to the *Inclined Sheet* that forms the northern boundary of this unit. The confined nature of the pristine aquifer resulted boreholes BH-4 and BH-5 becoming artesian after drilling. At this point, it is also likely that the aquifer was under normal conditions effluent to the river.

(iii) A deeper-seated, confined aquifer associated with discrete, open, fractures in the dolerite and meta-sediments at the base of the *Outer Sill* and *Inclined Sheet*, as well as presumably the *Inner Sill*. High yields were struck in a fracture system at the base of the *Outer Sill*. The temperature of the groundwater in borehole BH-7 is slightly elevated at 24° C, indicating upward movement of groundwater from a greater depth.

Drilling of the exploration boreholes BH-1, -4, -5, -7 and BH-8 resulted in an artificial connection between the various aquifer units. It is postulated that the drilling of BH-1, -4 and BH-5 resulting in a downward flow of groundwater from aquifer unit (ii) into the underlying unit (iii) (**Figure 31**).

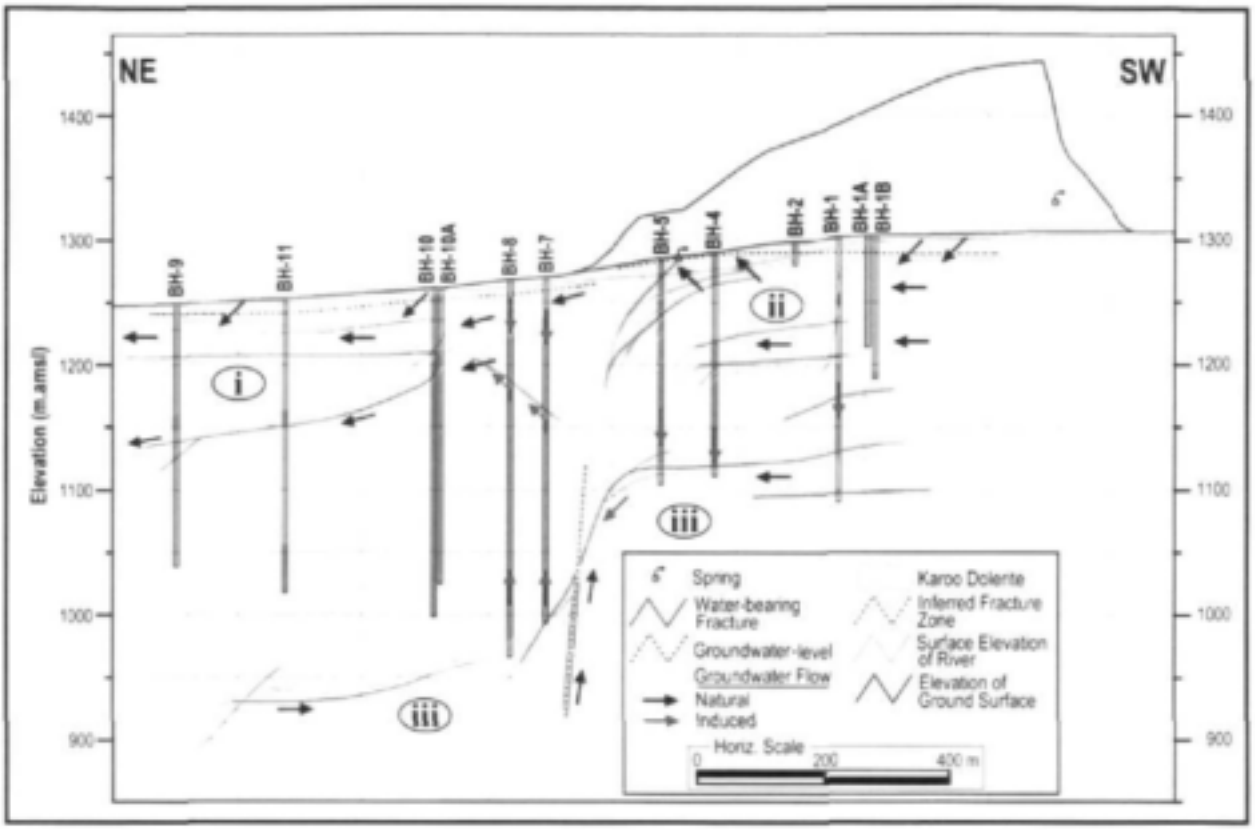

Figure 31: Natural and 'Induced' Groundwater Flow Regime at the Qoqodala Test Site

Table 12: Groundwater Fluctuations in Boreholes BH-1 to BH-11 since monitoring commenced

Borehole Number	Waterlevel (m.bgl) [Date]	Waterlevel (m.bgl) [Date]	Waterlevel Change (m)
BH-1	13.170 [9-Dec-02]	29.507 [17-Sep-03]	-16.337
BH-1A	23.216 [24-Jun-03]	28.822 [16-Sep-03]	-5.606
BH-1B	23.798 [24-Jun-03]	29.404 [16-Sep-03]	-5.606
BH-4	3.240 [9-Dec-02]	13.119 [16-Sep-03]	-9.879
BH-5	4.120 [9-Dec-02]	10.595 [17-Sep-03]	-6.475
BH-7	11.500 [9-Dec-02]	16.210 [15-Sep-03]	-4.710
BH-8	13.780 [9-Dec-02]	16.865 [24-Jul-03]	-3.085
BH-9	9.610 [9-Dec-02]	11.627 [18-Sep-03]	-2.017
BH-10	11.200 [24-Jun-03]	11.288 [16-Sep-03]	-0.088
BH-10A	11.153 [24-Jun-03]	11.265 [16-Sep-03]	-0.112
BH-11	14.910 [24-Jun-03]	15.152 [16-Sep-03]	-0.242
Borehole BH-5 was artesian after completion of the drilling in July 2002, then became sub-artesian when borehole BH-4 was drilling at 97m. Bh-4 was artesian until borehole BH-1 was drilled to 50m.			

3.8 ECOSYSTEM AND WETLAND MAPPING

The size of the study area and the lack of previous studies or data in the area make it an ideal area in which to use remote sensing to assist in the mapping process. The numerous veld types present in the study area have been previously mapped at a scale of one in one million (Acocks) and with the satellite imagery available, it is theoretically possible to refine the vegetation map to approximately 1: 50000. Acocks based his observations on the agricultural potential of the vegetation (http://www.ngo.grida.no/soesa/nsoer/Data/vegrsa/vegpref.htm) and the categories of mapping by Acocks did not included groundwater dependant ecosystems.

The aim of this chapter is to firstly produce a higher resolution vegetation map by using remote sensing mapping, secondly, to map any wetlands present in the study area using moisture and greenness indices derived from multi-temporal satellite imagery, and thirdly to use the spectral properties of a known seep to map this groundwater dependant ecosystem.

According to Hatton and Evans (1998) and Evans and Hatton (2000), groundwater dependent ecosystems can be classified into six categories:

Phreatophytic terrestrial vegetation does not rely on surface water for survival and exploits groundwater either constantly or periodically through the capillary root systems. The quality and depth of the groundwater will influence the distribution of the species.

Wetland ecosystems are vulnerable to change in groundwater regime and abstraction. These waterlogged environments (peat, swamps, and marshes) can be fed by rainfall, local runoff, perched water Table and seepages. They retain, absorb and release water throughout the year. They are vulnerable to change in land use.

Base flow contributes to the river flow, maintaining it during periods of drought. The amount of water available from base flow depends on the depth of the water table in the weathered zone, the

number and hydraulic characteristics of the fractured aquifers. Volume of the base flow, variability and changes in land use may significantly change or threaten the ecosystem.

Aquifer and cave ecosystems support a variety of subterranean organisms (fauna and flora). They occur in the groundwater in karstic terrain, porous or fractured-rock aquifers and are dependent on environmental conditions of darkness

Near shore marine and estuarine ecosystems use groundwater opportunistically or to a very limited extent. Some of the fresh groundwater can extend offshore and can support a variety of fauna (prawn) and flora such as sea-grass.

Terrestrial fauna can use groundwater discharge occasionally or seasonally for survival. Because of their mobility they also form part of larger ecosystem groups.

Phreatophytic terrestrial vegetation, wetland ecosystems and base flow are relevant and applicable to the study area. It is possible that there are aquifer and cave ecosystems within the study area but an investigation of this nature falls beyond the scope of the present project. Near shore marine and estuarine ecosystems fall outside the geographic and geomorphic framework of our study; and terrestrial fauna, although relevant, would require a regional ecological project on its own.

3.8.1 Vegetation Mapping

One Landsat ETM+ image (November 2000) was used for the broad ecosystem mapping. It was not necessary to combine the wet and dry season image for this processing as the aim was to map the various veld types that occur in the study area and the smaller seasonal variations are not necessarily relevant. In addition, the time span of 16 years between the capture of the dry season image (May 1984) and the wet season image (November 2000) may have led to land use changes in the urban and farming areas which may lead to confusing classification results.
The Landsat image was examined visually prior to any processing being carried out. This examination, coupled with observations made in the field led to a decision as to how many classes to choose as a maximum for the output of the unsupervised classification. These classes are listed

in **Table 13**. It must be noted that the names given to these initial classes may not necessarily be reflected in the results. A total of thirteen classes were identified prior to classification and, to allow for classes which may have been overlooked, two more classes were allowed in the classification. By limiting the number of output classes in the unsupervised classification, the classification is forced to have fewer output classes and is thus forced to clump classes together which may have otherwise have been separate classes.

The unsupervised classification resulted in 15 output classes which were then matched as best possible to the classes decided upon to prior to processing and given in **Table 13**. The classes which were easily identifiable were clouds, shadows, water, overgrazed grasslands and urban areas. The remaining classes were not as easily recognisable and their names were changed to more suitable names. In some cases, such as in the shrubs / mixed vegetation class, more than one output class fitted into this category. In these cases, output classes were merged. In addition, the following classes shadow, clouds and unclassified were merged as these classes are not relevant to the study. The results are shown on the map in **Figure 32**.

Table 13: Classes decided upon prior to image classification

Class Number	Provisional Class Name	Description	Provisional Veld Type (from Acocks veld types)
1	Bare soil	Exposed soil, badlands, overgrazed areas in the inner sill	
2	Overgrazed grasslands	Badlands, overgrazed areas in the inner sill	Pure Grassveld (dry cymbopogon-themedaveld)
3	Non-irrigated Crops	Cultivated land in the former Transkei which rely on rainfall for irrigation	
4	Fallow land	Farmland without crops, bare soil	
5	Urban areas	Built-up areas, including roads	
6	Clouds		
7	Water	Dams, Rivers, Wetlands	
8	Shadow	Cloud shadow, shadow caused by topography	
9	Grasslands	Predominantly grass in the low lying areas May be used as range land on commercial farms	Pure Grassveld (dry cymbopogon-themedaveld)
10	Shrubs/ mix	Succulent, hardy shrubs occurring on the slopes of the dolerite sills	Pure Grassveld (karroid danthonia and *mountain* veld)
11	Kloof Vegetation	Lush vegetation found in kloofs and next to rivers	Temperate and Transitional Forest
12	Dolerite Grasslands	Predominantly grass on the high lying dolerite sills	Pure Grassveld (dry cymbopogon-themedaveld)
13	Irrigated Crops	Cultivated land on commercial farms - irrigated	

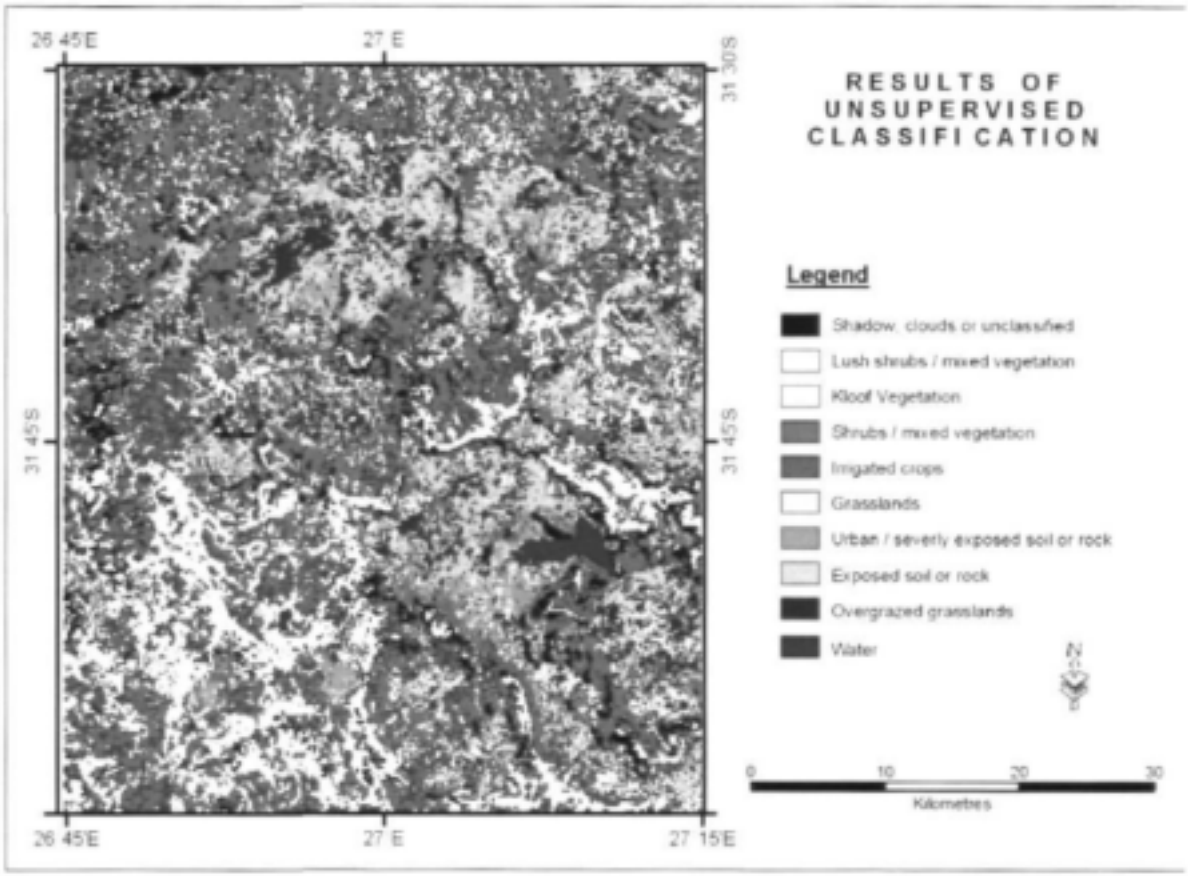

Figure 32: Results of the unsupervised classification

By examining the mapped result in conjunction with the three dimensional view of the Qoqodala ring in **Figure 33** below, trends regarding the location of the classes with respect to topography, relief, aspect and former national boundaries can be seen. In some cases these are backed up by the botanical field investigation which was carried out. A discussion of the trends for each class now follows:

Class 1: Bare soil: This class appears to be well mapped but was grown to include exposed rock as well as bare soil. There is no field data to verify the accuracy of this class. The bare soil class tends to occur on the flat inner ring in the areas which were incorporated in the Former Transkei. This is perhaps indicative of the land use practices in this area as the number of cattle on the land probably exceeds its carrying capacity and, as a result, soil erosion has occurred leaving exposed soil, dongas and badlands.

Class 2 & 3: Overgrazed grasslands and non-irrigated crops: These classes appear to have the same reflectance as there was only one output class which appeared to contain both non-irrigated crops and overgrazed grasslands. As with class 1 above, these classes mostly occur in Former Transkei.

Class 4: Fallow land: It was expected that this class would be found in the commercial farmlands however a class which matched this description was not identified.

Class 5: Urban: The built-up areas of Queenstown are well mapped by this class however large areas in the former Transkei have the same reflectance as the town of Queenstown. This is probably due to extreme land degradation which has occurred in parts of the former Transkei.

Class 6: Clouds: Clouds are well mapped in Class 6 and no other features are mistakenly identified as cloud.

Cloud 7: Water: Large water bodies such as the Xonxa Dam are accurately mapped. In some cases a thin line of pixels demarcates river lines and this is probably where the rivers are deep and wide.

Class 8: Shadow: This class includes shadow caused by clouds and topography; tar roads also fall into this category as do burn scars. Unfortunately a number of the botanical samples taken fall into in this class (shadow caused by topography) which reduces the number of botanical ground control points available.

Class 9: Grasslands: This category tends to occur at the foot of the slope of the dolerite rings and again on the high lying dolerite sills. This could be due to increased water availability due to increased precipitation in the high-lying areas and surface runoff at the foot of the slope. The grass occurring at the foot of the slope was noted during the botanical investigation in the Qoqodala Ring.

Class 10: Shrubs/ mixed vegetation: This is a very large category and is made up of three classes. It is also possible to split this class into two; namely lush shrubs and mixed vegetation and simply shrubs and mixed vegetation. The shrubs and mixed vegetation tends to occur on the north and east facing slopes of the dolerite sills and this finding is backed up by the botanical investigation which took place on the slope with a north-east aspect in the Qoqodala Ring (Qoqodala West in **Figure 34**). The lush shrubs and mixed vegetation was confirmed by botanical investigation in the Zingqutu area. It tends to occur on the south and west facing slopes and at the foot of cliffs formed by the outer sills.

Class 11: Kloof vegetation: This class appears to be well mapped. Kloof vegetation also seems to occur on the south facing slopes, at the foot of the high lying dolerite cliffs and within the kloofs themselves.

Class 12: Dolerite grasslands: This class can not be separated spectrally from Class 9: Grasslands.

Class 13: Irrigated crops: This class does not appear to be spectrally unique. In some cases it is successful in the commercial farming area, however there are many areas identified as irrigated crops which obviously are not crops. These areas are usually high lying areas of dolerite and it is probable that this is grasslands with an advanced stage of growth due to increased water supply either due to precipitation or possibly a water table at or near the surface.

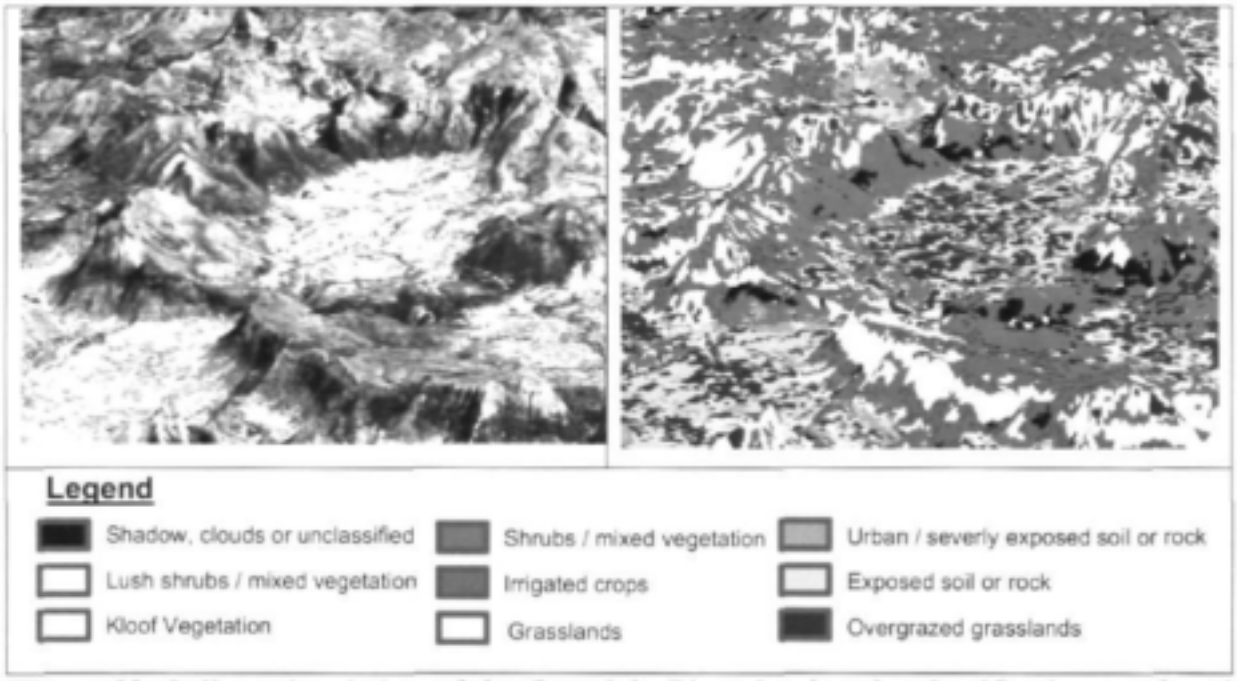

Figure 33: 3 dimensional view of the Qoqodala Ring showing the classification results (right) with an Aster image (left) displayed for reference

Field investigation and accuracy of classification results

Site visits were conducted 21 October 2001, from 16 to 19 November 2002 and from 2 March to 8 March 2003. Plant specimens were collected for identification and are listed below.

Specimens were collected within 10m X 10m quadrats along the dolerite slopes. The co-ordinates of each quadrat were recorded using a global positioning system (GPS) and are plotted in Figure 34. The lack of field data makes the drawing of significant conclusions on the accuracy of the classification results difficult. Using the data available, the results are discussed per micro region as shown in **Figure 34**.

Luxeni: The vegetation at this sample point is described as Aloe dominated thicket which matched the shrub / mixed vegetation class. The classification is therefore accurate in this instance.

Qoqodala North: The vegetation in this region comprises solely of grass species which grow on the sandy substrate however the classification reveals different vegetation types. It should be noted that large areas of grassland were identified in the proximity so it is possible that the classification is accurate but inaccuracies in the location may have occurred due to errors in the GPS reading or during image rectification.

Qoqodala West: The vegetation in this region is comprised of dense shrub thicket dominated by *Aloe sp., Rhus glauca, Olea europea* subsp *africana* and *Chrysanthemoides incana*, which occur on the rockier substrate. These shrubs and succulents are physiologically adapted to arid conditions. The shrubs tend to have longer roots systems and their leaf structures are adapted to reduce water loss. The succulents have thick, large leaves and store water in these leaves. The classification results were reasonably accurate in this region as the scrub vegetation was classified as shrub / mixed vegetation. The seeps were not detected, possibly due to their size.

Zingqutu North: The vegetation which characterises this region is grasslands interspersed with tall shrubs. The classification results were 50% accurate in this region as site 9 was incorrectly classified as lush shrubs / mixed vegetation when in fact grass is the dominant vegetation type found.

Zingqutu South: This region is situated within a valley and the vegetation is described as sparse thicket. This sparse thicket is found surrounded by grasslands which dominate the Zingqutu Ring.

The fact that the vegetation lies in a valley led to it being classified as shadow and the accuracy of the classification cannot be assessed in this situation.

The output classes, could not be matched to Acocks veld types or sub types with any degree of confidence and for this reason, it was not done. The unpublished vegetation map by Rutherford et al. (personal com.) was consulted and, with the exception of Tarkastad Montane Shrubland, which appears to correspond to the categories of shrubs and mixed vegetation and lush shrubs and mixed vegetation, the output classes could not be matched to vegetation types. It is believed that the principal reason for the classes not matching either of the vegetation maps is due to land use. Had the landscape been pristine, the differences in vegetation types may have been apparent due to differences in texture and spectral responses. The differing land practices between the former Transkei and South Africa seem to be the governing influences on the landscape with respect to image classification thus in this case; satellite image mapping would be more suited to creating a land use map than a vegetation map.

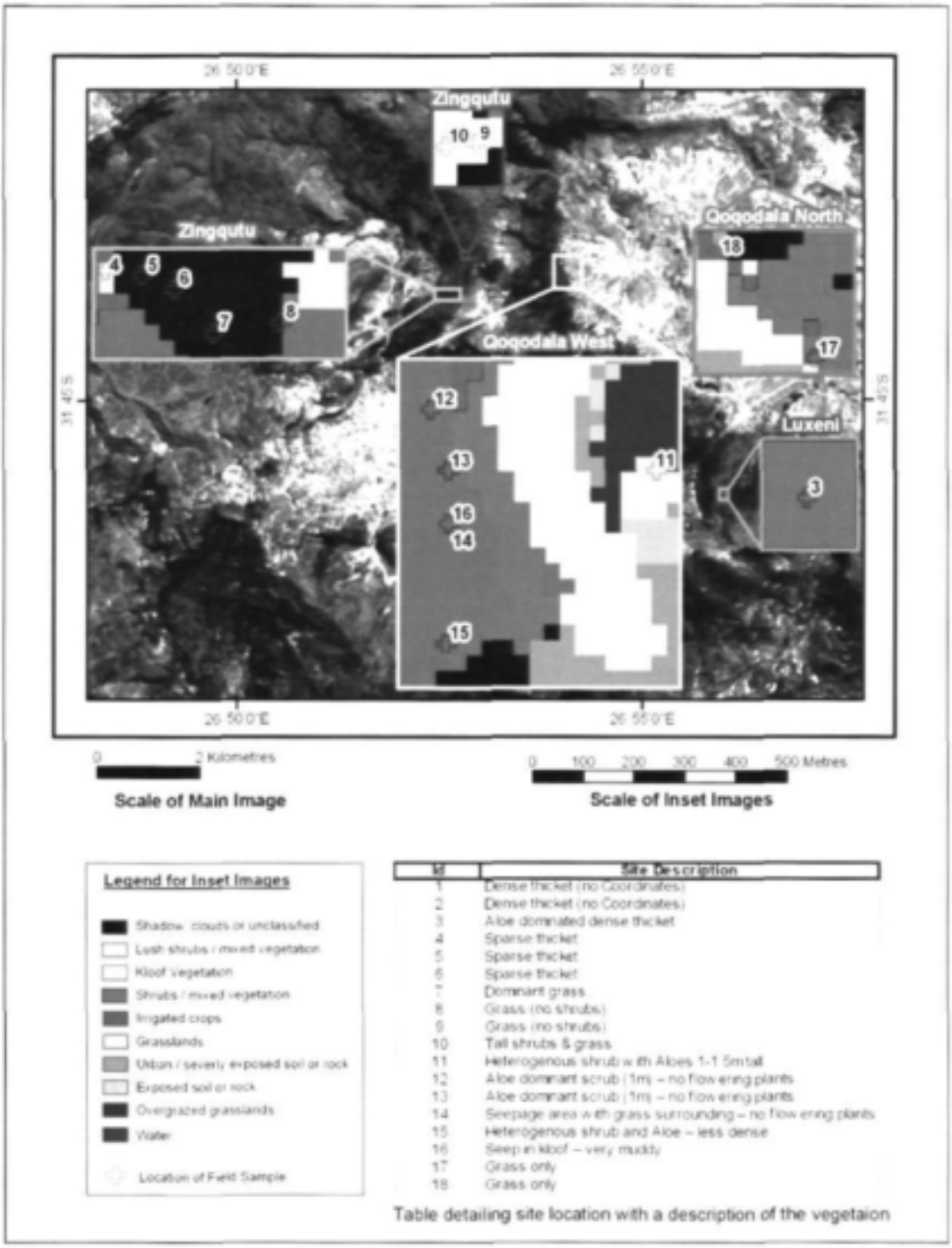

Id	Site Description
1	Dense thicket (no Coordinates)
2	Dense thicket (no Coordinates)
3	Aloe dominated dense thicket
4	Sparse thicket
5	Sparse thicket
6	Sparse thicket
7	Dominant grass
8	Grass (no shrubs)
9	Grass (no shrubs)
10	Tall shrubs & grass
11	Heterogenous shrub with Aloes 1-1.5m tall
12	Aloe dominant scrub (1m) – no flowering plants
13	Aloe dominant scrub (1m) – no flowering plants
14	Seepage area with grass surrounding – no flowering plants
15	Heterogenous shrub and Aloe – less dense
16	Seep in kloof – very muddy
17	Grass only
18	Grass only

Table detailing site location with a description of the vegetaion

Figure 34: Results of the classification compared with field data

The species list **(Table 14)** collected during field investigation does not include any species that are likely to be groundwater dependant or even wetland dependant (Low, 2003) and for this reason, ground water dependant ecosystems, even if they were detected in the classification, would not be able to be verified. However, the lush shrubs and mixed / vegetation and kloof vegetation which grow in the valley, fractures and southerly slopes may be phreatophytic. This should be verified by field work before any further conclusions are drawn.

Table 14: Species collected during field investigation

Acacia karoo	*Euclea racemosa*	*Lobelia setacea*
Aloe africana	*Euphorbia mauritanica*	*Lobostemon argenteus*
Aloe aristata	*Euphorbia cf. decepta*	*Lycium tetrandrum*
Aloe claviflora	*Felicia tenella*	*Matricaria sabulosa*
Aloe maculata	*Fern 1*	*Olea europea* subsp *africana*
Aloe pluridens	*"Grass"*	*Oxalis obtusa*
Aspalathus sp	*Helichrysum sp. 1*	*Pelargonium yrrhufolium*
Berkheya sp	*Helichrusum dasyanthum*	*Rhus glauca*
Chrysanthemoides incana	*Heliophila sp*	*Sarcocornia littorea*
Crotalaria capensis	*Hibiscus sp*	*Spiloxene sp*
Crassula arborescens	*Kedrostis nana*	*Zygophyllum morgsana*
Crassula rogersii	*Lachanalia sp*	

3.8.2 Wetland mapping

An initial field trip in July 2002 revealed seeps located on the slopes of the dolerite above the settlement areas. A seep, which is classified as a type of wetland, is defined as: "An area, generally small, where water [sic] percolates slowly to the land surface....used by some for flows too small to be considered springs" (Bates & Jackson, 1980).

The characteristics of the seeps found in the study area were somewhat unexpected. It is normally assumed that the presence of green vegetation indicates the presence of water. However, in

Qoqodala, the vegetation in the vicinity of the seep consists of grass which is dry, dead or dormant, whereas further away, the vegetation consists of greener shrubs and succulent bushes (**Plate 1**).

It is surmised that in the area immediately surrounding the seep, the water table is high and in the wet season after rain, the water table would be very close to the surface. The hardy shrubs, adapted to harsher, more arid conditions, are unable to grow and the grass and wetland vegetation thrive.

Wetland plants could not always be identified in the immediate vicinity of the seeps. However this does not imply that wetland vegetation is not present, as the vegetation on the seeps is grazed extensively by cattle, so the grass and other vegetation were cropped short making identification very difficult. In spite of this, a type of sedge, which is a typical wetland plant, was identified in the vicinity of some of the seeps. Furthermore, the seeps were characterized by dark organic and peaty soils in which mud cracks were apparent in the dry season. This indicates that these areas are saturated for at least some part of the year. Watering and dewatering of wetlands generally leads to the formation of landslides. The seeps commonly occur in small depressions created by fractures or lithological contacts. Depressions combined with landslides could be the start of future valleys. The individual seeps were typically smaller than $40m^2$ and sometimes as small as about $9m^2$. In addition, the seeps tend to occur in zones (**Plate 2**) of varying size and quantity.

In South Africa, there is no existing spatial data wetland inventory so wetlands needed to be mapped for the study area. The properties of multi-spectral satellite imagery are such that they contain bands that fall outside the wavelengths visible to the human eye. For example, wavelengths in the near infra red are very useful for vegetation mapping and these properties make it a more desirable mapping medium than colour or black and white aerial photography. Multi-spectral satellite imagery is recognized as being a very cost effective method of producing land cover maps at a regional scale and as wetland mapping can be seen as a form of land cover mapping, it was the chosen method for this research. It is assumed that the reader is familiar with basic remote sensing concepts, as these will not be explained in the text. However, Appendix A can be consulted for a brief overview of remote sensing principles and details of Landsat and Aster imagery can be found in Appendices B & C.

Plate 1: A wetland and seep in Luxeni (see Figure 34 for location). The seep is located to the right and in front of the author.

Plate 2: A zone of seeps on the southern rim of the Qoqodala Ring above Manelspoort village

The remote sensing processing was carried out on a small part of the Qoqodala sill and ring Complex i.e. the Qoqodala ring itself (**Figure 35**). The reason for choosing a small pilot area was to enable field verification of results to be carried out, it also includes the drill site, the wetland adjacent to the drill site, and the vegetation on the dolerite ring itself was of interest.

Methodology

The Department of Environment Affairs and Tourism (DEAT) has recognized the need to create an inventory of wetlands in order to effectively manage and conserve wetlands in South Africa. With this aim in mind, a pilot project (Thompson, Marneweck, Bell, Kotze, Muller, Cox & Smith, 2002) was commissioned to develop a methodology for establishing a cost-effective, accurate and comprehensive National Wetland Inventory. The remote sensing imagery chosen was multi-temporal Landsat TM and Landsat ETM+. Landsat was identified as having the best combination of spatial, spectral and costing characteristics when compared to other medium resolution satellite sensors. The study used a multi-temporal, multi-stage classification approach and attempted to map vegetated, as well as non-vegetated wetlands. The conclusion on using Landsat imagery for wetland mapping was as follows (Thompson et al., 2002):

1. Satellite based mapping is not suitable for detailed wetland mapping, if Landsat-type imagery is used, and the minimum mapping standards were as was specified[1].
2. It would be possible to use an alternate form of satellite imagery to increase spatial resolution. However the costs of this are not comparable to the costs of using Landsat imagery.
3. If higher mapping accuracies are desired, field work combined with aerial photography techniques are recommended.
4. Wetland mapping using Landsat imagery is essentially limited to a generic "presence or absence" mapping of "core" wetland areas.

[1]The terms of reference stated that the aim was to map 90 percent of all wetlands >1 ha and 50 percent of all wetlands >0.5 ha

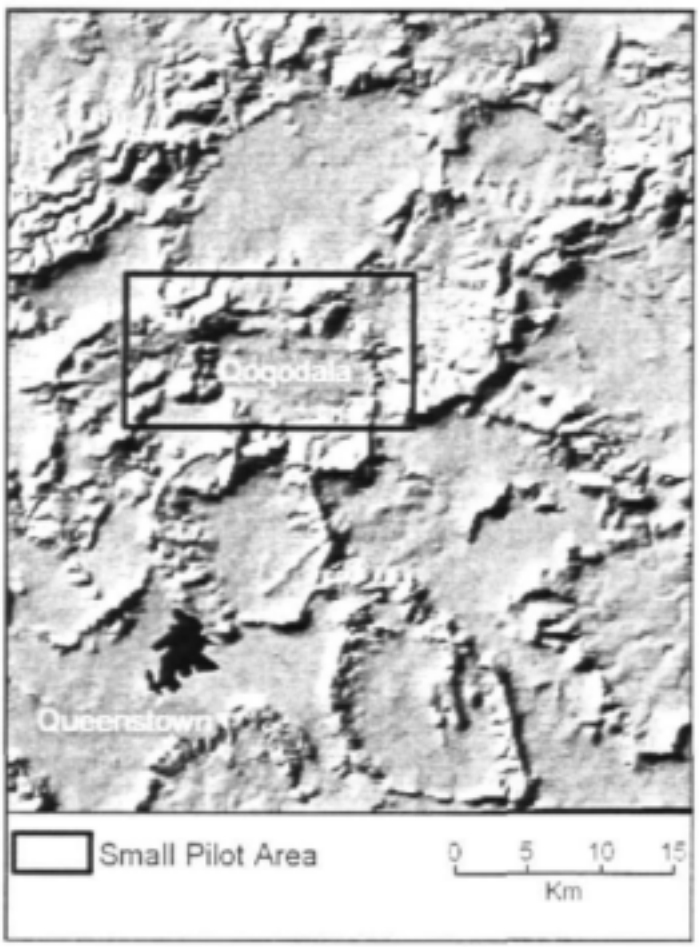

Figure 35: A hillshade of the study area showing the location of the area selected for wetland mapping and remote sensing processing

For a full description of the methodology used in the pilot wetland mapping project, Thompson et al. (2002) may be consulted. It was also concluded that the mapping accuracy of open-water wetlands is generally much higher than that of vegetated wetlands. This is due to the fact that open-water wetlands differ spectrally to the surrounding land-covers far more than vegetated wetlands do.

As multi-temporal Landsat imagery was one of the datasets available for the present research, it was decided to adapt and apply the above methodology in the study area. The available Landsat imagery was utilised in the processing. In addition, Aster imagery which has a higher resolution both spatially and spectrally than Landsat imagery was available. It was postulated that due to the higher resolution, it may present a viable alternative with higher mapping accuracies. On this basis,

the above methodology was further adapted and modified for use with Aster imagery (Gibson, 2003). If high level mapping accuracies were not achieved but general presence or absence of wetlands indicated, this may be an acceptable result.

The best time of year for the satellite images to be acquired is when the wetlands exhibit the most differences spectrally to the surrounding vegetation. This is especially true in the case of vegetated wetlands. This period is usually during the transitional 'wet-up' or 'dry-down' periods. In the summer rainfall areas, within which the study area falls, the optimum wet-period image period is likely to be from September to November. This is just after the onset of the summer rains when the wetlands are inundated and experiencing vigorous early season growth compared with the surrounding non-wetland vegetation. By the same reasoning, the optimal dry season image acquisition time is from March to May as wetlands are likely to remain wetter and greener for longer into the dry season than the surrounding non-wetland vegetation. Multi-temporal datasets (one wet-up and one dry-down image) are highly desirable. However where only single date imagery exists, it is possible to utilize this provided the image acquisition period is optimal. (Thompson et al, 2002).

The rainfall of Queenstown was carefully studied as Queenstown is the weather station in the study area with complete rainfall data and using this data, optimal dates for two Landsat images and an Aster image selected (Figure). The dry season Landsat TM image was selected from May 1984, a wet-season Landsat ETM+ image was selected from November 2000; and as only wet-season Aster imagery was available, October 2000 was selected. These dates fulfil the above criteria laid out by Thompson et al. (2002) for optimal image acquisition dates and all images were virtually cloud free.

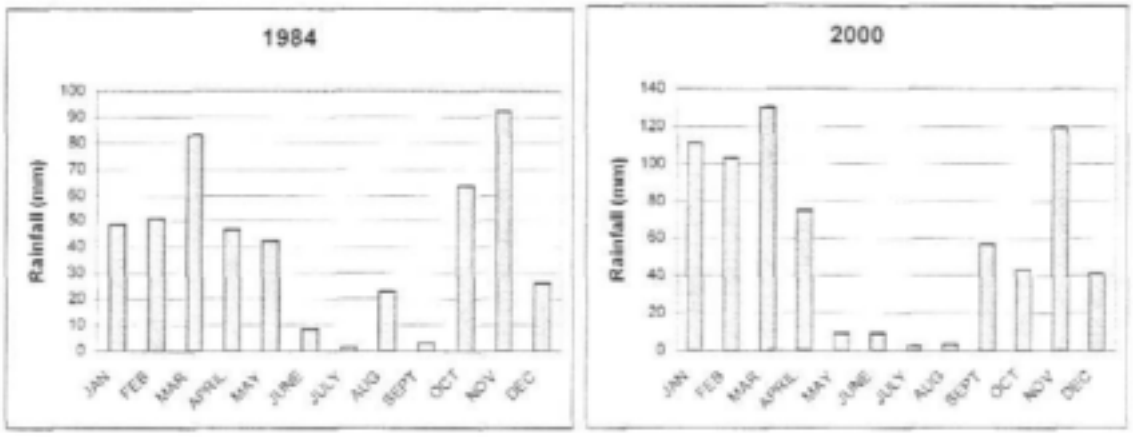

Figure 36: Rainfall data of Queenstown for 1984 and 2000 respectively (Data obtained from S.A. Weather Services).

Dry Season Landsat TM: May 1984

Wet Season Landsat ETM+: November 2000

Wet Season Aster: October 2000

A base map was prepared using data gathered during the initial field trip; then during subsequent field trips, the base map was expanded. This base map was used to assess the validity of results obtained in the office before field verification was undertaken (**Figure 37**).

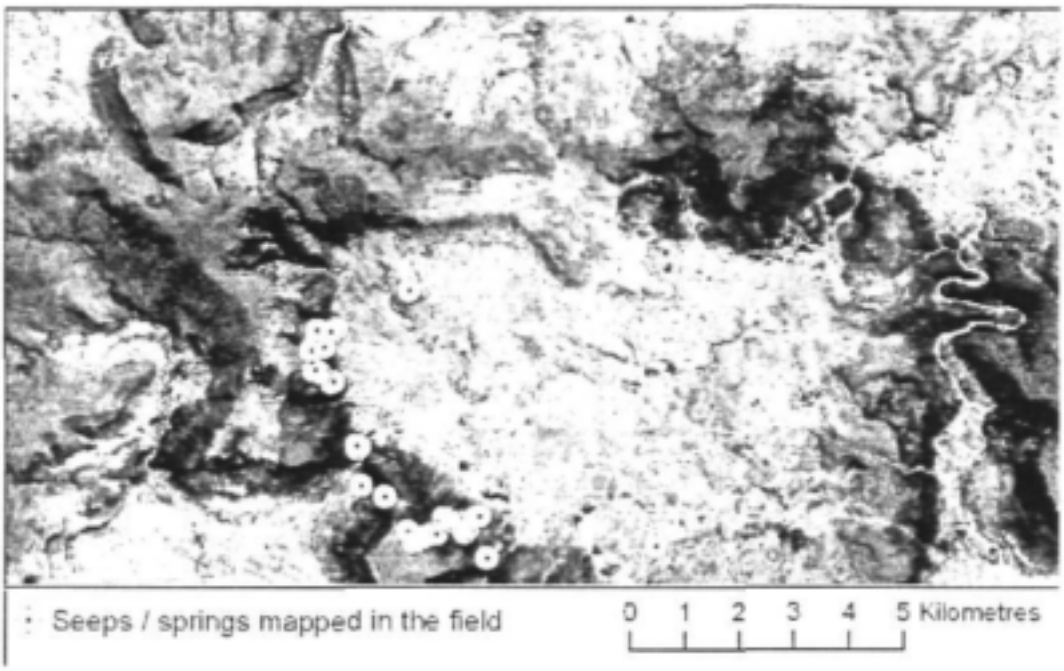

Figure 37: The base map showing the known seeps visited in July and November 2002 and used to assess the validity of results in the office.

The Landsat Classification Approach

The methodology is based largely on the proposal by Thompson et al. (2002) with two major exceptions (Gibson, 2003). Firstly, the process of creating a land cover map to exclude areas which cannot contain wetlands was modified. Secondly, the final hydrological modelling stage was also excluded from the research. A flow chart depicting the various steps in this approach can be seen in **Figure 38.**

Figure 38: Flow Chart of methodology used in the Landsat Classification Approach (Gibson, 2003).

Instead of creating an initial land cover map, it was decided to rather exclude the flat inner ring from processing. The reason for doing this is threefold. Firstly the seeps tend to occur either on the dolerite ring or on the contact between the dolerite ring and the sediment. Due to the fact that the people rely on rainfall for irrigation, it is highly likely that if wetlands existed in the inner ring in the past, they made an ideal location for crop or pasture and have been changed beyond recognition. Finally, the more homogeneous an image, the better the classification results will be (Smith, Wickham, Stehman and Yang, 2002), so it was decided to exclude the heterogeneous portions of the image which is the flat inner ring and only work with the more homogeneous dolerite upland portion of the image, as seen in **Figure 39.**

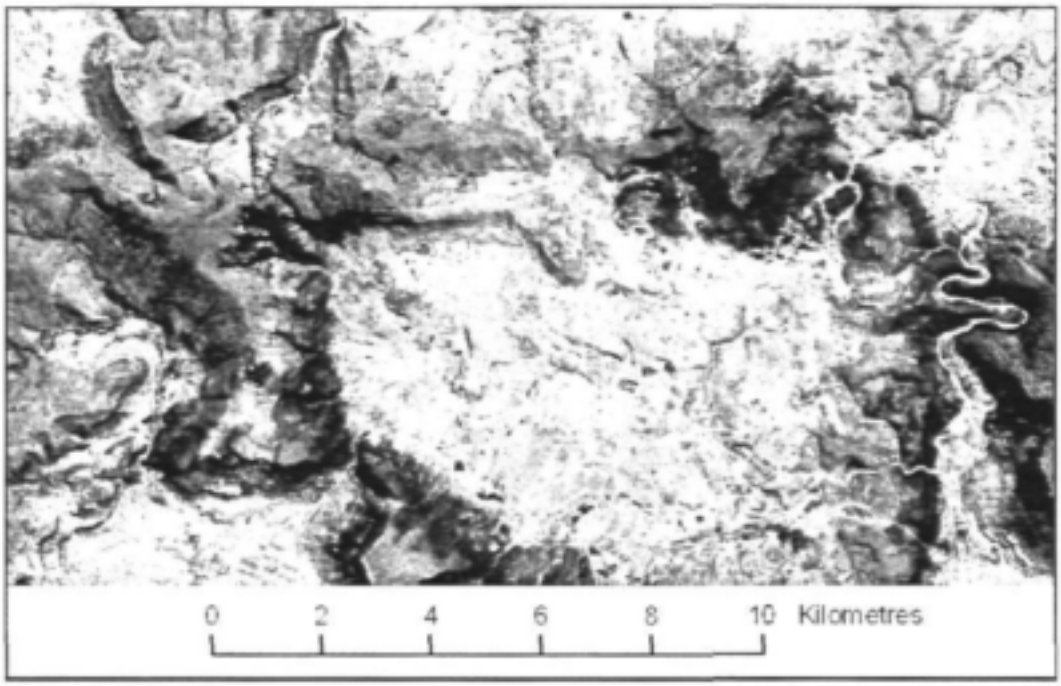

Figure 39: Aster band 1 image of Qoqodala. Note the heterogeneous nature of the inner ring due to haphazard land use.

Following on from the above reasoning, a mask was created in the following manner:

1. An ArcView® shape file of the dolerite had been digitized at a scale of 1: 50 000. The dolerite was then buffered by 200m to include areas of sediment immediately adjacent to the dolerite, as seen in **Figure 40A**. The reasoning behind this is that seeps often occur at the contact between two different lithological units so it was important to include these areas.

2. The inner ring does not always consist entirely of sediment. In some cases, the sediment has been eroded leaving the dolerite of the lower sill exposed. This is the case in the Qoqodala ring. However, it was still felt necessary to exclude the inner ring in order to exclude the highly heterogeneous portions of the image. A slope analysis was performed using a digital elevation model (DEM) and all areas with a slope of less than 5 degrees were clipped from the buffered dolerite layer, as seen in **Figure 40B**. The areas to be included in processing were given a code of one and those areas to be excluded a code of

zero. The vector layer was then converted to a raster layer and this was used as the masking band (**Figure 40C**).

The tasseled cap transformation is designed to rotate the axes in such a way that the data in which we are most interested is extracted. It was first proposed in 1976 by Kauth and Thomas who found that in four dimensional MSS[2] data space, there is a line, oblique to all four axes, which represents soils, and a triangular area which represents various stages of growth in vegetation (Crist & Cicone, 1984).

Crist & Cicone (1984) adapted the tasseled cap transformation for use with Landsat TM data. It was found that data in the six reflective bands occupy three dimensions. Two of these dimensions relate to the original Tasseled Cap Greenness and Brightness index; and the third component is affected mainly by the short wave infrared (SWIR[3]) bands.

This third dimension has been called Wetness, as absorption by vegetation in the mid-infrared bands is caused primarily by soil moisture content.

The influence of each Landsat TM band in the creation of the new indices is as follows:

- Brightness: a weighted average of the six Landsat TM bands
- Greenness: visible, near infrared (NIR) contrast with little contribution from mid infrared (MIR) - Bands 5 and 7.
- Wetness: contrast between MIR (bands 5 and 7) and the red and NIR (bands 3 and 4). Mather (1999)

[2] MSS: Multi-spectral Scanner. Landsat satellite preceding Landsat TM. Landsat MSS consisted of only four spectral bands which explains the reference to four dimensional space.
[3] Short wave infrared is also known as mid infrared (MIR)

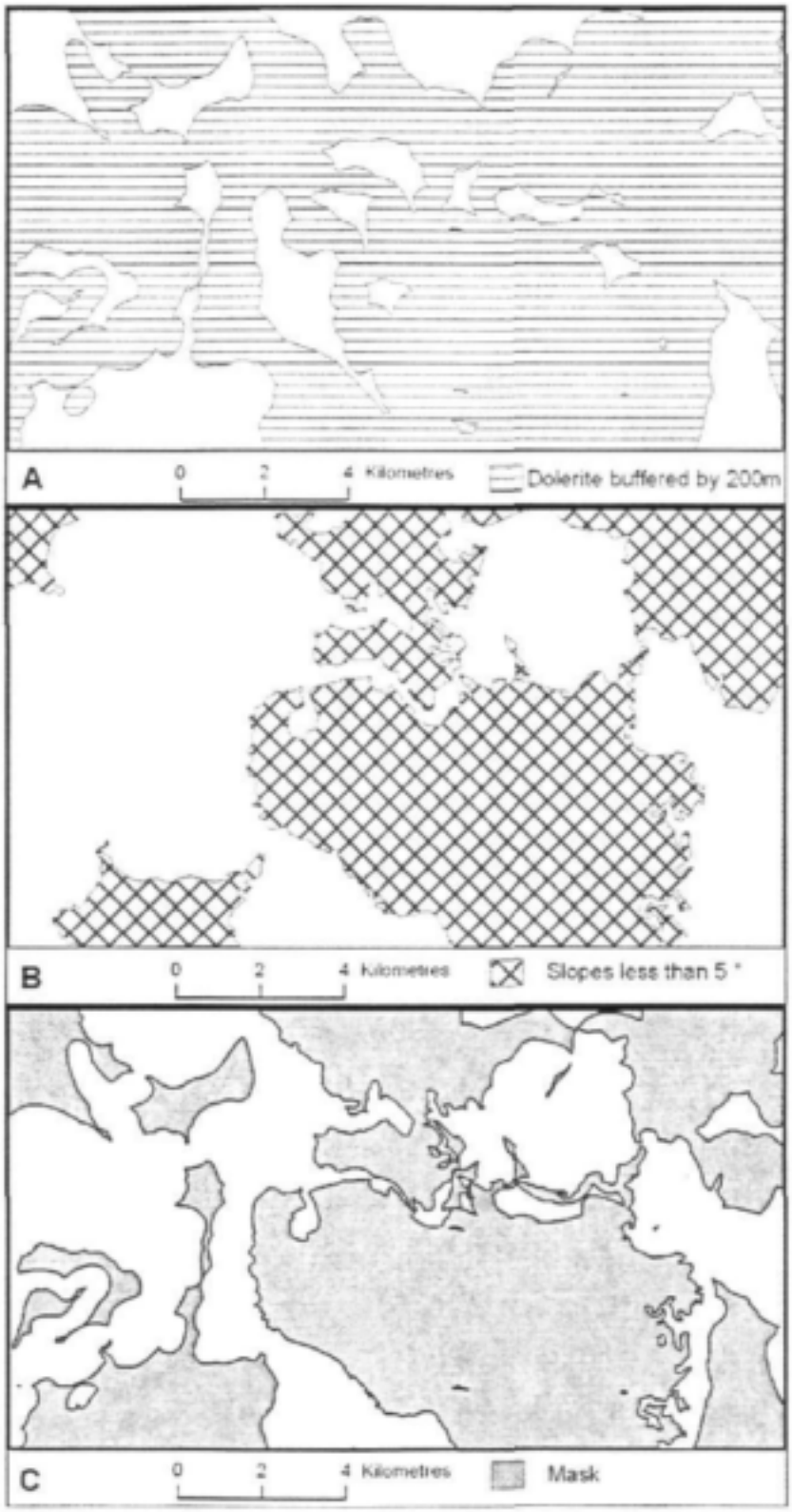

Figure 40: The mask creation process. A: The dolerite is buffered by 200m; B: all slopes less than 5° are isolated and C: A and B are combined to produce a mask.

The normalised difference vegetation index (NDVI) uses a ratio of the visible red and near infrared bands of an image to create a 'greenness' or biomass index. The NDVI can be applied to any satellite image which contains bands in the red and near infrared wavelengths. It is used on a global or continental scale using coarse resolution imagery to study patterns in vegetation change, and can be used on a more regional or local scale using Landsat or Aster. The NDVI is based on the differences in reflectance by healthy vegetation of the visible red and near infrared wavelengths

The TCT was performed on each of the Landsat images, using the above mentioned mask to exclude the inner ring. Similarly a NDVI for each image was produced. These six resulting files were then stacked to create a multi-layered file on which the classification was to be performed.

As per the recommendations by Thompson et al. (2002), an unsupervised method of classification was chosen for this research. Unsupervised classifiers do not use training data as the basis for classification; algorithms cluster pixels in a data set based on statistical relationships. These algorithms examine the pixels in an image and assign them to a class, based on the natural grouping or clustering of the digital number values. The basic premise is that values within a given cover type should be close together in measurement space, whereas data in different classes should be well separated. (Lillesand & Kiefer, 2000; Research Systems, Inc, 2001).

An unsupervised classification was run using Research Systems, Inc. software (ENVI) with a maximum output of 20 classes.

Results of the Landsat Classification Approach

The classification image that was produced did not indicate any one class representing the known seeps so it was presumed that these wetlands were too small to be detected. It is possible that perhaps larger wetlands were present higher up the slopes in areas that had not been visited in the field and visual interpretation of the image revealed the probably occurrence of grasslands. Since the seeps lower down the slopes are characterized by grass, it was presumed that the grass on the higher slopes could potentially contain wetlands. In addition, dense vegetation growing in river valleys could be identified by visual inspection of the unprocessed image. As these valleys and

kloofs are potentially moister areas, these areas are also of interest to the study. With the above in mind, five classes which could potentially contain wetlands were selected with three 'types' of potential wetlands being identified. The three types were identified visually using differences in colour and texture to distinguish between them (**Figure 41**).

The first type consisted of one class and was provisionally called kloof vegetation. It was believed that this class constituted vegetation growing in kloofs, high shadow and moist areas or along riverbanks. No field work was done on this class but it is thought that this class may correspond to the groundwater dependant ecosystem known as base flow. Two further types were identified and provisionally called wetlands type one (made up of one class) and wetlands type two (made up of two classes). Wetlands types one and two were mostly located on the highest parts of the slope in areas that probably received the most precipitation and as a result, the potential for finding wetlands is greater. The three types of wetland classes were then vectorised. Area calculations are given later in the text where the results of the Landsat classification approach are compared with the results of the Aster classification approach (**Table 17**).

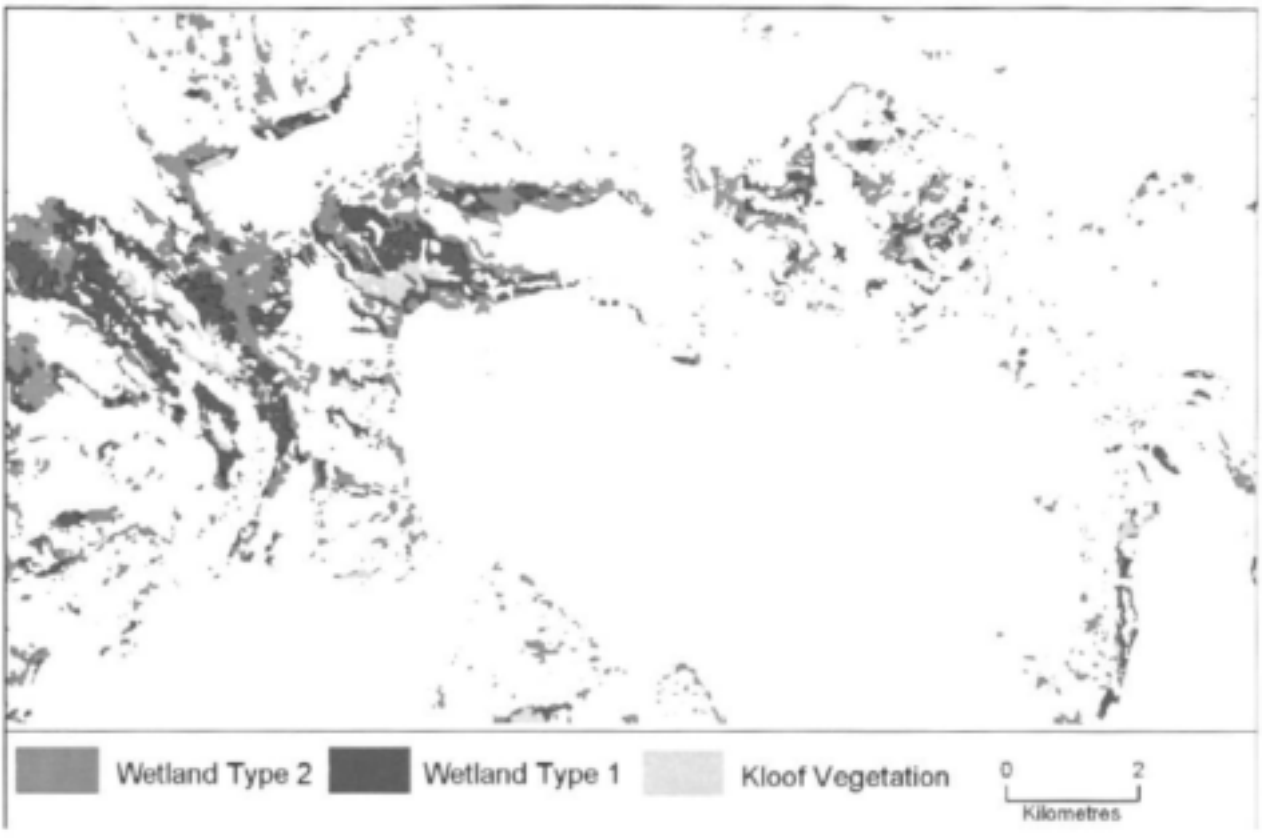

Figure 41: The results of the Landsat Classification Approach.

The Aster Classification Approach

The method proposed by Thompson et al (2002) was then modified further for use with the Aster image available for the study area. A flowchart of the methodology is given in Figure. As can be seen in Appendix, Aster has three bands with a fifteen metre resolution making it a better option for detecting smaller wetlands. However, there are two drawbacks with using Aster in this study. Firstly, only a single date image was available for the study area and, secondly, the wavelengths represented by Aster bands do not correspond exactly with the wavelengths represented by Landsat bands (see Appendix C). This necessitated the further modification of the technique (Gibson, 2003).

Ideally, the methodology requires multi date imagery for this processing but where only one image is available, a single date image can suffice provided that the image was acquired at an optimal time of year. For vegetated wetland detection the optimal time of year would be at the onset of the rainy season, as it is at this time that the vegetation in the wetland will show the most difference compared with the surrounding non-wetland vegetation. Wetlands are the first to be inundated with water after the first rains, so wetland vegetation responds earlier in the season than non-wetland vegetation (Thompson et al., 2002). An Aster image was available for 16 October 2000 and as the summer rains began in September that year, this date is considered ideal if using single date imagery. This resulted in the dataset built for classification consisting of only three layers excluding the mask layer: the NDVI for the wet season and the greenness and wetness indices (from the tasseled cap transformation) for the wet season. This is in contrast to the six layers, excluding the mask layer used in the Landsat classification approach.

The differences in band wavelengths between Aster and Landsat presented a particular challenge. The methodology required the application of the tasseled cap transformation (TCT) to the data. This is problematic as the TCT was developed for Landsat imagery and not Aster imagery. A concern of the author was whether the application of a technique specially developed for Landsat image on Aster image is scientifically valid. Personal correspondence with Prof. Paul Mather suggested a method whereby coefficients of the tasseled cap transformation could be calculated specifically for Aster image data. This method is dependent upon the definition of the soil line and involves the identification of pixels of bare wet soil and bare dry soil. Since it is crucial that these pixels are recorded at the time of the satellite passing overhead, it was not possible to attempt this method. The reader can consult Mather (1999) for further reading on this subject. Since it was not possible to calculate coefficients for Aster imagery and the results were to be used qualitatively and not quantitatively, it was decided to use the standard coefficients and assess the results.

As illustrated in Appendix C, the band wavelengths for Landsat and Aster are not equivalent. There is no equivalent for Landsat band 1 in the Aster bands and conversely there are four Aster bands that fall in the range of Landsat band 7. There appeared to be no alternative but to simply use Landsat band 1 resampled to 15m for the TCT on the Aster data. The ratio of input of each band to

output index (**Table 15**) was examined and it was discovered that band 1 most influences the output of the dryness and to a lesser extent the greenness index. Band 1 also has minimal influence on the wetness output index. It was thus decided that this was an acceptable solution.

Table 15: Coefficients for the tasseled cap functions 'brightness', 'greenness', and 'wetness' for Landsat Thematic Mapper bands (from Mather, 1999).

TM Band	**1**	**2**	**3**	**4**	**5**	**7**
Brightness	0.3037	0.2793	0.4343	0.5585	0.5082	0.1863
Greenness	-0.2848	-0.2435	-0.5436	0.7243	0.0840	-0.1800
Wetness	0.1509	0.1793	0.3299	0.3406	-0.7112	-0.4572

Landsat band 7 covers the wavelengths represented by Aster bands 5, 6, 7 & 8. Correlation statistics were carried out in order to determine which of these bands correlated best to Landsat band 7. Additionally, the mean of the five bands was calculated, as was the first principal component and correlations between these two outputs and Landsat band 7 was also examined. The results, shown in **Table 16** below, indicated that all the outputs were similarly correlated with Aster band 7 slightly outperforming the rest.

Table 16: Correlations between Landsat band 7 and Aster bands.

	Landsat Band 7	Aster Band 5	Aster Band 6	Aster Band 7	Aster Band 8	Mean Aster 5-8	1st PC Aster 5-8
Landsat Band 7	1	0.771876	0.761988	0.772333	0.767489	0.772188	0.772201

The study area was processed in the manner modified and described by Gibson (2003) and shown in the flow diagram in **Figure 42**: It is summarised as follows:

A pseudo-Landsat file was built as follows:

Band 1 = Landsat band 1

Band 2 = Aster band 1

Band 3 = Aster band 2

Band 4 = Aster band 3

Band 5 = Aster band 4

Band 7 = Aster band 7

The tasseled cap transformation was run on this file using Research Systems, Inc.® software and the Greenness and Wetness Index was extracted and saved for later processing.

A multi-layer dataset was then created using the NDVI and the Greenness and Wetness Indices from the TCT. An ISODATA unsupervised classification was run on this dataset in the same way and using the identical parameters as in the case of the Landsat Classification Approach.

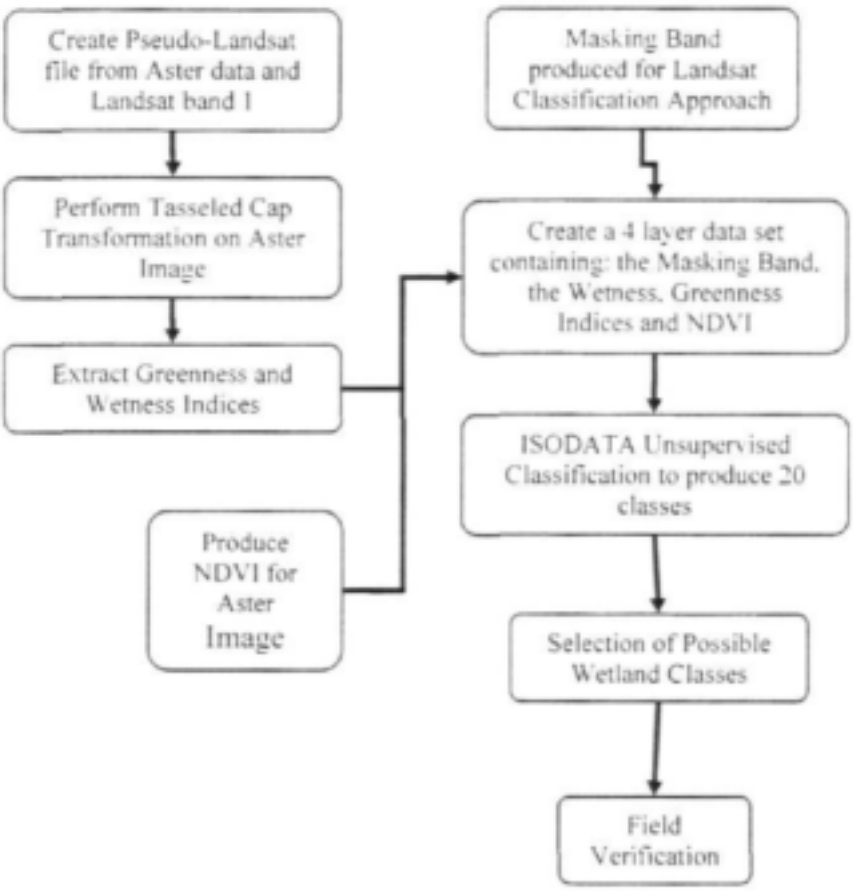

Figure 42: Flowchart of Methodology for Aster Classification Approach

Results of the Aster Classification Approach

Similar to the Landsat processing, the results of the processing on the Aster imagery produced 20 classes with no one class representing the known seeps. The three wetland types identified using the Landsat images were matched to the results from the Aster classification (**Figure 43**). The difference in the Results of the Landsat and Aster Classification Approaches in total area covered by wetland type one and two (with the exception of kloofs) does not appear to be significant (**Table 17**). However, it is apparent that the Aster classification approach tends to select smaller areas for each class than Landsat Classification Approach as the Aster Classification approach yielder many more polygons. By implication, the Landsat Classification approach results in fewer areas defined as wetlands but these wetlands are large. Contrarily, the Aster Classification Approach results in many more areas being identified as wetlands but these areas tend to be small.

Table 17: Total area covered by each wetland type.

	Total Area (m2)	Mean Area m2)	No polygons	No classes
ASTER: Kloof	4474125	2048	2184	3
ASTER: Type 1	7343837	1380	5319	1
ASTER: Type 2	9014726	1550	5813	2
Landsat: Kloof	2130217	8486	251	1
Landsat: Type 1	8909743	9027	987	1
Landsat: Type 2	12699987	8627	1472	2
Total ASTER (excluding kloof) = 16358563m^2				
Total Landsat (excluding kloofs) = 21609730m^2				

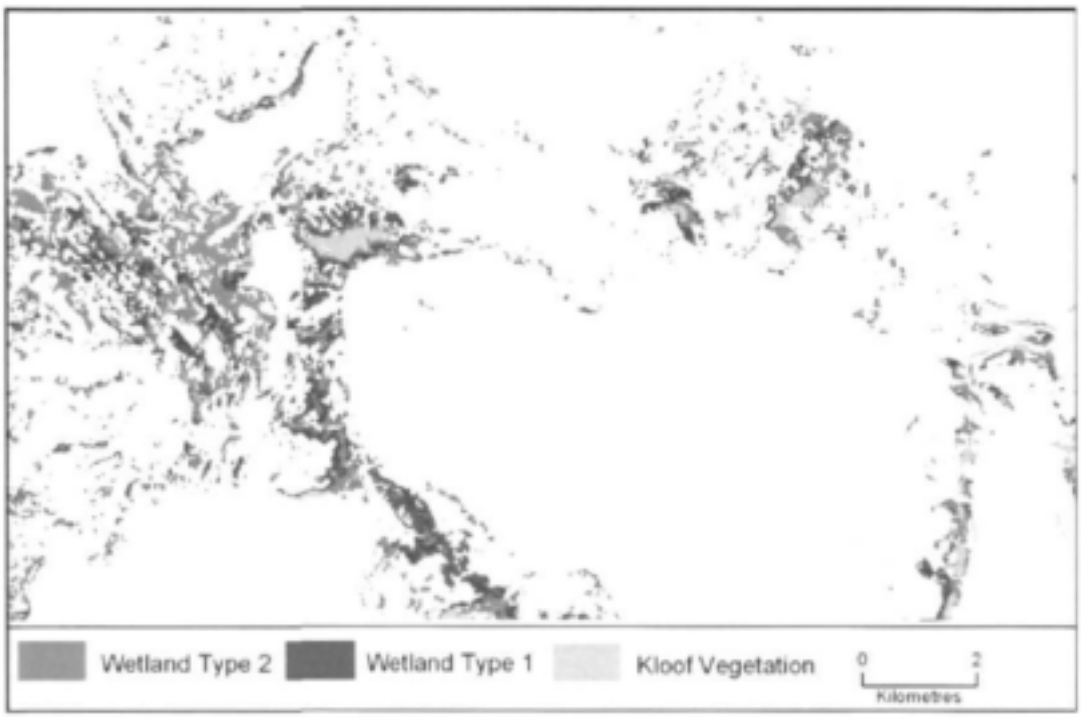

Figure 43: Results of the Aster Classification Approach

Fieldwork and discussion of results

The results of both classification approaches were matched to the base map (**Figure 44**). The following conclusions can be drawn.

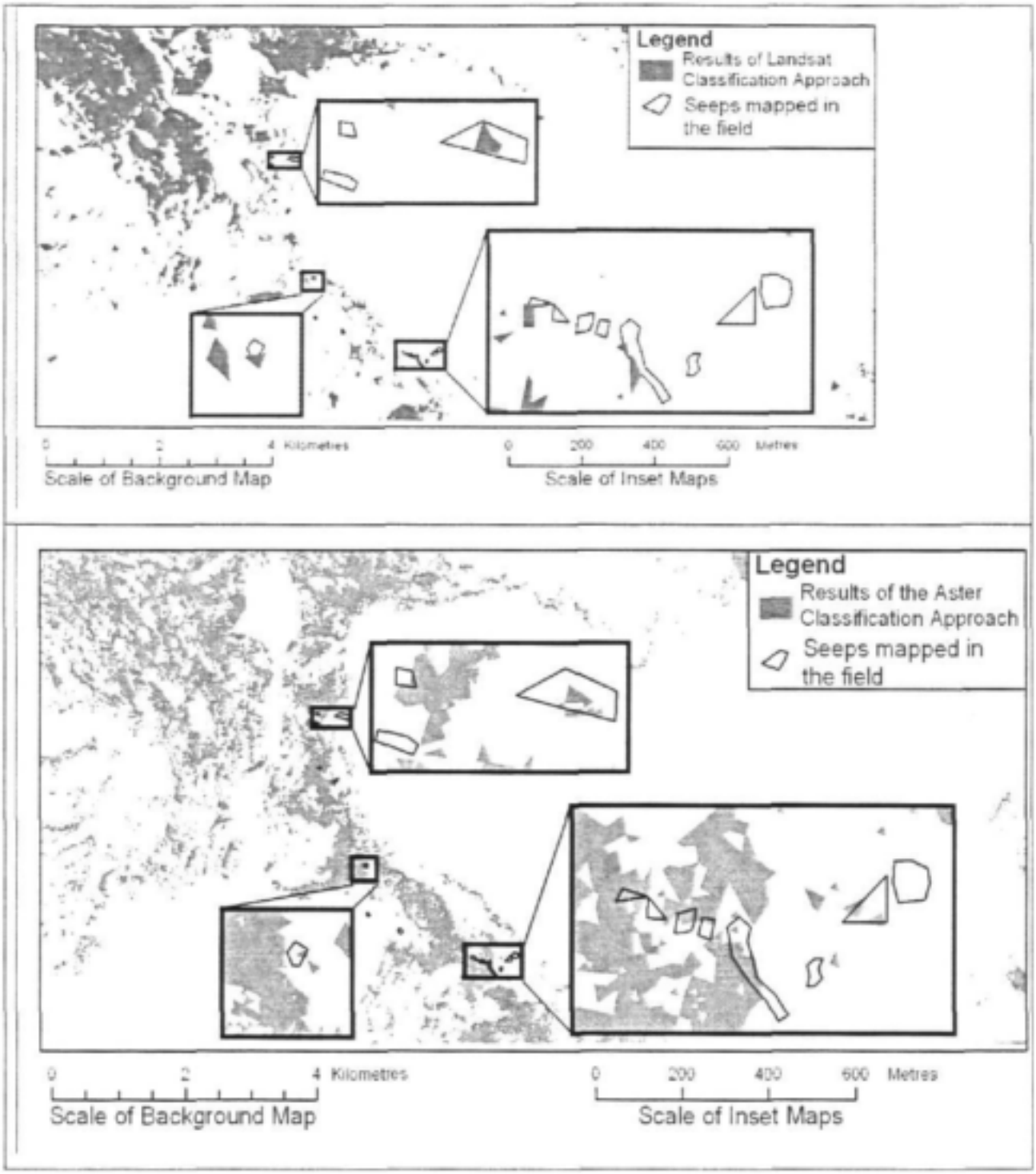

Figure 44: A: Results of the Landsat Classification Approach compared with the location of known seeps. B: Results of the Aster Classification Approach compared with the location of known seeps.

It can be seen examining **Figure 44** that the results of both approaches were not very accurate. In the Landsat Classification Approach no seep was completely detected however four out of a possible twelve were partially detected. In the Aster Classification Approach, eight out of twelve seeps were partially detected. What is most apparent from examining the maps is the amount of wetland type one & two was detected in the high lying areas which had not been visited during field work. It was possible that wetlands existed on the high lying areas that had not been previously visited in the course of field work.

For this purpose, fieldwork was carried out in March 2003. The study area was divided into four areas that covered the largest areas of suspected wetlands (**Figure 45**). The aim was twofold. Firstly to visit the four areas and do a "presence or absence" check to determine whether or not the classes selected are in fact wetlands. Secondly if there are wetlands present, one area would be chosen and the accuracy of the results of the Landsat classification approach to the results of the Aster classification approach would be compared.

After a field trip to all four areas, it became apparent that what had been identified as being wetland type 1 and wetland type 2 was in fact grassland which was being used as pasture for cattle. There was no visible difference between 'wetland' type 1 and type 2 except that perhaps type 2 was more of a mixed type of grass and small loose boulders or interspersed with small shrubs, whereas type one tended to consist mostly of grass.

The following could explain why the Aster classification approach did not detect as many grass/lands/ wetlands as the Landsat classification approach: The Aster image was acquired in October 2000 and the Landsat image was taken in November 2000. The summer rain of 2000 began in September which means that the landscape captured by the Landsat image was exposed to a month more rain than the landscape captured by the Aster image. In that month the temperature would have increased, the daylight hours would have extended and these coupled to the additional rainfall would have induced grass growth. So the landscape captured in the Aster image simply does not have as much green grass as the landscape captured by the Landsat image.

From this result, it was unnecessary to conduct a more detailed survey of one of the four areas as there were no wetlands to be surveyed. It was also not practical to try to determine the respective accuracy of the Landsat classification approach and the Aster classification approach in terms of pasture mapping, as the season in which the fieldwork was being conducted (March) differed to the time of year of image acquisition (October and November).

Figure 45: Areas selected for checking presence or absence of wetlands.

It can be seen by the results presented that the methodology selected for this research was inconclusive. Possible reasons for the limitations of the methodology will now be discussed.

a) Small patch size and heterogeneous landscape

The smaller the patch size of individual land covers, the more heterogeneous the landscape and the less accurate the classification result (Townshend et al., 2000). According to Smith et al (2002), landscape characteristics that have been hypothesized to contribute to pixel misclassification include high land cover heterogeneity, small patch size and convoluted shapes all of which result in pixels being harder to classify. They concluded that as heterogeneity increases, the probability of misclassifying pixels increases, while as patch size increases, the probability decreases. Although the most heterogeneous inner ring was masked from the image classification, the landscape was

nonetheless too heterogeneous with the patch size of the wetlands too small to be detected using this imagery and this method.

b) Spectral signature of the wetlands is not unique

According to Gorte (In Stein et al. 2002), in order to obtain information from multi-spectral imagery; the multi-dimensional, continuous reflection measurements have to be transformed into discrete objects which are distinguished from each other by a discrete thematic classification. However, within different objects of the same class and even within a single object, the reflection is not always the same. Conversely, different thematic classes cannot always be distinguished in a satellite image because they display almost the same reflection. In cases such as these, deterministic methods such as unsupervised classification will not be successful and an alternative method should be found.

3.8.3 Mapping a groundwater dependant ecosystem

An attempt was made to determine if a specific vegetation type (vegetation found on seeps) could be mapped and how its distribution is influenced by the dolerite structures. It must be emphasized that this was an experimental attempt using a combination of image processing and slope analysis. The aim of this experimental mapping attempt is twofold: firstly to see if any trends can be identified and secondly to illustrate how remote sensing and GIS could be used for the purpose of ecosystem mapping.

The approach used for this stage of the remote sensing part of the project differed to that used for wetland mapping. The properties of Aster imagery are shown in Appendix B. Summed up here: Aster consists of 14 bands ranging from visible light to thermal infrared. The resolution for the visible and near infrared wavelengths is 15m, for the shortwave infrared 30m and for the thermal infrared 90m. It was decided not to use the thermal infrared bands as the resolution is too coarse for the purposes of this project. This brings the number of available bands down to nine at a resolution of 15m (SWIR bands resampled to 15m). Although theoretically Aster is a multispectral sensor, with nine bands one can began to use it as a hyperspectral image and, as such, apply hyperspectral processing techniques to the image. Various hyperspectral processing techniques

were investigated and ultimately the technique chosen was matched filtering. A very simple explanation of this technique now follows but interested readers are referred to Research Systems, Inc., 2001; Van der Meer, De Jong and Bakker, 2001; and Jacobsen, Heidebrecht & Nielsen (1998) for a more detailed explanation. A few basic principles must first be outlined. In remote sensing, the object which one wishes to map seldom falls precisely within the boundaries of one pixel or alternatively the object being mapped sometimes occurs at a sub-pixel level. This is known as a mixed pixel effect where the spectral response of a pixel is made up of the spectral response of all land cover types present within that pixel. Matched filtering is a technique whereby it is possible to calculate the influence of the spectral response of a specified input pixel - or group of pixels - on the spectral response of every pixel present in the image. The result is a greyscale image with values ranging around one. A value of one indicates a perfect match which means that it contains the exact spectral response as the input (reference spectrum). The further away the value moves from one, the less similar the spectral response of the pixel to the reference spectrum and the less likely the pixel is to contain that input land cover.

Before applying the matched filtering technique, a Minimum Noise Fraction (MNF) Transform is applied to the image. The MNF transform is a modified version of the Principal Component Analysis that orders the output components by decreasing signal to noise ratio. This methodology results in a set of components in which noise levels increase uniformly with increasing component number. In other words, the low-order components should contain most of the image information (signal) and little image noise (Microimages, 2001). The matched filtering algorithm is applied to the first five MNF transform bands as these bands should contain maximum signal and minimum noise.

Water-linked ecosystems are of most interest in this study therefore the chosen input was a pixel in a known seep (**Figure 46**). The methodology used is illustrated in the flowchart in **Figure 47**. The same rationale in which a mask excluded the inner rings from processing in Landsat and Aster classification approaches was applied here, and only the dolerite and adjacent sediment was analysed. The matched filtering algorithm contained in Research Systems, Inc. software was run and a greyscale image of the local study area was produced. The output greyscale image is difficult

to analyse as the value of interest (1) lies somewhere in the middle of the data range. Threshold limits need to be determined whereby pixels between these determined values are deemed to consist mostly of the input land cover type; in this case the vegetation on the known seep. Pixels with values of between 0.8 and 1.2 were chosen as having a relatively high degree of match to the reference spectrum and as such were selected as being the same as the input pixel. A map was produced illustrating all pixels comprising mostly of the same vegetation as found on the known seep (loosely referred to as 'seeps' from now on).

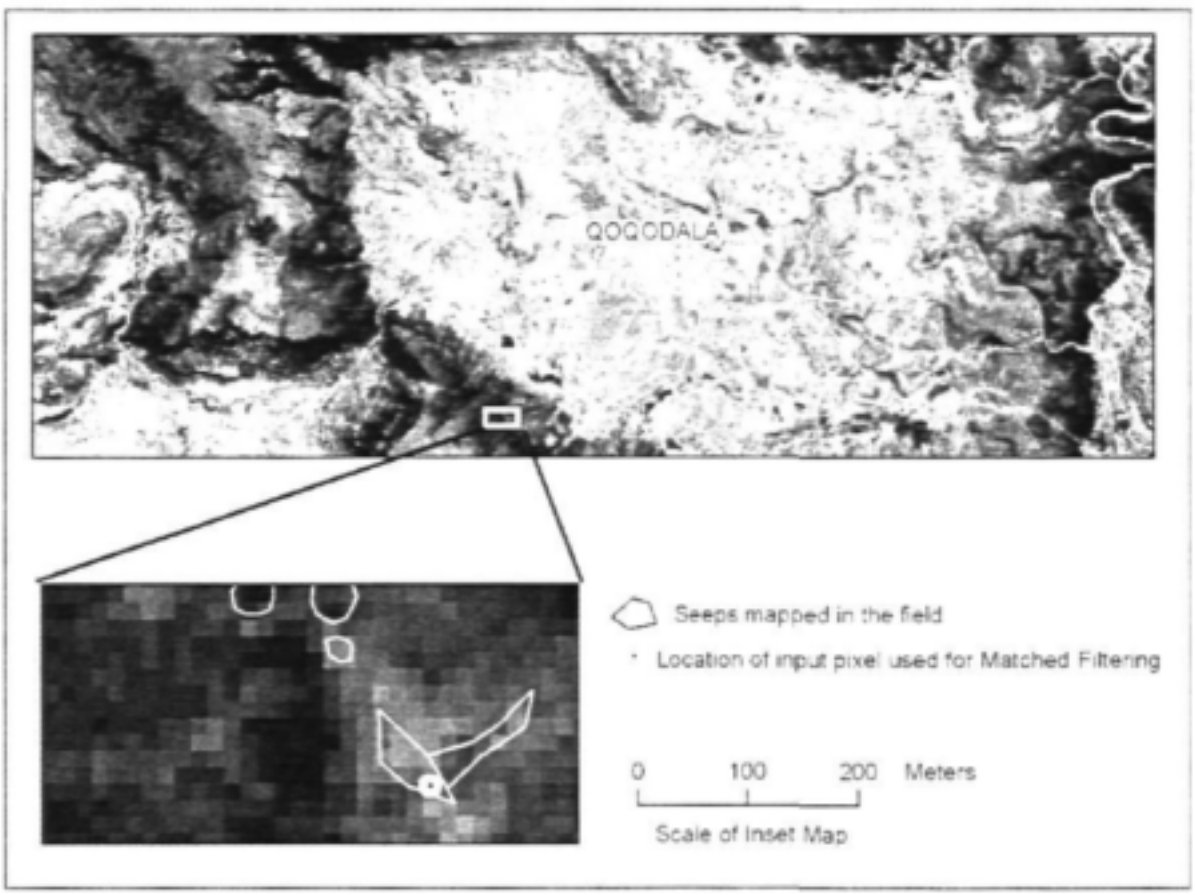

Figure 46: The location of the input pixel of the known seep used in the matched filtering processing

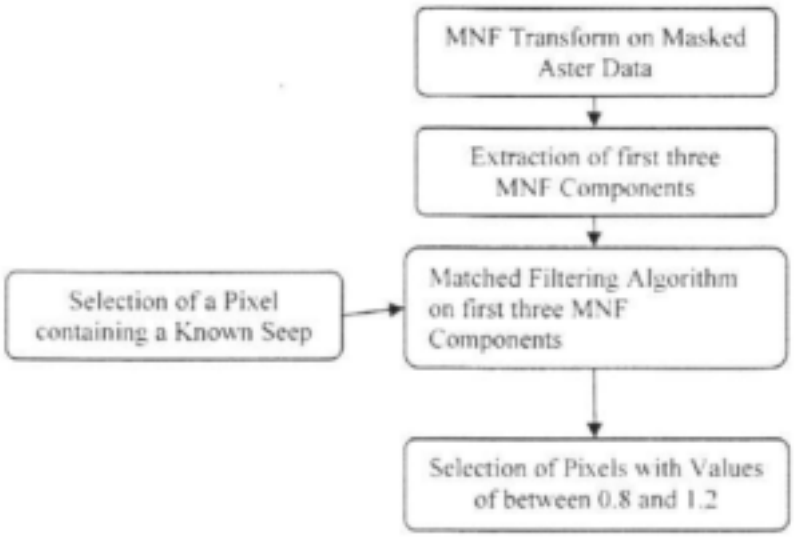

Figure 47: A flowchart showing the methodology used in the groundwater dependant ecosystem mapping

Results

As with the wetland mapping results described in Chapter 3.4.2, the results of seep mapping when compared to known seeps mapped in the field were disappointing (**Figure 48a**). However in other areas where seeps are known to occur such as Luxeni, a large number of seeps were detected (**Figure 48b**). It must be noted that field work was not aimed at checking the results of the ecosystem mapping and field work of this nature would be very labour intensive and time consuming.

The second step was to combine the 'seeps' with the DEM with the aim of comparing the elevation of the seeps to the elevation of the dolerite. The 'seeps' image originally had a resolution of 15m whereas the DEM has a resolution of 50m. The effect of combining the two images was to reduce the resolution to the coarser of the two being 50m. This resulted in many seeps comprising of individual pixels being removed from the processing but on the other hand the smallest 'seep' was now represented as being 50m by 50m. The dolerite as discussed earlier had been divided into 5 elevation classes as follows : Class 1 = 340 – 942m; Class 2 = 943 – 1181m; Class 3 = 1182 – 1389m; Class 4 = 1390 – 1628m; Class 5 = 1629 – 3000m. The sediment adjacent to the dolerite

was included in the analysis as it was included in the image processing (see **Figure 17**). This sediment was called Contact Zone and the elevation of this class was not taken into account.

A slope analysis was carried out for each class of dolerite class and definite trends were highlighted and discussed in Chapter 3.2. To summarize here, slopes were divided into 5 categories based on the natural breaks in statistics and are dolerite elevation classes are described in terms of their position on the dolerite ring (**Table 18**).

Table 18: Dolerite elevation classes with dominant slope and position on dolerite ring.

Class	**Dominant Slope Category**	**Position on Dolerite Ring**
Contact Zone		Steep slopes at the foot of cliffs
Class 1	slopes $\leq 8°$	Flat slopes transition to flat sill
Class 2	$8° \leq$ slopes $\leq 28°$	The inclined sheet
Class 3	$8° \leq$ slopes $\leq 28°$	The inclined sheet
Class 4	$8° \leq$ slopes $\leq 28°$	The inclined sheet
Class 5	All	Outer sill

A density analysis of the seeps present in each dolerite elevation class was then run and the results presented in the graph in (**Figure 49**). It was found that Class 1 contained the most seeps relative to the area covered by Class 1 and Class 5 contained the lowest density of seeps.

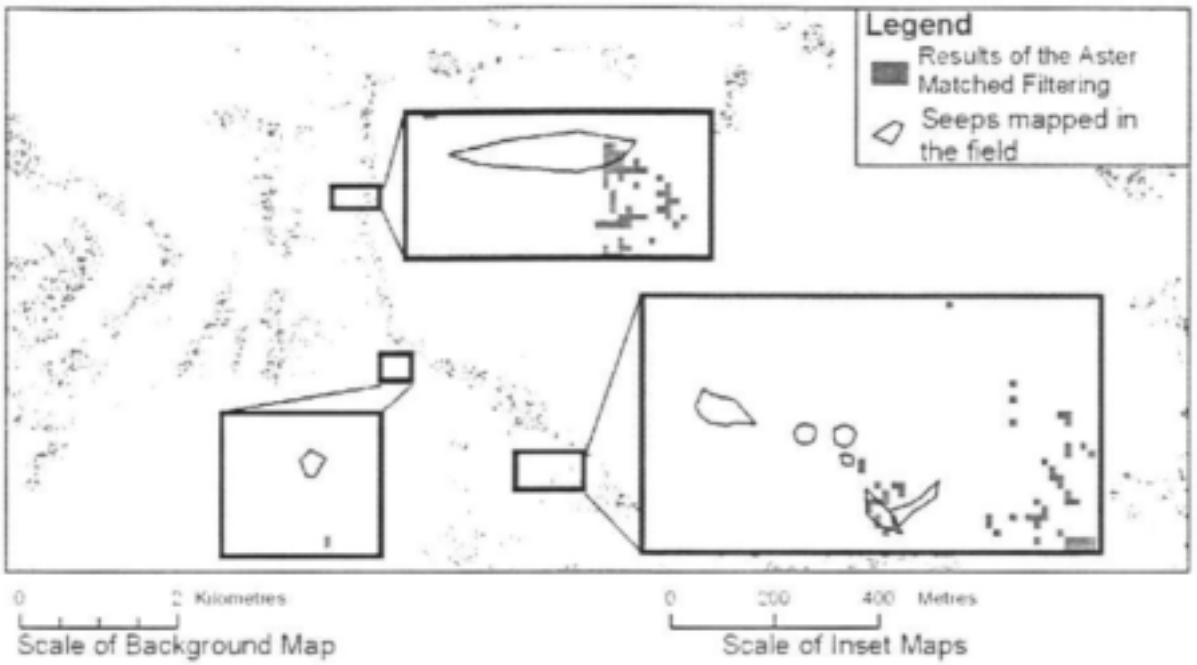

Figure 48: A: The results of groundwater dependant ecosystem mapping as compared to the base map of known seeps.

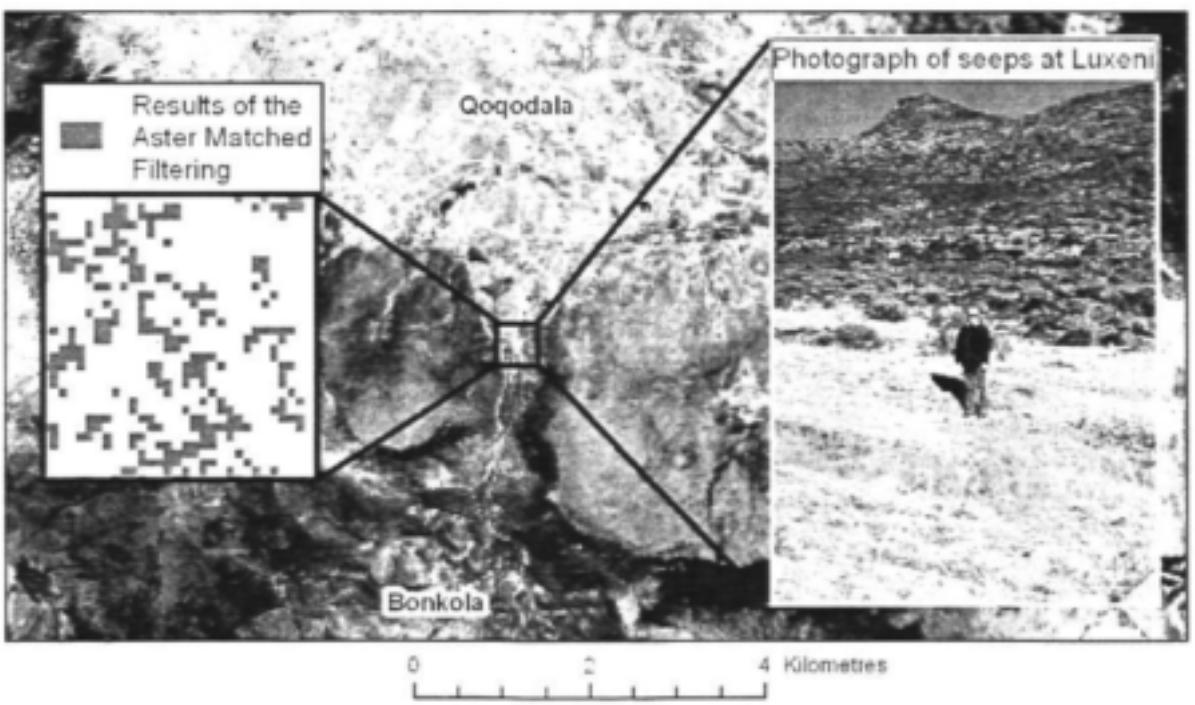

Figure 48: B: The results of groundwater dependant ecosystem mapping compared to an area of known seeps but precise locations unknown.

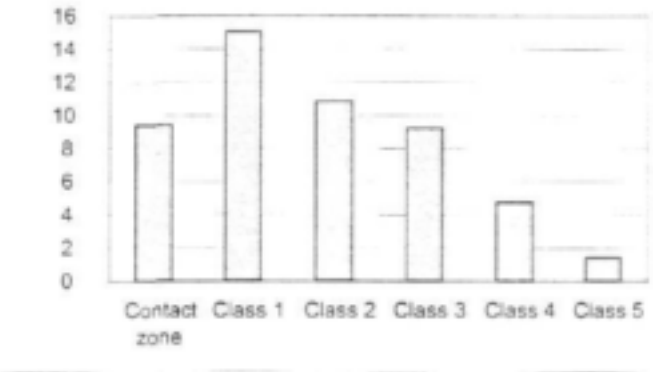

Figure 49: Percentage area of seeps per dolerite elevation class.

The graph (**Figure 50**) shows the proportion of representation in the study area. It can be seen that Class 1 is statistically underrepresented in the study area (an area of $2km^2$) so any conclusions drawn by analysing the results in Class 1 must be assessed cautiously. However the other classes cover areas in excess of $50km^2$ so these results can be meaningfully analysed.

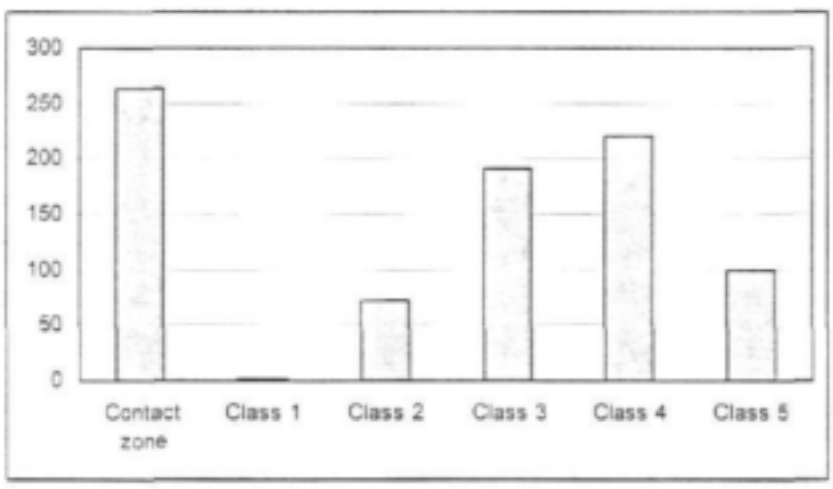

Figure 50: Area in km^2 covered by each dolerite elevation class in the study area.

The study was taken one step further and a density analysis of 'seeps' on each category of slope and within each dolerite slope class was undertaken. The results are presented in the graphs in Figure 52 below. It is interesting to note that the trends. In general, the density of seeps decreases with elevation and with slope steepness. Notable exceptions are Elevation Class 1 and Elevation Class 5. Class 1 is underrepresented so conclusions cannot be drawn from those results. Elevation Class 5 is made up of the cliff face and flat outer sills (see Chapter 3.2 and **Tables 2 & 3**) which may be influencing the occurrence of the 'seeps' and therefore skewing the results. However the slight increase with slope in Elevation Class 5 is not significant compared to the variations in other classes. The conclusions which can be drawn are as follows: the optimal location for the occurrence of 'seeps' is on dolerite with an elevation of between 943 and 1389m. Furthermore the optimal slope on which the 'seeps' occur at these altitudes is on slopes of less than eight degrees closely followed by slopes of between eight and 14 degrees.

It was mentioned at the beginning of the chapter that the aim of this methodology is to identify trends and to illustrate how remote sensing and GIS can be used in tandem for this type of research. The next step would be fieldwork to determine whether the remote sensing techniques utilised produced meaningful results. If fieldwork determines the results are valid, one would be able to apply the elevation and slope parameters identified in the local study area, where Aster imagery is available, to the rest of the catchment where Aster imagery has not been purchased. By applying these parameters to the rest of the catchment which has similar geomorphology as the study area, this type of methodology can negate the necessity of purchasing expensive satellite imagery on a regional scale as instead a DEM alone can be used to identify areas where seeps are most likely to occur.

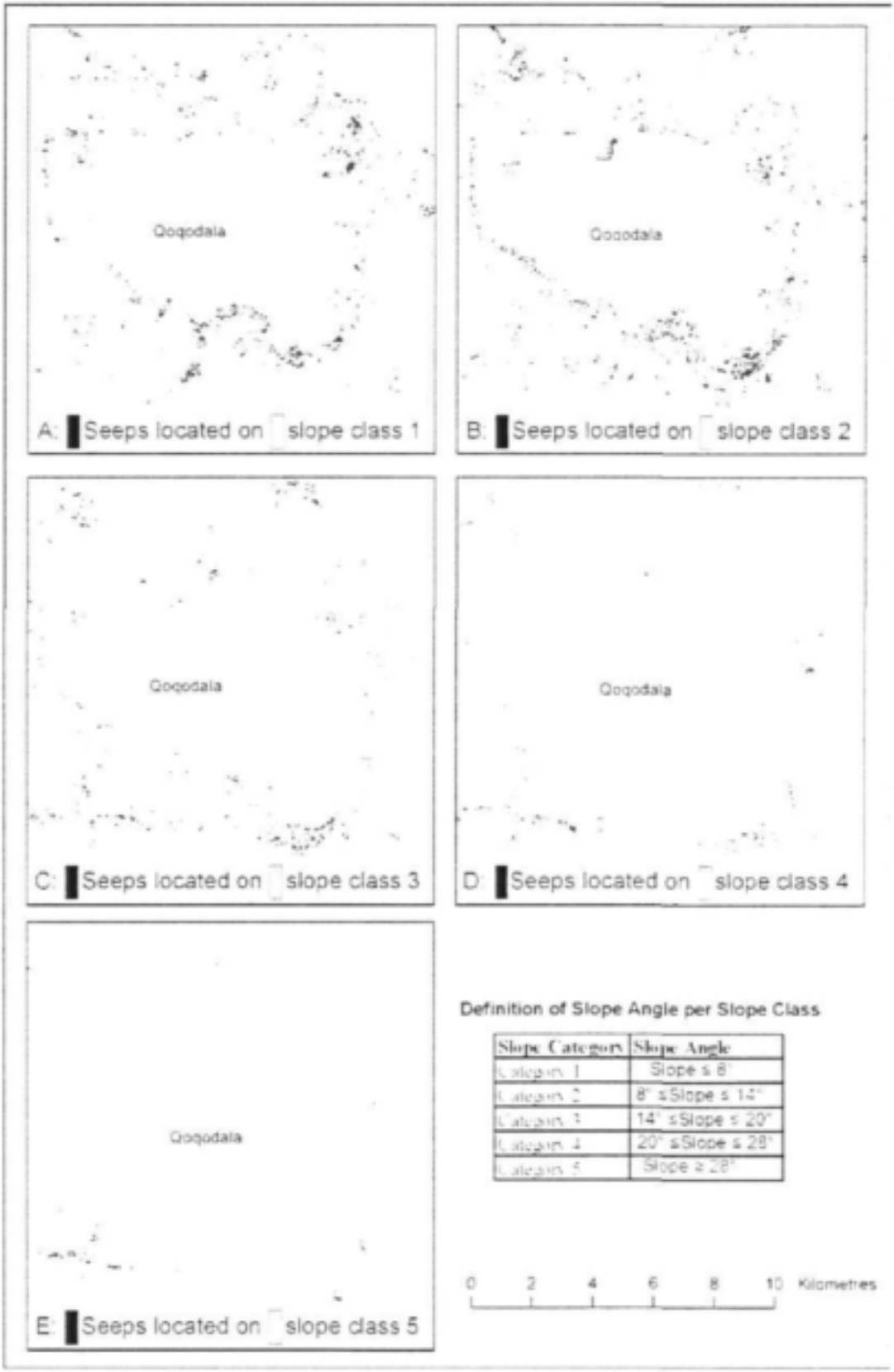

Figure 51: Results of seep mapping per slope category.

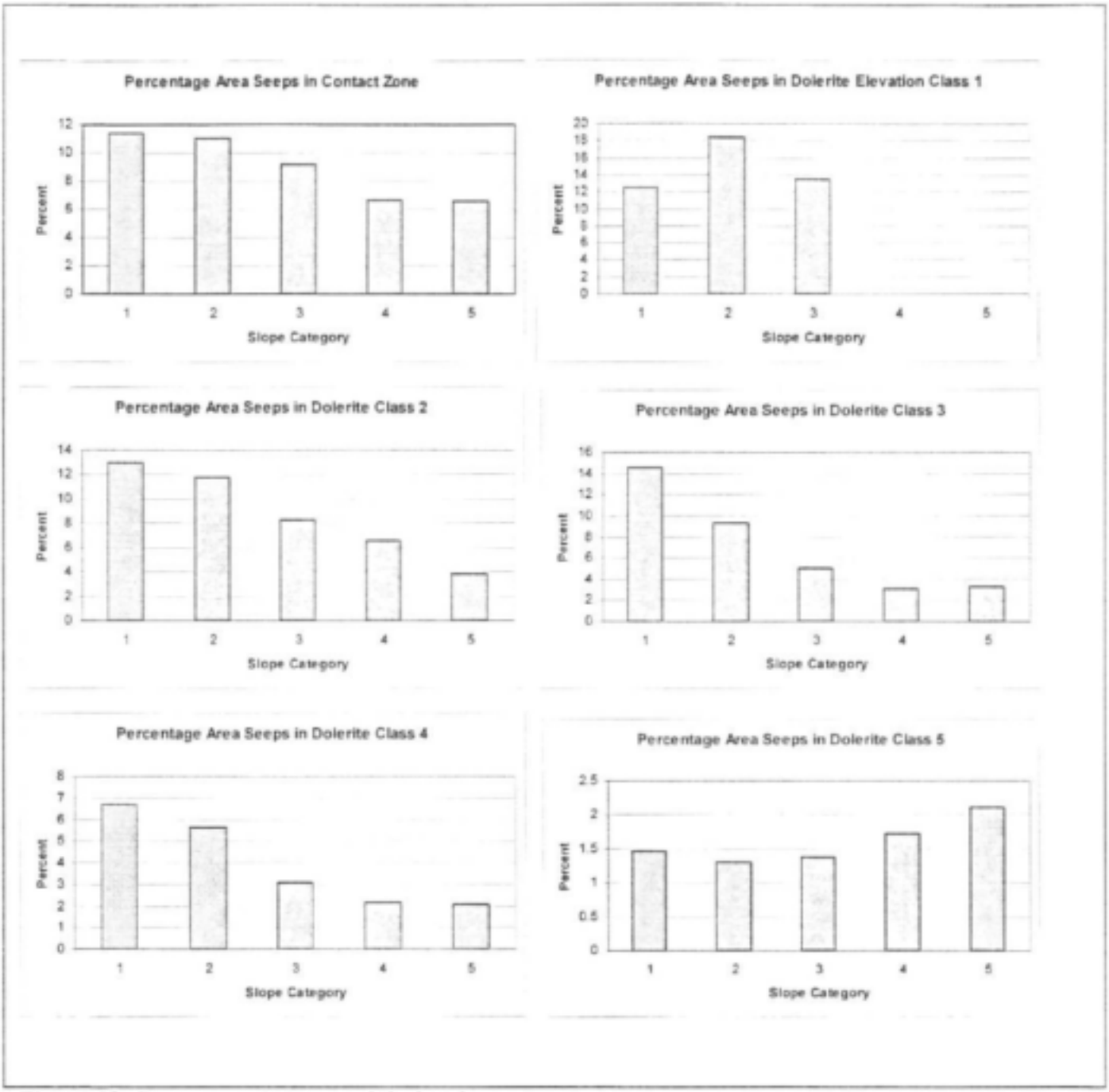

Figure 52: Percentage seeps per dolerite class.

3.9 GROUNDWATER RESOURCE POTENTIAL

3.9.1 Groundwater Management Units

The study area of 313 km^2 was subdivided into six groundwater management units (**Figure 53**) in order to provide a preliminary estimates of the groundwater resource potential based upon possible aquifer units (i.e. zones of similar groundwater flow and sharing common aquifer boundaries). It must be noted that, due to the complex and multi-layered nature of both the primary and fractured-rock aquifer systems, groundwater may flow from one groundwater management unit to another via preferential flow paths (i.e. faults) or even from a deeper-seated aquifer.

The groundwater management units fall within the S10D and S31F Quaternary Drainage Regions and are numbered using these catchment numbers as a prefix followed by a sequential alphanumeric value, i.e. management unit S10D-a falls in the S10D Quaternary Drainage Region and is unit number 'a'. The name and size of each management unit is presented in **Table 1**.

3.9.2 Groundwater Recharge

Sustainable groundwater utilization depends upon adequate recharge to replace the water being removed from the aquifer system by pumping. Rainfall is the main source of this recharge to the shallow Karoo fractured-rock aquifer systems. Historically, estimated recharge rates for most aquifer systems in South Africa range between 5% and 10% of the annual precipitation. For the purposes of this study, aquifer recharge refers to the amount of rainwater that infiltrates into the vadose zone and then actually passes into the main underlying aquifer system, i.e. effective recharge.

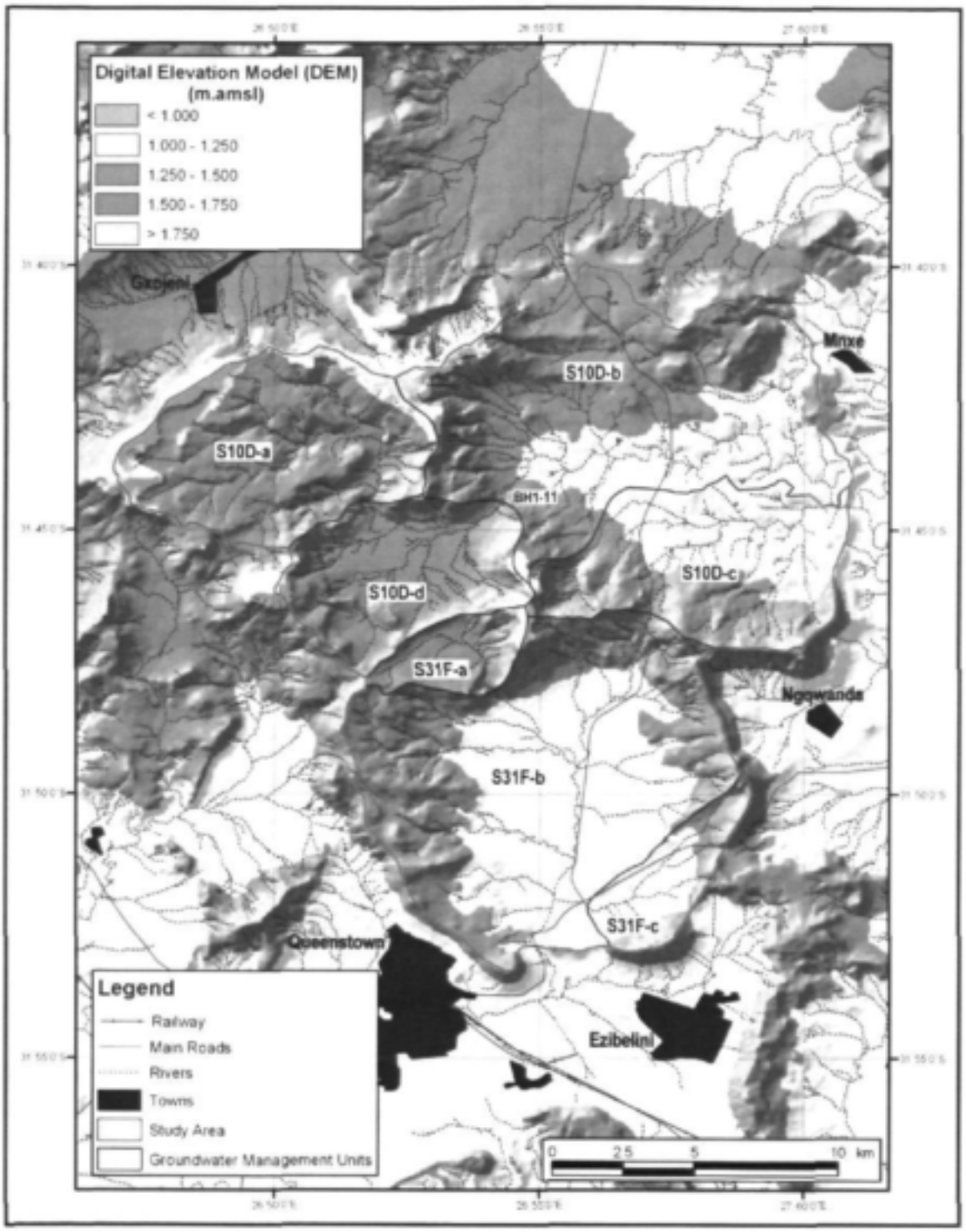

Figure 53: Groundwater Management Units of the study area showing the Qoqodala test site (BH-1 to -11)

The mean annual effective recharge (R_e) from rainfall to each groundwater management unit was estimated using the following GRID-based GIS modelling technique:

1. A 50x50m grid of variable recharge rate or factor (R_f) was derived from the mean annual precipitation (MAP) dataset (Schultze, 1997), as follows:

R_f = [MAP (mm) / 10 000]

2. A 50x50m runoff factor (S_f) grid was derived from a percentage slope grid (calculated from 50x50m digital terrain model), as follows:

S_f = [100 - Slope%] / 100

3. A 50x50m lithology factor (L_f) was derived to take into account the variable recharge rates with the various lithological units as follows:

Lithological Unit	Recharge Factor (L_f)
Quaternary Deposits	0.87
Karoo Dolerite	0.94
Burgersdorp Formation	0.95
Molteno Formation	1.05

4. A 50x50m mean annual effective recharge or R_e (mm) grid was derived for the study area as follows:

R_e (mm) = MAP x R_f x S_f x L_f

5. The Lower and Upper Limits of R_e were estimated from Shultze's (1997) Coefficient of Variation (%) of Annual Precipitation, which they refer to as an 'index of climatic risk'.

The resultant mean annual effective recharge (mm) for the study area is presented in **Figure 54**. The mean annual effective recharge (MAER) from rainfall for the entire study area is estimated at

14.6 x 10^6 m^3, which equates to an average recharge rate of 6.4% of the mean annual precipitation. The MAP and MAER for each groundwater management unit are presented in **Table 1**.

DWAF's produced a *Harvest Potential* map of South Africa (Seymour and Seward, 1996), which provides an estimate of the theoretical volume of groundwater that could be abstracted from an area on a sustainable basis based upon regional estimates of groundwater storage and recharge. The Harvest Potential of the study area is approximately 4.8 x10^6 m^3 per year (**Table 1**), which is a third of the MAER estimate obtained for this study. This Harvest Potential is considered to be unrealistically low.

Smart (1998) produced an *Abstraction Potential* map as part of his 1/500,000 scale 3126 hydrogeological mapsheet. The Abstraction Potential (AP) provides an estimate of the quantity of groundwater that can be practically, economically and/or feasibly abstracted from an area. It is determined using aquifer transmissivity, which is estimated from borehole yield information, and an assumed feasible density of production boreholes. The aquifer transmissivity is the only limiting factor considered and not the volumes of groundwater stored in or recharging the aquifer. In the study area the groundwater AP varies between 20 000 and 40 000 $m^3/km^2/a$. If an average value of 30.000 $m^3/km^2/a$ is used then the AP of the study area is ±9.4 x10^6 m^3 per annum, which is less than the MAER but similar to the drought estimate of annual rainfall recharge (**Table 1**)

Smart (1998) also produced a regional *Development Potential* (DP) map which he described as the lesser of his 'adapted' Harvest Potential and Abstraction Potential estimates, which Smart states is probably as close as one can get to what might actually be abstracted. Smart's DP values vary between 7 000 to 40 000 $m^3/km^2/a$ across the study area, which equates to approximately 6.57 x 10^6 m^3 per annum. This figure appears somewhat conservative and the mean annual recharge estimate provided in **Table 1** is accepted as a reasonable preliminary estimate of the long-term sustainable groundwater yields available from each of the management units. It may however, be necessary to downscale abstraction from a unit to the 'Drought' recharge value during prolonged periods of below average rainfall.

Table 19: Estimated groundwater recharge to Groundwater Management Units

Groundwater Management Unit	Area (km^2)	MAP (mm / year)	Recharge Rate %	Mean Recharge (m^3/ year)	Drought Recharge (m^3/ year)	Harvest Potential (m^3/ year)
S10D-a	45.7	713	6.6%	2,158,908	1,558,485	686,619
S10D-b	81.1	721	6.7%	3,941,029	2,847,975	1,108,271
S10D-c	40.3	697	6.5%	1,820,457	1,303,581	594,309
S10D-d	30.8	714	6.6%	1,442,360	1,039,445	420,824
S31F-a	9.6	673	6.2%	399,395	283,4890	131,615
S31F-b	92.5	710	6.7%	4,389,657	3,159,046	1,626,932
S31F-c	12.5	630	5.8%	458,355	322,506	220,992
TOTAL	**312.5**	**694.0**	**6.4%**	**14,610,161**	**10,514,528**	**4,789,578**

When comparing the MAER per groundwater management unit with the actual estimates of the long-term sustainable yield of the borehole as derived from the analysis of the pumping-tests (**Table 2**), it is evident that the two are in agreement with one another. Note that these estimates do not take into account any other groundwater abstraction that may be taking place within the vicinity of the production boreholes.

Table 20 Comparison of long-term sustainable borehole yields with Mean Annual Recharge Estimates

Groundwater Management Unit	Pro-Rata Mean Recharge (m^3/year)	Production Borehole	Long-Term Sustainable Yield from Pump-Test (m^3/year)	
S10D-b	155 000	BH-1	68 400	
S10D-d	175 000	BH-7 and BH-11	152 000	
Note: The pro-rata volume of MAER available to the production boreholes was estimated using the ratio of the borehole 'capture-zone' in relation to the total area of the unit; BH-1 = 3.3 / 30.8 km^2 = 0.107, BH-7+11 = 3.6/81.1 km^2 = 0.044				

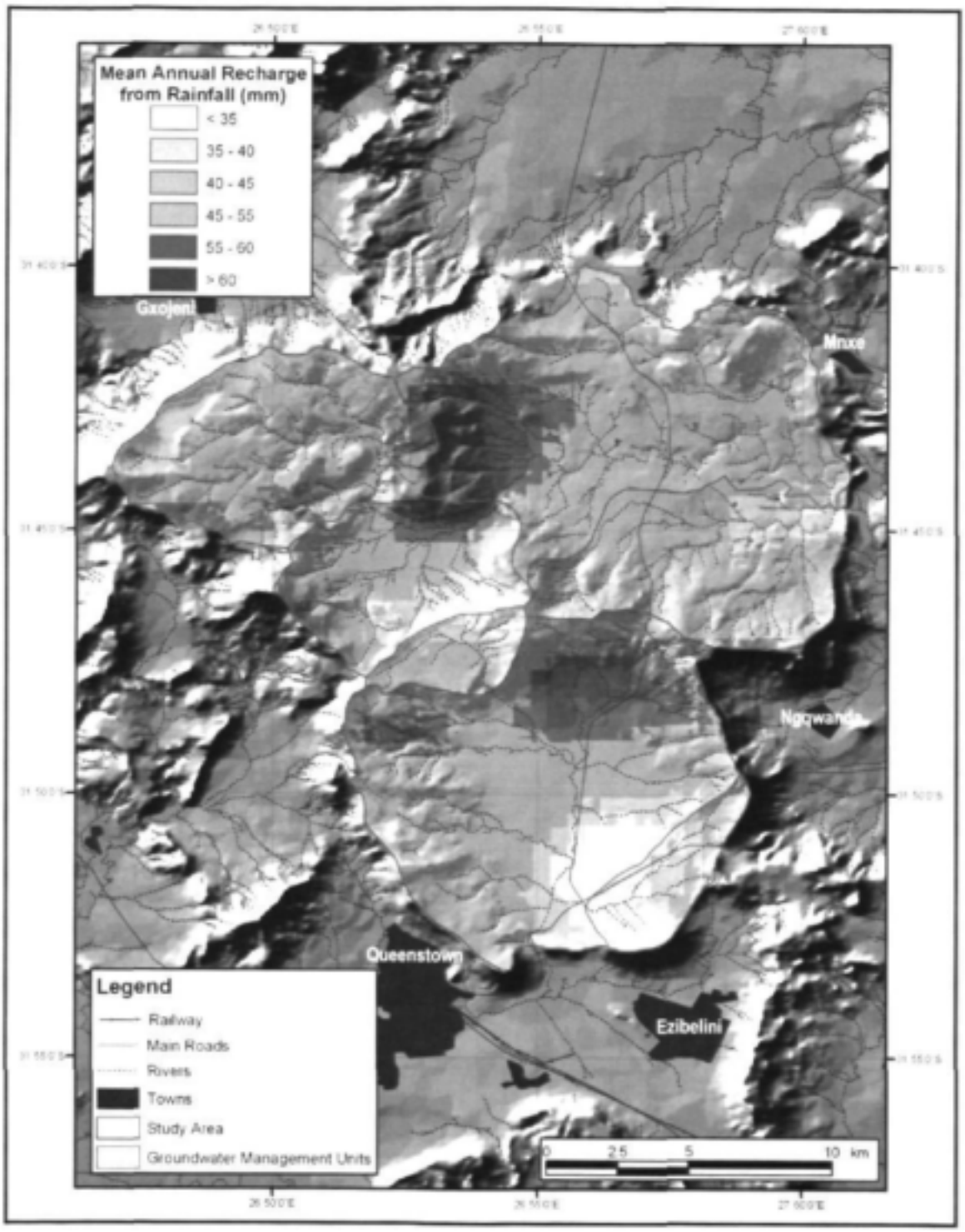

Figure 54: Mean Annual Effective Recharge from rainfall for the study area

4 DISCUSSION, CONCLUSION AND RECOMMENDATION

4.1 ECO-GEOHYDROLOGICAL MODEL OF THE QOQODALA RING COMPLEX

The geological and structural analysis of the Qoqodala dolerite sill and ring system has confirmed the results obtained in the Western Karoo during a previous investigation and the hydro-morpho-tectonic model of Chevallier et al. (2001) (see Figure 1). Regional fracture zones have controlled the intrusion of major dolerite dykes and the emplacement of ring-forming inclined sheets along NE, NW, NNE and EW directions. The inclined sheet forms the structural back bone of the ring system and the transition between the inner sills inside the ring and the outer sills outside the ring (**Figure 55**). Lineament analysis over the study area showed that the ring part of the system is densely fractured along these regional trends. At the drilling site across the Qoqodala ring NW fractures are very prominent; the inclined sheet, which is feeding several sills, is probably fed by a regional dyke. The outer sill of a specific ring can becomes the inner sill of another ring. For instance one of the outer sill of the Qoqodala ring forms the inner sill of the Bonkolo ring. Morpho-tectonic and elevation analysis of the sills complemented by drilling results have shown at least six levels of sill intrusion over the study area.

This dolerite plumbing system has been conducive to the formation of fractured rock aquifers with complex geometries and ground water flow dynamics (**Figure 55**). Exploration drilling at Qoqodala has shown that aquifers are multilayered but not necessarily interconnected. The upper fractured aquifer system (depth beween 15 and 80 m) is situated above the Zingqutu outersill and the thin Qoqodala inner sill. Extensive subhorizontal fractures affect the western compartment behind the inclined sheet and the eastern compartment in front of the inclined sheet. This upper aquifer is unconfined and the video log has shown water movement in some of these fractures. The inclined sheet is excessively fractured but no major transgressive fractures seem to connect the two compartments and the flow between the two is slow. Drilling in borehole 1, 4 and 5 has created an artificial connection to these fractures and drained the water table down. At the base of the Zingqutu outer sill and the thin inner sill (between elevations 1100 and 1160 m), where steeply dipping or subvertical fractures are dominant, water movement is seen in these fractures.

However the western and eastern compartments do not seem to be connected, the inclined sheet being a massive, hard, non-fractured dolerite. A very deep aquifers system (around 250 m) was intercepted at the base of Qoqodala inner sill. This aquifer system might be linked to the base of the outer sill via fracturing along the inclined sheet and a possible feeder dyke. In borehole 7 uprising of warm, non-oxygenated water is now feeding into the upper fractured aquifer.

Ecosystem and wetland studies have shown that grassland is very common on high lying outer dolerite sills and this could be due to increased water availability via moisture conditions and precipitations (**Figure 55 and Plate 3**). These grassland areas do not however host large wetlands or spongy areas (spongy dolerite) that could act as water reservoir or perched water table. On the North facing and East facing slopes of the dolerite rings Aloe dominated thicket is predominant (such as at the drilling site). These shrubs and succulents are adapted to more arid conditions than the grassy highlands. None of these plants however are likely to be groundwater dependant. Lush tall shrubs with a tree component dominate in the kloofs and at the foot of dolerite cliffs and seem to prefer South and West facing steep exposures. These luxuriant thickets may be phreatophytic i.e. a combination of moist conditions in valley or shadowy places and periodic use of non-perennial seeps at the base of dolerite cliffs. Groundwater dependant plants occur around perennial seeps. The vegetation on these ecosystems consists mainly of grass and sedges growing on peaty black soil forming small wet areas from few meters to several tens of meters wide. Shrubs adapted to harsher conditions are unable to grow. They typically occur in depressions along fractures or created by morphological breaks along lithological contact zone i.e. mudstone-sandstone or dolerite sediment. They also tend to occur at low elevation and on slopes of no more than 14°. These seeps and small wetlands might not significantly contribute to the overall water recharge but they are very vulnerable to change in groundwater regime via drilling or abstraction as proven at Qoqodala drilling site. In the middle of the ring extreme land degradation occurs; bare soil and overgrazed grassland dominate, however this does not necessarily imply that wetland vegetation did not exist in the inner ring in the past.

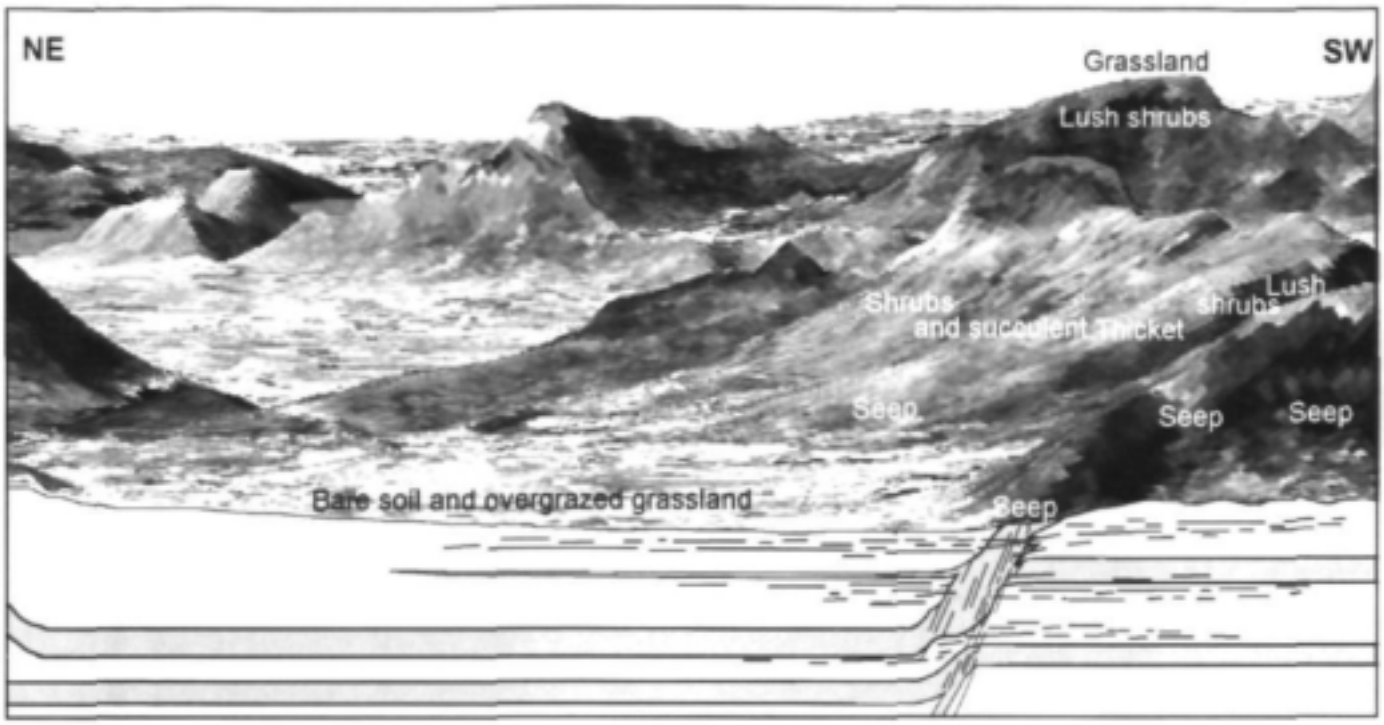

Figure 55: The Eco-geohydrological model of the Qoqodala dolerite ring complex.

Plate 3: Ecosystem and dolerite ring at Qoqodala drilling site. The foreground is occupied by the shrubs and succulents typical of dolerite slopes.

The most vulnerable eco-hydrogeological system corresponds to the upper unconfined aquifer above the low outer sill and to the seeps occurring at low elevation. The bulk of the groundwater recharged during rainfall events is stored in this aquifer layer. Because of the high density of

fracturing of the ring and the high connectivity of these shallow fractures, badly planned drilling can induced water flow regime and deplete the aquifer and therefore affect these ecosystems. The location of wetlands or seeps at low elevation, the direction and density of fracturing, the slope of the inclined sheet, and the presence of an outer sill at depth are factors which should be taken into account when developing dolerite ring related groundwater.

4.2. APPLICABILITY OF RESULTS TO THE GREAT KEI CATCHMENT

The hydrostratigraphy and the groundwater flow regime at Qoqodala can be applied to the rest of the catchment which is characterized by dolerite rings and stacks of sills emplaced at specific elevations. The parameters that play a role in the groundwater flow and the vulnerability of the groundwater dependent ecosystems are expected to be the same at the catchment scale and the results of our study could be generalized with a good degree of confidence to the rest of the basin.

The role of dolerite rings is primordial in the compartimentalisation of the unconfined shallow aquifer and its recharge. Aquifers located behind the inclined sheets will be recharged by inter-ring catchments especially where a kloof (generally guided by a fracture) is cutting through a ring. Aquifers in front of the inclined sheet (i.e inside the ring) are recharged by water collected by the dolerite ring itself.

Morphotectonic factors will be indicators of the complexity of the fractured aquifers at depth. A thick, steeply dipping and fractured ring will have the same structural complexities found at Qoqodala exploration site i.e. several intrusive phases, several outer sills and several inner sills leading to several confined or semi confined aquifers. Whereas a thin and shallow dipping inclined sheet will create a simpler structural pattern (see Victoria West ring investigation, Chevallier et al., 2001).

Flats sills are very extensive and can be found cutting through the entire catchment. High elevation sills around the catchment correspond to high rainfall areas and usually any perched

watertable will not be affected by groundwater abstraction occurring below the vadose zone. Low elevation sills form the inner sills of many ring complexes and are below the vadose zone. High yielding aquifers are expected from these open fractures. However they do not seem to extend laterally. The influence of abstraction from these deep, extensive but probably discontinuous aquifers on the ecosystem on a regional scale is unknown.

The mapping of ecosystems within the Qoqodala Ring Complex has shown that medium resolution satellite imagery such as Landsat and Aster is more suitable to creating a land use map than a vegetation map and that mapping small wetlands and ground water dependant ecosystem i.e. seeps, cannot be successful. The mapping of wetlands at a primary catchment scale however, may be more successful. It is probable that within the Great Kei River Catchment large open water wetlands exist, as do larger vegetated wetlands with significantly different spectral responses than the surrounding non-wetland vegetation. If this is the case, the proposed methodology can probably be applied successfully to the Great Kei River Catchment. It must be noted that stringent field verification would need to be carried out in order to determine the accuracies of the results and small wetlands and seeps will not be detected using this method.

Should it be necessary to create a preliminary vegetation map for the Great Kei River Catchment, it is recommended that the methodology be altered. As the Catchment covers a larger area and as such encompasses a larger number of vegetation and land use types, the maximum number of output classes would have to be increased.

4.3 APPLICATION TO RURAL DEVELOPMENT

The dolerite ring-complexes of this part of the Eastern Cape strongly control the vegetation, geomorphology and drainage systems of the area, resulting in very distinctive semi-circular catchments where a centripetal drainage system often exits the catchment at a single point. The inclined-sheet and outer-sill of the dolerite ring-complex forms the high-lying perimeter of the catchment, whilst the flat-lying central portions are often covered by overburden. This in turn

has led to a rather distinctive pattern of settlement in the rural areas. The local inhabitants tend to build their dwellings at or near to the foothills of these circular catchments, where the:

(i) vegetation is more lush for the grazing of animals, collection of wood and general aesthetics,
(ii) unpolluted fresh-water springs and seeps emanate from these higher-lying areas and are tapped for drinking purposes (**Figure 56**), and
(iii) protection from infrequent flooding of the lower lying areas etc.

Crops are generally planted on the more flat-lying, central portions of these catchments where the soils are thicker and more fertile.

This research project and similar research conducted elsewhere on dolerite ring- and sill-complexes have indicated that high-yielding production borehole can be sited with a high degree of success at specific zones associated with the inclined-sheet. This project has also high-lighted that in the Eastern Cape these exploration targets are not always easily accessible due to the ruggedness of the terrain, and quite often access is restricted to the narrow 'poorts' incised by the drainage system along the perimeter of the catchments. Nevertheless, it should be possible to establish a 'ring-main' of high-yielding production boreholes along the perimeter of these dolerite-ring complexes that can be developed as part of a bulk groundwater supply scheme, rather using the more 'traditional' approach of establishing local supplies using hand-pumps and low-yielding boreholes. Such an idealized system is presented for the south-western portion of the Qoqodala dolerite ring-complex (**Figure 56**).

This study has also highlighted the importance of low-yielding springs/ seeps to the local communities in these rural areas as a source of fresh drinking water, as well as their vulnerability within the groundwater system to pollution and depletion by over-exploitation of the aquifer by boreholes. During the exploration drilling programme at the Qoqodala dolerite ring-complex, a number of deep boreholes were drilled alongside a spring that dried-up as a result of the dewatering of the upper aquifer unit, which fed the spring, due to leakage of groundwater into a deeper seated aquifer unit via the borehole. No waterlevel monitoring was conducted during or

directly after the drilling operations and therefore the problem was only discovered after the spring had dried up.

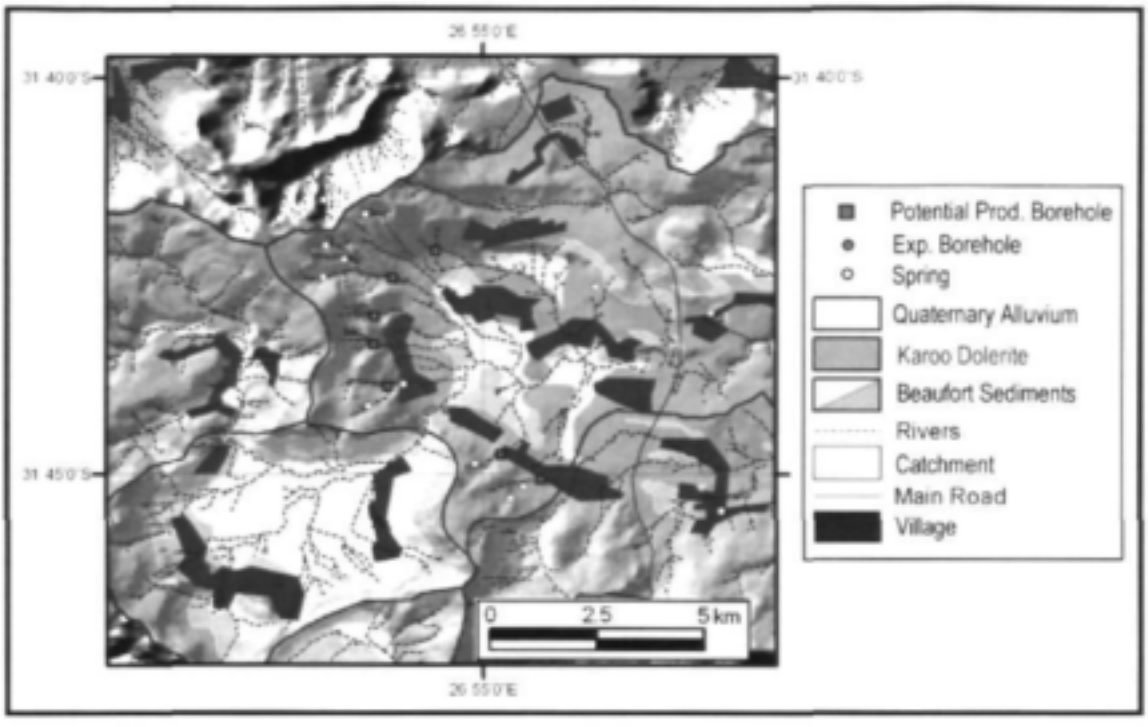

Figure 56: Idealized layout of Wellfield of High-Yielding Production Borehole tapping the Qoqodala Dolerite Ring-Complex in relationship to villages

4.4 RECOMMENDATIONS FOR FUTURE RESEARCH

Future research should focus on integrated studies at catchment level over the Mzimvubu to Keiskamma Water Management Area (WMA), in order to assist in the development of a Decision Support System (DSS).

There is therefore a need to do an assessment of the balance of the water resources: surface water budget, groundwater reserves, ecosystem and land use, and propose integrated long-term scenarios taking into account human impact studies. Factors such as vulnerable spring and

wetland use, intermittent bad quality run-off, silted dams and shallow low-yielding aquifers are problematic. Overgrazing and increasing erosion have also led to fast land degradation with possible elimination of wetlands and desertification, and diminution of water budget. An integrated study should quantify the role that sustainable groundwater could play in the total water budget.

Regional assessment of the groundwater exploration potential is problematic in water-stressed rural areas where water supply is carried out by insufficient ad hoc water schemes. In order to gain an understanding of this, it is important to initially collect, collate and assess all available geological and geohydrological information at the scale of the management area. The region can be subdivided into a number of hydrogeological domains, where groundwater occurrence and exploration targets are similar. It is important to characterize these areas in terms of potential high-yielding exploration targets, and identify problem areas for groundwater development.

6 REFERENCE LIST

Acocks, J.P.H. 1988. Veld Types of South Africa 3rd edition, *Memoirs of the Botanical Survey of South Africa* 57: 1-46.

Bates, J. A. & Jackson, J. A. 1980. Glossary of Geology. *2nd ed.* Viginia: American Geological Institute.

Batten, A. & Bokelmann, H. 1966. Wild flowers of the Eastern Cape. Cape Town: Books of Africa.

Burger C.A.J., Hodgson F.D.I. & Van der Linde P.J. 1981. Hidrouliese eienskappe van akwifere in die Suid-Vrystaat. Die ontwikkeling en evaluering van tegnieke vir die bepaling van die ontginninspotensiaal van grondwaterbronne in die Suid-Vrystaat en in Noord-Kaapland, Volume 2, Instituut vir Grondwaterstudies, Oranje Vrystaat Universiteit.

Catuneaunu, O., Hancox, P.J & Rubidge, B.S., (1998). Reciprocal flexural behaviour and contrasting stratigraphies: a new basin development model for the Karoo retroarc foreland system, *South Africa. Basin Research*.10: 417-439.

Chevallier, L., Goedhart, M & Woodford, A. 2001. The influence of dolerite sill and ring complexes on the occurrence of groundwater in Karoo fractured aquifers: a morpho-tectonic approach. Water Research Commission No 937. Pretoria: Water Research Commission.

Chevallier L. & Woodford A. 1999. Morpho-tectonics and mechanism of emplacement of the dolerite rings and sills of the Western Karoo, South Africa. *South African Journal of Geology* 102: 43 - 54.

Cleaver, G, Brown, N., Bredenkamp, G.., Smart, M.C. and De W. Rautenbach C.J. 2003. Assessment of environmental impact of ground water abstraction from TMG aquifer on ecosystem in the Kamanassie nature Reserve and environsWRC report No 1115/1/03.

Cole, D.I. 1992. Evolution and development of the Karoo Basin. In de Wit M.J. & Ransome I.G.D. (eds) *Inversion tectonics of the Cape Fold Belt, Karoo and Cretaceous Basins of Southern Africa* pp87 – 99. Rotterdam: Balkema.

Conrad, J., Hughes, S. & van der Voort, I. 2000. The new National Water Act: a case study on the applicability of commercial multi -spectral data for determining the groundwater reserve. 28th International Symposium on Remote Sensing of Environment, Cape Town. Proceedings on CD ROM.

Crist, E. P. & Cicone, R. C. 1984. Application of the Tasseled Cap concept to simulated Thematic Mapper data. *Photogrammetric Engineering and Remote Sensing*. 50:343-352.

Duncan R.A., Hooper P.R., Ehacek J., Marsh J.S. and Duncan R.A. (1997): The timing and duration of the Karoo igneous event, Southern Gondwana. J. Geophys.Res., 102, 18127 - 18138.
Du Toit, A.L., 1905. Geological survey of Glen Grey and parts of Queenstown and Woodehouse, including the Indwe area. Geological Commission of the Cape of Good Hope, tenth annual report, 95-140.

Du Toit, A.L. 1920. The Karoo Dolerites- a study in Hypabyssal Intrusion. Transactions of the Geological Society of South Africa 23: 1-42.

Evans, R. & Hatton, T. 2000. Environmental Water requirements of groundwater dependent ecosystems. Canberra: Environment Australia.

Gibson, L.A. 2003. The detection of wetlands using remote sensing in Qoqodala, Eastern Cape. Masters thesis. Cape Town: University of Cape Town, School of Architecture, Planning and Geomatics.

Gorte, B. 1999. Supervised image classification. In Stein A., van der Meer, F., Gorte, B. *Spatial Statistics for Remote Sensing* pp 153 - 164. Dordrecht: Kluwer Academic Publishers

Groenewald, G.H. 1996. Stratigraphy and sedimentology of the Tarkastad Subgroup, Karoo Basin, South Africa. Doctoral dissertation. Port Elizabeth: University of Port Elizabeth.

Hallbauer-Zadorozhnaya, V, Chevallier, L, Nhleko, L and Wheeler, W. 2003. Detection of aquifers above and below dolerite sills: A successful application of TDEM in the Eastern Cape. South African Geophysical Association, Pilanesberg Nature Reserve, unpublished.

Hancox, P.J. 1998. A stratigraphic sedimentological and palaeoenvironmental synthesis of the Beaufort-Molteno contact in the Karoo Basin. Doctoral dissertation. Johannesburg: University of the Witswatersrand.

Hartnady, C. J. & Hay, E. R. 2000. Reconnaisance investigation into the development and utilisation of the Table Mountain Group artesian groundwater, using the E10 catchment as a pilot study area. Report by Umvoto Africa CC to the Department of Water Affairs and Forestry.

Hatton, T. & Evans, R. 1998. Dependence of ecosystems on groundwater and its significance to Australia. Occasional Paper No 12/09. Canberra: Land and Water Resources Research and Development Corporation.

Jacobsen, A., Heidebrecht, K. B. & Nielsen, A. A. 1998. *Monitoring Grasslands using Convex Geometry and Partial Unmixing – A Case Study*. 1st EARSel Workshop on Imaging Spectroscopy, University of Zurich, Switzerland. Proceedings edited by: M. Shaepman, D. Schlafer & K. Itten.

Jamtveit, B., Svensen, H., Podladchikov, Y. and Planke, S. (in press). Hydrothermal vent complexes associated with sill intrusions in sedimentary basins. Submitted manuscript.

Johnson, M.R., Van Vuuren, C.J., Visser, J.N.J., Cole, D.I., Wickens, H. de V., Christie, A.D.M., Roberts, D.L., & Brandl, G., 1997. *The foreland Karoo Basin, South Africa.* In R.C. Selley (Ed.), African Basins. Sedimentary Basins of the World, 3. Amsterdam: Elsevier,.

Kent, L.E., 1972. Springs. In Eeden, O.R. *The geology of the Republic of South Africa. An Explanation to the 1:1 000 000 map.* Special publication 18, Geological Survey, Department of Mines: 71-74.

Kok, T.S. 1992. Recharge of springs in South Africa. Department of Water Affairs Technical Report, GH 3748.

Le Maitre, D., Scott, D.F. & Colvin, C. 1999. A review of information on interactions between vegetation and groundwater. *Water SA* 25 2:137 – 152.

Lillesand, T. M. & Kiefer, R. W. 2000. Remote Sensing and Images Interpretation. 4th ed. New York: John Wiley & Sons.

Low, B. 2003. Comment on the Botany of Groundwater Systems within the Dolerite Rings of the Great Kei Catchment. Report compiled for the Council for Geoscience (unpublished).

Low, B. & Rabelo, T. 1998. Preface to New Vegetation Map. [Online]. Available: http://www.ngo.grida.no/soesa/nsoer/Data/vegrsa/vegpref.htm [13/11/2003]

Mather, P. M. 1999. Computer Processing of Remotely-Sensed Images. An Introduction. 2nd ed. Chichester: John Wiley & Sons.

Mather, P. M. 2002. Personal Communication. Email on 29 July 2002 about Tasseled Cap Transformation on Aster data.

McMaster, C & McMaster, R. 2001. Survey of the montane grassland of the eastern section of the Amatola Range. SA Forest Company Ltd.

Microimages. 2001. Getting Started. Analysing Hyperspectral Images. [Online]. www.microimages.de/support/tutorial/hyprspec.pdf. [30.3.2003].

Midgley, D.C., Pitman W.V. & Middleton, B.J., 1994. Surface water resources of South Africa 1990, Book of maps. Water Research Commission Report 298/5.2

Milton S.J. (1990) Life styles of plants in four habitats in arid karoo shrubland. *South African Journal of Ecology*. 1: 63-72.

Research Systems, Inc. 2001. ENVI User's Guide. Boulder: Research Systems, Inc.

Rutherford, M.C. 1997. Categorization of biomes. In *Vegetation of Southern Africa.* Cowling, R.M, Richardson, D.M. & Pierce, S.M. (Eds) pp.91-98. Cambridge: Cambridge University Press.

Rutherford, M.C. 2003. Personal Communication. Meeting on 22 July 2003 about unpublished National Vegetation Map.

Rural Support Services. 1994. Qoqodala Groundwater Investigation. Unpubl.

Sabins, F. F. 1997. Remote Sensing. Principles and Interpretation. 3rd ed. New York: W. H. Freeman and Company.

Schultz, R. E., Maharaj, M., Lynch, S. D., Howe, B. I. & Melvil-Thomson, B. 1997. South African Atlas of Agrohydrology and Climatology. Data on CD ROM.

Shand, N. 1999. Eastern Cape Water Resources situation Assessment. Department of Water Affairs and Forestry Report. Directorate of Water Resources Planning.

Seymour, A and Seward, P. 1996. 1: 3 000 000 Groundwater Harvest Potential map of South Africa.

Smart, M.C. 1998. An explanation of the 1:500 000 General Hydrogeological Map, Queenstown 3126. Department of Water Affairs and Forestry, 14- 43.

Smart, M.C. 2002. The vulnerability of spring flow to groundwater abstraction in the Kammanassie Mountain Range – An assessment technique for a case with limited groundwater level data. Groundwater Division, Western Cape Branch Conference: Tales of a Hidden Treasure. Somerset West, Sept. 2002, extended abstract 297 – 302.

Smith, R.M.H., Eriksson, P.G., & Botha, W.J. 1993. A review of the stratigraphy and sedimentary environments of the Karoo-aged basins of Southern Africa. Journal of African Earth Science. 16: 143–169.

Smith, J.H, Wickham, J.D, Stehman, S.V. & Yang, L. 2002. Impacts of Patch Size and Land-Cover Heterogenity on Thematic Image Classification Accuracy. *Photogrammetric Engineering & Remote Sensing*. 68: 65 - 70.

Statistics South Africa. 2001. Selected 1996 Census Data by Electoral Ward (With Maps). Data on CD ROM.

Svensen, H., Jamtveit, B. and Planke, S. 2001. Interaction between sills, sediments and fluids in the Karoo basin, South Africa, Preliminary results. Fourth International Dyke Conference, June 2001, KwaZulu-Natal, South Africa, abstract, 21.

Terra Sounding and Analytical. 2003. TDEM Measurements in the Qoqodala Area, Eastern Cape. Unpublished report for the Council for Geoscience.

Thompson, M, Marneweck G, Bell S, Kotze D, Muller J, Cox D & Smith R, 2002. A Methodology Proposed for a South African National Wetland Inventory. Prepared for Dept. Environment Affairs and Tourism by CSIR Environmentek. March 2002.

Townshend, J. R. G., Huang, C., Kalluri, S. N. V., Defries, R. S. & Liang, S. 2000. Beware of per-pixel characterization of land cover. *International Journal of Remote Sensing*. 21: 839-843.

Van der Meer, F. D., de Jong, S.M. & Bakker, W. 2001. In van der Meer, F.D. & de Jong, S.M. (eds) *Imaging Spectrometry: Basic Principles and Prospective Applications*, pp38-61. Dordrecht: Kluwer Academic Publishers.

Vandoolaeghe, M.A.C. (1979 a) Geohydrological investigation, Middelburg C.P.. Department of Water Affairs, Comprehensive Technical report No 3072 . 101 pp, 25 Fig., 33 enclosures (maps and sections, 20 tables. Unpubl.

Vandoolaeghe, M.A.C. (1980a). Queenstown geohydrological investigation, Main report. Department of Water Affairs Unpublished Technical Report, Gh 3153, Pretoria. 26 pp. plus A0 maps

Vandoolaeghe, M.AC. (1980b). Queenstown geohydrological investigation, Part I Geology, Borehole survey, levelling. Department of Water Affairs Unpublished Technical Report, Gh3153, Pretoria. 63 pp.

Water and Rivers Commission (2001). Identification of Groundwater Dependent Ecosystems in the Jurien Arrowsmith Groundwater areas (Australia), Literature review. Report by PPK.

Woodford, A.C & Chevallier, L., 2002a. Hydrogeology of the main Karoo Basin: Current Knowledge and Future research needs. Water Research Commission Report No TT 179/02.

Woodford, A. & Chevallier, L., 2002b. Regional characterization and mapping of Karoo fractured aquifer systems. An integrated approach using a Geographical Information System and digital Image processing. Water Research Commission project. Report 653/1/02.

APPENDIX A

PHOTOGRAPHS OF THE STUDY AREA FROM THE ACOCKS ARCHIVE

4551: - Acacia Karroo in Grassveld. 16/11/1945

4552: - Acacia Karroo in Grassveld. 16/11/1945

4958: - Themda trainda in Dohne Sourveld
Mtaba Mthuru Nek, 26/7/1946

4959: - Elynurus argenteus in Dohne Sourveld
Mtaba Mthuru Nek, 26/7/1946

4960: - Elynurus argenteus in Dohne Sourveld
Mtaba Mthuru Nek, 26/7/1946

4961: - Outlier of Valley Bushveld
Cacadu Gorge

4962: - Snow storm in thorn invaded Dohne Sourveld

4963: - Snow storm in thorn invaded Dohne Sourveld

Plate A1: Photographs from the Acocks Archive. The number before the title denotes the reference number given by Acocks. Photographs courtesy of the National Botanical Institute.

APPENDIX B

BASIC PRINCIPLES OF REMOTE SENSING

Numerous definitions have been found in the literature for remote sensing. Campbell (1996) defines remote sensing as: "the practice of deriving information about the earth's land and water surfaces using images acquired from an overhead perspective, using electromagnetic radiation in one or more regions of the electromagnetic spectrum, reflected or emitted from the earth's surface."

Campbell (1996), Mather (1999) and Lillesand & Kiefer (2000) all give excellent introductions to the concepts of remote sensing. The following discussion is adapted from their texts.

Electromagnetic radiation/energy (EMR) is generated by several mechanisms, including changes in the energy level of electrons, acceleration of electrical charges, decay of radioactive substances, and the thermal motion of atoms and molecules. Nuclear reactions within the sun produce a full spectrum of EMR, which is transmitted through space without experiencing major changes. As this radiation approaches the earth, it passes through the atmosphere before reaching the earth's surface. However, oxygen, carbon dioxide and water vapour present in the atmosphere, all absorb different ranges of wavelengths more or less completely. This means that only some of the continuum of electromagnetic radiation can be used for remote sensing of materials at the earth's surface. These "block-outs" are known as atmospheric windows. Other atmospheric interactions further restrict what is possible. Clouds prevent all radiation, with the exception of wavelengths in the microwave region, from reaching the earth's surface. The presence of molecules of oxygen, nitrogen, water vapour and dust particles cause scattering which produces haze in the visible wavelengths. Refraction (the bending of light), occurs as EMR passes through atmospheric layers of varied clarity, humidity, and temperature. These atmospheric effects may have a substantial impact on the quality of images and the data generated by sensors, so it is important to understand these interactions.

As EMR reaches the earth's surface, it is reflected, absorbed or transmitted. Reflection occurs when a ray of light is redirected as it strikes a non-transparent surface. The nature of the reflection depends upon the size of surface irregularities in relation to the wavelength of the radiation considered. If the surface is smooth relative to wavelength, specular reflection occurs, whereby almost all incident radiation is redirected in a single direction. If a surface is rough relative to wavelength, diffuse or isotropic reflection occurs. In this case, energy is scattered more or less equally in all directions. Transmission of radiation occurs when radiation passes through a substance without significant attenuation (reduction in intensity). Water bodies are an example of good transmitter of EMR, and leaves of plants transmit significant amounts of radiation in the infrared wavelengths.

A fundamental premise in remote sensing is that we can learn about objects and features on the earth's surface by studying the radiation reflected and/or emitted by these features. A set of observations or measurements observed over a range of wavelengths, constitutes a spectral response pattern, also known as a spectral signature. Wolff, 1965 in Campbell (1996) states: "Everything in nature has its own distribution of reflected, emitted and absorbed radiation. These spectral characteristics can - if ingeniously exploited - be used to distinguish one thing from another or to obtain information about shape, size and other physical and chemical properties".

APPENDIX C
LANDSAT AND ASTER IMAGERY

Since the 1960s a very large number of satellites have been launched. For this research, data from two different sensors was used (Landsat and ASTER), and thus only these two will be discussed. Both Landsat and ASTER imagery can be ordered via the Internet and there is extensive information regarding these sensors available on these sites. Most introductory texts to remote sensing dedicate a chapter to describing the available sensors. However, as ASTER was only recently launched, only electronic texts on ASTER were found in the literature.

The Earth Resources Technology Satellite (ERTS) Program launched the first of a series of satellites (ERTS1) in 1972. Part of the National Aeronautics and Space Administration's (NASA) Earth Resources Survey Program, the ERTS programme and ERTS satellites were later renamed Landsat. This was to better represent the civil satellite program's prime emphasis on remote sensing of land resources. The latest satellite, Landsat7 was launched on 15 April 1999. This satellite carried the enhanced thematic mapper plus (ETM+). ETM+ is an enhanced version of the thematic mapper (TM) sensor flown aboard the previous landsat4 and -5 satellites. Sensor enhancements include the addition of the panchromatic band and two ranges, improved spatial resolution for the thermal band and two solar calibrators. (USGS, 2002)

Aster (Advanced Spacebourne Thermal Emission and Reflection Radiometer) is an imaging instrument that is flying on Terra, a satellite launched in December 1999 as part of NASA's Earth Observing System (EOS). Aster will be used to obtain detailed maps of land surface temperature, emmissivity, reflectance and elevation. The EOS platforms are part of NASA's Earth Science Enterprise, whose goal is to obtain a better understanding of the interactions between the biosphere, hydrosphere, lithosphere and atmosphere. The ASTER instrument was built in Japan for the Japanese Ministry of Economy, Trade and industry. A joint United States/Japan team is responsible for instrument design, calibration and validation. (California Institute of Technology, 2002)

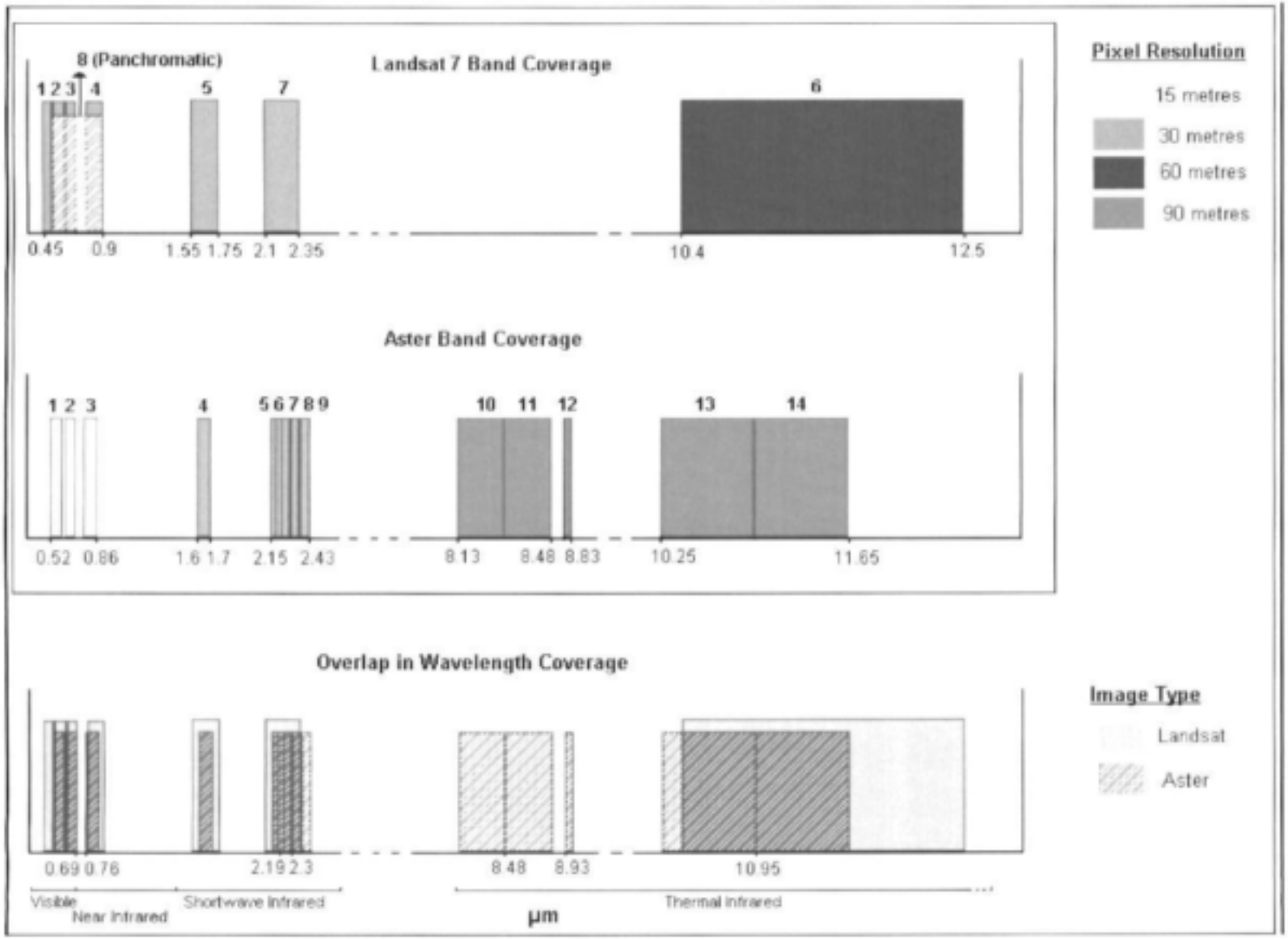

Figure C.1: Characteristics of Landsat and Aster Imagery

APPENDIX D

GLOSSARY

Aster image: satellite image of higher resolution than Landsat TM (see Appendix C for more information).

Badland: degraded land characterized by the formation of deep dongas/gulleys. It results from bad land practice, soil erosion, lowering of the water table and change in the drainage profile.

DEM: Digital Elevation Model.

Dolerite offshoot: small, thin and minor intrusion branching out of a major and thicker dolerite intrusion. Offshoots are usually a meter or less thick.

Dolerite sill and ring complexes: Dolerite sill and ring complex are typical of Karoo dolerite intrusions. They are commonly saucer-shaped with a disc-like flat sill in the middle, an inclined sheet all around and an outer sill on the rim at a higher elevation. Although sometime fed by sub-circular dykes, these structures are not ring complexes which one are typical of alkaline volcanic centers and characterized by multiple intrusions of various compositions.

Effluent: Secondary river or stream flowing into a larger river. It does also apply to a river when the water flows and feeds into an aquifer.

Ground water dependent ecosystems: have been classified into six categories (see Evans ad Hatton, 2000): phreatophytic terrestrial vegetation, wetlands, base flows, Aquifers and caves, near shore marine, terrestrial fauna.

Hydro-morpho-tectonic model: 3 D graphic conceptual model showing the relation between tectonics (dolerite sills and rings), morphology (ring system at surface) and hydostratigraphy (aquifer layering). See Chevallier et al. (2001).

Hydrostratigraphy: Description (depth, size, type etc...) of the vertical succession of aquifers in a rock mass. Ex: succession of a deep aquifer, medium-depth aquifer, shallow aquifer, and sub-surface aquifers.

Inclined sheet: Shallow to strongly inward dipping sub-circular intrusion forming the peripheral "ring" per saucer-shape dolerite ring system (see Chevallier et al., 2001).

Induced ground water flow: Ground water flow artificially created by drilling. Boreholes can connect two, or several different fractured aquifers lying at different elevations, resulting in a loss of water from one aquifer to the other.

Inner sill: flat lying sill forming the base of the saucer-shape dolerite ring system (see Chevallier et al., 2001).

Magnetic fabric: Magnetic field intensity data where low frequency information has been removed. The resulting map shows a greater degree of contrast between deep-seated ghost structures and shallow dolerite intrusions.

Multi-temporal satellite imagery: Remote sensing technique using and comparing satellite images taken at different times (different year) or at different times of the same year.

Morpho-tectonics: Study of the relations between morphology and tectonics (rock deformation). Both are closely linked and morphology often reflects a specific tectonic style. The Karoo dolerite rings display different tectonic s features (inner sill, inclined sheet, outer sills) each of them characterized by specific morphological features.

Outer sill: flat lying sill forming the outside rim of the saucer-shape dolerite ring system, usually eroded away (see Chevallier et al., 2001).

Plumbing system: term used in volcanology to describe the complex network of dykes, sills, pipes, bulges, blobs etc.. underlying volcanoes and acting as "fractured" magma chamber or magma storage (ex; the Kilauea Plumbing System , in Hawaii).

Shapefile: vector file format used for spatial data. It stores the location, the attribute and information for points, lines and whole areas. Each shapefile is a single feature file structure which consists of at least 4 files: .Shp, .Shx, .Dbf, and.Brj.

Spongy dolerite: fractured surface of a dolerite sill forming a small localised catchment. It retains and releases water via seeps or wetlands. Always high lying and recharged by rain or mist, these features.

Storativity: Coefficient of storage of an aquifer

Stream ordered rivers: coding system for vectorized drainage systems. Rivers or effluents are coded according to their order: principal river, secondary river, tertiary stream etc..

Transmissivity: Aquifer thickness multiplied by permeability.

Unsupervised classification: an automatic image classification procedure which does not require the selection of classes prior to classification. It is often used when there is an absence of large amounts of ground data.

Other related WRC reports available:

Hydrogeology of the main Karoo Basin: Current knowledge and future research needs

AC Woodford • L Chevallier (editors)

A large part of South Africa (approximately 50% of the country as a whole) is underlain by the Karoo Supergroup of geological formations. A major characteristic of the Karoo Supergroup, which consists mainly of sandstone, mudstone, shale and siltstone. The majority of boreholes drilled in Karoo formations have very low yields . However, large volumes of groundwater are pumped from wellfields supplying towns, mines and the basements of buildings on a daily basis in areas underlain by the Karoo formations, which is not what one would expect from aquifers with a limited yield.

Karoo aquifers have a very complex and unpredictable behaviour. The general view is thus that Karoo aquifers are not reliable sources of water. However, there is no doubt that these aquifers played a significant part in the development of South Africa. This is evident in numerous place and area names, such as De Aar, Bitterfontein, Koffiefontein, Springfontein, Lelieput, Syfergat and Putsonderwater.

The Water Research Commission (WRC) has co-ordinated and funded numerous research projects aimed at understanding the hydrogeology, flow characteristics and exploitability of Karoo fractured-aquifers over the past 20 years. The research was conducted by various research institutions, governmental organisations and private consultants, involving both intensive localised and more extensive regional studies.

This document review and collate the vast amount of existing knowledge on Karoo fractured-aquifers and identify future research priorities.

Report Number: TT 179/02 **ISBN: 1 86845 851 2**

TO ORDER: Contact **Publications** - Telephone No: 012 330 0340
Fax Number: 012 331 2565
E-mail: publications@wrc.org.za

Water Research Commission
Private Bag X03, Gezina, 0031, South Africa
Tel: +27 12 330 0340, Fax: +27 12 331 2565
Web: http://www.wrc.org.za